



<http://mc.manuscriptcentral.com/fems>

**Adhesive Organelles of Gram-Negative Pathogens  
Assembled with the Classical Chaperone/Usher Machinery:  
Structure and Function with a Clinical Bend**

Journal:	<i>FEMS Microbiology Reviews</i>
Manuscript ID:	FEMSRE-09-06-0029.R2
Manuscript Type:	Review - Invited
Date Submitted by the Author:	
Complete List of Authors:	Zaviyalov, Vladimir; University of Turku, Joint Biotechnology Laboratory Zavialov, Anton; Swedish University of Agricultural Sciences, Department of Molecular Biology Zaviyalova, Galina; University of Turku, Joint Biotechnology Laboratory Korpela, Timo; University of Turku, Joint Biotechnology Laboratory
Keywords:	Adhesins, Gram-Negative Pathogens, Chaperone/Usher Machinery



## INTRODUCTION

1  
2  
3  
4  
5  
6  
7 A necessary step for the development of an infectious disease in the host organism is the  
8  
9 formation of a firm link between the pathogen and target cells of the host. The link is mediated  
10  
11 by surface-exposed adhesive organelles and is required for internalization of bacteria or  
12  
13 extracellular colonization of host tissues. The adhesive organelles mediate bacterial adhesion via  
14  
15 specific interaction with surface structures presented on host cells. The adhesin-binding to the  
16  
17 target cells triggers subversive signals that allow pathogens to evade immune defense and  
18  
19 facilitate bacterial colonization or invasion (reviewed by Zavialov *et al.*, 2007).  
20  
21

22  
23 There are two major classes of protein adhesins of Gram-negative pathogens:  
24

- 25  
26 (1) The fimbrial adhesins, represented by the linear homopolymers or heteropolymers (up to 7  
27  
28 distinct subunits) of hundreds to thousands of subunits;  
29  
30 (2) The non-fimbrial adhesins consisted of a single protein or homotrimers.  
31  
32

33 The fimbrial adhesins in Gram-negative bacteria are typically formed by non-covalent homo-  
34  
35 or hetero- polymerization of subunit proteins (reviewed by Fronzes *et al.*, 2008; Kline *et al.*,  
36  
37 2009; Waksman & Hultgren, 2009; Zavialov *et al.*, 2007). In contrast, the more recently  
38  
39 discovered fimbrial adhesins in Gram-positive bacteria are formed by covalent polymerization of  
40  
41 protein subunits in a process that requires a dedicated sortase enzyme (reviewed by Proft &  
42  
43 Baker, 2009).  
44  
45

46  
47 The assembly of fimbrial and non-fimbrial adhesins of Gram-negative pathogens involves  
48  
49 the function of different secretion systems. Protein transport across the outer membrane of  
50  
51 Gram-negative bacteria can be subdivided into Sec-independent and Sec-dependent pathways  
52  
53 (reviewed by Gerlach & Hensel, 2007). Depending on the system of secretion, adhesive proteins  
54  
55 presented on the surface of Gram-negative bacteria may be divided in a few major families:  
56  
57

- 58  
59 (1) The fimbrial adhesins, assembled on outer membrane by the classical chaperone/usher  
60  
61 pathway (Choudhury *et al.*, 1999; Hung *et al.*, 1996; Fronzes *et al.*, 2008; Knight *et al.*, 2000;

1  
2 Remaut *et al.*, 2006, 2008; Sauer *et al.*, 1999, 2000, 2002, 2004; Thanassi *et al.*, 1998; Verger *et*  
3  
4 *al.*, 2007; Waksman & Hultgren, 2009; Yu *et al.*, 2009; Zavialov *et al.*, 2001, 2002, 2003, 2005,  
5  
6 2007; Zavialov & Knight, 2007).

7  
8  
9 (2) CS pili, assembled on outer membrane by the “alternate chaperone/usher pathway” (Soto &  
10  
11 Hultgren, 1999). Assembly of the surface antigen 1 (CS1) pili of enterotoxigenic *Escherihia coli*  
12  
13 shows high functional similarities to the classical chaperone/usher pathway but the proteins  
14  
15 involved share no detectable sequence similarities. Poole *et al.* (2007) demonstrated that like the  
16  
17 classical chaperone/usher pathway the donor strand complementation mechanism governs  
18  
19 intersubunit interaction of fimbriae of the alternate chaperone/usher pathway.  
20  
21

22  
23 (3) Type IV pili, formed in distinction to (1) and (2), by polymerization of pilin subunits at the  
24  
25 cytoplasmic membrane. The assembled pilus structure is extruded across the outer membrane  
26  
27 and forms long and flexible surface appendages (Craig *et al.*, 2004; Fronzes *et al.*, 2008,  
28  
29 2009a,b). Components of the type IV pilus assembly machinery are structurally related to Type 2  
30  
31 secretion system, where homologous proteins are called “pseudopilins”.  
32  
33

34  
35 (4) Curli or thin aggregative fimbrial adhesins, assembled at the bacterial surface through  
36  
37 extracellular nucleation precipitation: the major fiber subunit CsgA polymerizes on the surface-  
38  
39 exposed nucleator CsgB (Hammar *et al.*, 1996; Fronzes *et al.*, 2008).  
40  
41

42 (5) The non-fimbrial “trimeric autotransported adhesins”, secreted by the Type 5 secretion  
43  
44 system (Linke *et al.*, 2006). Adhesin YadA is the prototypical member of non-fimbrial adhesins.  
45  
46 YadA is expressed by several *Yersinia* species and is a member of the family of very stable  
47  
48 trimeric autotransporter adhesins anchored in the outer membrane with a  $\beta$ -barrel.  
49  
50

51 (6) Integral outer-membrane proteins (e.g. OmpA, invasins and intimin), anchored to the outer  
52  
53 membrane with a unique mechanism, in which the bacteria provide the cognate receptor for the  
54  
55 adhesin intimin by translocating it into the host cell in a Type III secretion system-dependent  
56  
57 manner (Niemann *et al.*, 2004).  
58  
59  
60

1  
2 (7) Non-fimbrial adhesins, secreted by the Type 1 secretion system (Delepelaire, 2004). E.g.  
3  
4 two-partner-secreted filamentous hemagglutinins from *Bordetella pertussis* exist in a membrane-  
5  
6 bound and secreted form, each having distinct functions.  
7

8  
9 Dominant class (1) of the fibrillar adhesive organelles of Gram-negative pathogens is  
10 assembled by the conserved classical chaperone/usher protein secretion system (Choudhury *et*  
11 *al.*, 1999; Hung *et al.*, 1996; Fronzes *et al.*, 2008; Knight *et al.*, 2000; Remaut *et al.*, 2006, 2008;  
12 *al.*, 1999; Hung *et al.*, 1996; Fronzes *et al.*, 2008; Knight *et al.*, 2000; Remaut *et al.*, 2006, 2008;  
13 Sauer *et al.*, 1999, 2000, 2002, 2004; Thanassi *et al.*, 1998; Verger *et al.*, 2007; Waksman &  
14 Hultgren, 2009; Yu *et al.*, 2009; Zavialov *et al.*, 2001, 2002, 2003, 2005, 2007; Zavialov &  
15 Knight, 2007). This system can assemble fimbrial organelles of diverse subunit composition,  
16 architecture and function. The assembled organelles consist of two main structurally and  
17 functionally distinct families. One family consists of only one or two types of subunits and at  
18 low resolution typically shows non-pilus, amorphous or capsule-like morphology (Hung *et al.*,  
19 1996; Remaut *et al.*, 2006; Soto & Hultgren, 1999; Zavialov *et al.*, 2003; 2005; 2007). The  
20 assembly of this family is assisted with the FGL (having a long F1-G1 loop) family of  
21 periplasmic chaperones (Hung *et al.*, 1996; Remaut *et al.*, 2006; Zavialov *et al.*, 2003; 2005;  
22 2007; Zavialov & Knight, 2007; Zav'yalov *et al.*, 1995b). The notable property of the organelles  
23 is that all subunits possess two independent binding sites specific to different host cell receptors  
24 (Anderson *et al.*, 2004a, b; Korotkova *et al.*, 2006a,b; 2008a; Pettigrew *et al.*, 2004). Because of  
25 this function-structural property they were named as “FGL chaperone-assembled polyadhesins”  
26 (Zavialov *et al.*, 2007). The other family consists of thick rigid and thin flexible adhesive pili  
27 (also known as adhesive fimbriae) of a complex subunit composition (up to 7 different subunits).  
28 The majority of the pili displays only one adhesive domain on the tip of the pilus (mono-  
29 adhesive fimbriae/pili) (Choudhury *et al.*, 1999; Hung *et al.*, 1996; Fronzes *et al.*, 2008; Knight  
30 *et al.*, 2000; Remaut *et al.*, 2008; Sauer *et al.*, 1999, 2000, 2002, 2004; Thanassi *et al.*, 1998;  
31 Verger *et al.*, 2007; Waksman & Hultgren, 2009). The assembly of mono-adhesive pili/fimbriae  
32  
33  
34  
35  
36  
37  
38  
39  
40  
41  
42  
43  
44  
45  
46  
47  
48  
49  
50  
51  
52  
53  
54  
55  
56  
57  
58  
59  
60

1  
2 is assisted with the FGS (having a short F1-G1 loop) family of periplasmic chaperones (Hung *et*  
3  
4 *al.*, 1996).

5  
6 The discovery of two families of organelles and chaperones was based on the different  
7  
8 morphologies of organelles and the sequence comparison of chaperones (Hung *et al.*, 1996;  
9  
10 Zav'yalov *et al.*, 1995b). The relevance of the division was confirmed later by high-resolution  
11  
12 3D analysis of the typical representatives of the two families of chaperones and the organelle  
13  
14 subunits folded by them (Choudhury *et al.*, 1999; Remaut *et al.*, 2006; Sauer *et al.*, 1999, 2002;  
15  
16 Salih *et al.*, 2008; Verger *et al.*, 2007; Waksman & Hultgren, 2009; Zavialov *et al.*, 2003, 2005,  
17  
18 2007; Zavialov & Knight, 2007). Both types of organelles are made of fibers of linearly  
19  
20 polymerized subunits. The subunits are connected with the donor strand exchange mechanism  
21  
22 (Salih *et al.*, 2008; Sauer *et al.*, 1999; Verger *et al.*, 2007; Waksman & Hultgren, 2009; Zavialov  
23  
24 *et al.*, 2003, 2005, 2007). Comparison of the subunit 3D structures in fiber and bound to  
25  
26 chaperone (Sauer *et al.*, 2002; Zavialov *et al.*, 2003) together with calorimetric studies (Zavialov  
27  
28 *et al.*, 2005) revealed that the fiber formation in both of the families is driven by the chaperone-  
29  
30 preserved folding energy.  
31  
32  
33  
34  
35  
36

37 The last comprehensive review on the superfamily of Gram-negative bacterial adhesins  
38  
39 assembled via the classical chaperone/usher pathway was published a decade ago (Soto &  
40  
41 Hultgren, 1999). A remarkable progress in understanding the structure and function of the  
42  
43 classical chaperone/usher assembly-translocation machinery (Remaut *et al.*, 2008; Yu *et al.*,  
44  
45 2009), the structure and function of the surface-exposed adhesive organelles (Anderson *et al.*,  
46  
47 2004a,b; Bouckaert *et al.*, 2005, 2006; De Greve *et al.*, 2007; Korotkova *et al.*, 2006a,b, 2008a;  
48  
49 Li *et al.*, 2007; Pettigrew *et al.*, 2004; Salih *et al.*, 2008; Verger *et al.*, 2007; Westerlund-  
50  
51 Wikström & Korhonen, 2005; Zavialov *et al.*, 2003, 2005, 2007), and the phylogenesis of  
52  
53 ushers/chaperones (Nuccio & Bäumlér, 2007) has been achieved since that time. It has become  
54  
55 now evident that adhesins trigger subversive signals directed to mislead the immune system  
56  
57 (Bergsten *et al.*, 2005; Betis *et al.*, 2003a, b; Cane *et al.*, 2007; Diard *et al.*, 2006; Sharma *et al.*,  
58  
59  
60

1  
2 2005a, b; Sodhi *et al.*, 2004). Numerous examples of application of the organelles for  
3  
4 development of vaccines have been described (Alvarez *et al.*, 2006; Chichester *et al.*, 2009; Del  
5  
6 Prete *et al.*, 2009; Elvin *et al.*, 2006; Eyles *et al.*, 2000; Honko *et al.*, 2006; Glynn *et al.*, 2005;  
7  
8 Goluszko *et al.*, 2005; Hu *et al.*, 2009; Jones *et al.*, 2006; Langermann *et al.*, 2000; Lopes *et al.*,  
9  
10 2006; Powell *et al.*, 2005; Remer *et al.*, 2009; Santi *et al.*, 2006; Strindelius *et al.*, 2004;  
11  
12 Verdonck *et al.*, 2009; Williamson *et al.*, 2005). In addition, it has been demonstrated that  
13  
14 adhesive domains of monoadhesins and chaperone/usher assembly-translocation machinery are  
15  
16 promising targets for new generations of antimicrobials that specifically inhibit adhesion  
17  
18 (Wellens *et al.*, 2008) or interfere the fimbrial adhesion assembly (Aberg & Almqvist, 2007;  
19  
20 Pinkner *et al.*, 2006).

21  
22 Although several excellent reviews have been published recently, they either focused on  
23  
24 specialized aspects of the chaperone-usher assembly (Fronzes *et al.*, 2008; Sauer *et al.*, 2004) or  
25  
26 covered the results of studies of only particular chaperone-usher system (Waksman & Hultgren,  
27  
28 2009). Our previous review was also devoted only to FGL chaperone-assembled polyadhesins  
29  
30 (Zavialov *et al.*, 2007). We believe that recently accumulated significant new knowledge on  
31  
32 different aspects of biogenesis of the superfamily of Gram-negative bacterial adhesins assembled  
33  
34 via the classical chaperone/usher pathway and their medical applications require new analysis  
35  
36 and generalizations. During this work we found that number of different types of subunits,  
37  
38 composing the organelles, strongly correlates with the length of F1-G1 loop of chaperone  
39  
40 proteins. Based on this, we suggest here a novel function-structural classification of the  
41  
42 superfamily of adhesive organelles assembled with the classical chaperone/usher machinery.  
43  
44  
45  
46  
47  
48  
49  
50  
51  
52  
53  
54

### 55 **General Properties of Adhesive Organelles**

56  
57  
58 Adhesive organelles assembled with the classical chaperone/usher machinery are found in  
59  
60 Gram-negative bacteria, primarily in genera *Escherichia*, *Klebsiella*, *Photobacterium*, *Proteus*,

1  
2 *Salmonella*, and *Yersinia* of *Enterobacteriaceae*. The organelles are also found in species from  
3  
4  
5  
6  
7  
8  
9  
10  
11  
12  
13  
14  
15  
16  
17  
18  
19  
20  
21  
22  
23  
24  
25  
26  
27  
28  
29  
30  
31  
32  
33  
34  
35  
36  
37  
38  
39  
40  
41  
42  
43  
44  
45  
46  
47  
48  
49  
50  
51  
52  
53  
54  
55  
56  
57  
58  
59  
60  
*genuses Bordetella* of *Alcaligenaceae*, *Haemophilus* of *Pasteurellaceae* family, *Pseudomonas* of  
*Pseudomonadaceae* family, and *Acinetobacter* of *Moraxellaceae*. All these bacteria cause  
various diseases including fatal systemic diseases, like bubonic and pneumonic plague (*Yersinia*  
*pestis*), enteric typhoid fever (*Salmonella typhi* and *Salmonella paratyphi A*), sepsis or extra-  
intestinal focal infections (*Salmonella choleraesuis*), gastroenteritis (*Yersinia*  
*pseudotuberculosis*, *Salmonella typhimurium* and *Salmonella enteritidis*), pyelonephritis, cystitis,  
diarrhea (different pathogenic *E. coli* strains and *Proteus mirabilis*), whooping cough (*Bordetella*  
*pertussis*), Brazilian purpuric fever, meningitis, otitis media (*Haemophilus influenzae*),  
pneumonia (*Klebsiella pneumoniae*), insect infections (*Photorhabdus temperata*) and plant  
infections (*Pseudomonas syringae*).

Table 1 describes assembly assisting proteins, species distribution and associated diseases  
for fifty currently known adhesive organelles, the assembly of which on bacterial surface has  
been confirmed experimentally and is assisted with the classical chaperone/usher machinery.  
The information is placed in Table 1 in alphabetical order of the names of the chaperone/usher  
proteins.

### Gene Clusters Encoding for Adhesive Organelles

Genes of proteins involved in expression and assembly of adhesive fibres via the classical  
chaperone/usher pathway are arranged into compact gene clusters, which are located either on  
the chromosome or plasmids of Gram-negative bacteria. Depending on the structural properties  
of periplasmic chaperones they can be divided into two families:

- (1) FGL chaperone-comprising gene clusters;
- (2) FGS chaperone-comprising gene clusters.



1  
2 **FGL chaperone-comprising gene clusters.** Encoded by the *caf* gene cluster fraction 1  
3  
4 (F1), capsular antigen from *Y. pestis* is comprised of aggregated high-molecular-weight linear  
5  
6 polymers of a single subunit Caf1 (Zavialov *et al.*, 2002, 2003, 2005, 2007). The genes of *caf*  
7  
8 gene cluster, *caf1*, *caf1M*, *caf1A* and *caf1R*, encode, respectively, for Caf1 subunit, periplasmic  
9  
10 chaperone Caf1M, an outer membrane assembler, the molecular usher Caf1A, and the protein  
11  
12 Caf1R regulating of the gene cluster transcription (Galyov *et al.*, 1990, 1991; Karlyshev *et al.*,  
13  
14 1992a, b; 1994).  
15  
16  
17

18  
19 The *psa* gene cluster from *Y. pestis* encodes proteins for expression and assembly of the  
20  
21 fimbrial pH6 antigen comprised of high-molecular-weight polymer of PsaA subunit (Lindler &  
22  
23 Tall, 1993). PsaB functions as the periplasmic chaperone, PsaC is the molecular usher. Two  
24  
25 additional proteins, PsaE and PsaF, have been shown to regulate transcription of *psaA* gene  
26  
27 (Yang & Isberg, 1997). Another transcriptional regulator, RovA, interacts with the *psaE* and  
28  
29 *psaA* promoter regions, suggesting that RovA is an upstream regulator of *psa* gene cluster  
30  
31 (Cathelyn *et al.*, 2006). Identical *psa* gene clusters are present in *Y. pestis* and *Y.*  
32  
33 *pseudotuberculosis* (Lindler & Tall, 1993).  
34  
35  
36

37  
38 Closely related to *psa* gene cluster of *Y. pestis*, *Y. enterocolitica* contains *myf* encoding the  
39  
40 Myf fimbriae, which are built up of MyfA subunits. The *psa* and *myf* clusters have similar  
41  
42 general organisation. Moreover, proteins encoded by these gene clusters display a significant  
43  
44 sequence similarity, suggesting that pH6 antigen and Myf fibriae have a common function in the  
45  
46 different species of *Yersinia*. As PsaE and PsaF encoded by *psa*, the MyfE and MyfF proteins  
47  
48 encoded by *myf* have a role in regulation of the cluster transcription (Iriarte & Cornelis, 1995).  
49  
50  
51

52  
53 The *cs-3* gene cluster from *E. coli* encodes for proteins for expression and assembly of the  
54  
55 colonization factor-3 that forms CS-3 fimbriae comprised of high-molecular-weight polymer of  
56  
57 CS-3 subunit (Jalajakumar *et al.*, 1989). CS3-E functions as the periplasmic chaperone, and CS3-  
58  
59 D is the molecular usher.  
60



1  
2 The *nfa* gene cluster from *E. coli* encodes proteins for expression and assembly of the  
3 nonfimbrial adhesin, NFA-I, comprised of high-molecular-weight polymer of NfaA subunit  
4 (Ahrens *et al.*, 1993). NfaE functions as the periplasmic chaperone, and NfaE is the molecular  
5 usher.  
6  
7  
8  
9

10 A group of *E. coli* gene clusters, *afa-3*, *afa-8*, *agg*, *aaf*, *agg-3*, *dafa*, *dra*, *daa*, that encode  
11 proteins for expression and assembly of the afimbrial adhesins Afa-III and AfaE-VIII, the  
12 aggregative adherence fimbria type I, II and III (AAF/I, AAF/II and AAF-III), the diffuse  
13 adherence fibrillar adhesin (Dafa), the Dr hemagglutinin flexible fimbriae and the F1845 (DaaE)  
14 fimbrial adhesin, respectively, have a peculiar feature: each gene cluster encodes additional  
15 subunit D for which an invasive function was suggested (putative invasin subunit; Jouve *et al.*,  
16 1997; Servin, 2005). DraE and AfaE-III adhesins may assemble into a flexible fibre that provides  
17 the link between the usher at the outer membrane and the putative invasin subunit located at the  
18 tip of the fibre (Anderson *et al.*, 2004a, b; Pettigrew *et al.*, 2004). However, expression of DraD  
19 invasin subunit is independent of the DraC usher and DraE fimbrial subunit (Zalewska *et al.*,  
20 2005). In addition, polymerization of DraE fimbrial subunits into fimbrial structures does not  
21 require expression of DraD. Recently, Zalewska-Piątek *et al.* (2008) showed that type II  
22 secretion in *E. coli* strain Dr<sup>+</sup> leads to DraD translocation to the bacterial cell surfaces. Very  
23 recently, Korotkova *et al.* (2008b) and Guignot *et al.* (2009) demonstrated that the DraD subunit  
24 is not required for  $\beta_1$  integrin recruitment or bacterial internalization. Therefore, the function of  
25 D subunits is still under the question.  
26  
27  
28  
29  
30  
31  
32  
33  
34  
35  
36  
37  
38  
39  
40  
41  
42  
43  
44  
45  
46  
47  
48

49 A group of *Salmonella* spp. gene clusters *saf*, *sef*, *cs6-1*, *cs6-2* that encodes proteins for  
50 expression and assembly of the atypical fimbriae Saf, the filamentous fimbriae-like structures  
51 SEF14/18, and the colonization factors CS6-1 and -2 has another common peculiar feature: all of  
52 these gene clusters encode two adhesin subunits. The SefB chaperone of *S. enteritidis* assists in  
53 the assembly of two distinct cell-surface structures, SEF14 and SEF18, which are homopolymers  
54 of SefA and SefD subunits, respectively (Clouthier *et al.*, 1994). The CscC chaperone assists in  
55  
56  
57  
58  
59  
60

1  
2 assembling thin CS6 fibrillae that are composed of two heterologous CssA and CssB subunits  
3  
4 (Wolf *et al.*, 1997).  
5

6  
7 **FGS chaperone-comprising gene clusters.** A group of two gene clusters *atf* and *pef* that  
8  
9 encodes proteins for expression and assembly of the ambient-temperature fimbriae ATF of *P.*  
10  
11 *mirabilis* (Massad *et al.*, 1996) and plasmid-encoded (PE) fimbriae of *S. typhimurium* have  
12  
13 common peculiar feature: they encode only one structural subunit which is probably functioning  
14  
15 as an adhesin subunit. Recently a cosmid carrying the *pef* operon was introduced into *E. coli* and  
16  
17 expression of fimbrial filaments composed of PefA was confirmed by flow cytometry and  
18  
19 immune-electron microscopy (Chessa *et al.*, 2008). Plasmid-encoded fimbriae were purified  
20  
21 from the surface of *E. coli* and the resulting preparation was shown to contain PefA as the sole  
22  
23 major protein component. Binding of purified plasmid-encoded fimbriae to a glycan array  
24  
25 suggested that this adhesin specifically binds the tri-saccharide Galss1-4 (Fuca1-3) GlcNAc, also  
26  
27 known as the Lewis X (Lex) blood group antigen.  
28  
29  
30  
31  
32

33 The *aciad* gene cluster of *Acinetobacter sp.*, strain ADP1 (Barbe *et al.*, 2004; Gohl *et al.*,  
34  
35 2006) encodes only one structural subunit which may function as an adhesin subunit. This cluster  
36  
37 contains genes for two periplasmic chaperones.  
38  
39

40 A group of gene clusters *f17a*, *acu* and *fim/fha* that encodes proteins for expression and  
41  
42 assembly of the F17 pili of *E. coli* (Lintermans *et al.*, 1988), thin pili of *Acinetobacter sp.*, strain  
43  
44 BD413 (Barbe *et al.*, 2004; Gohl *et al.*, 2006) and type 2 and 3 pili of *B. pertussis* (Willems *et*  
45  
46 *al.*, 1992). They encode one structural and one adhesin subunit that are exposed on the tip of pili.  
47  
48

49 A group of gene clusters *hif*, *haf*, *mrk*, *lpf* and *pmf* that encodes proteins for expression and  
50  
51 assembly of the *H. influenzae* fimbriae (van Ham *et al.*, 1994), *H. influenzae* biogroup aegyptius  
52  
53 fimbriae (Read *et al.*, 1996), *K. pneumoniae* type 3 fimbriae (Allen *et al.*, 1991), *S. typhimurium*  
54  
55 long polar fimbriae (Bäumler & Heffron, 1995) and *P. mirabilis* PMF pili (Massad & Mobley,  
56  
57 1994) encode two structural subunits and one adhesive subunit that is exposed on the tip of  
58  
59 fimbriae.  
60

1  
2 A group of gene clusters *fas*, *csw* and *fort* that encodes proteins for expression and assembly  
3  
4 of the 987P (Edwards *et al.*, 1996), CS12 (EMBL accession number Q9ALL0) and CS18  
5  
6 (Honarvar *et al.*, 2003) fimbriae of *E. coli* have very unusual feature since they encode three  
7  
8 distinct chaperones which assist in assembling of fibers composed of two structural subunits and  
9  
10 one adhesive subunit exposed on the tip of fimbriae. E.g., in the case of 987P fimbriae the FasB  
11  
12 was shown to be a periplasmic chaperone for the major fimbrial subunit, FasA (Edwards *et al.*,  
13  
14 1996). The periplasmic chaperone FasC specifically interacts and stabilizes the adhesin FasG  
15  
16 (Edwards *et al.*, 1996). FasE, a chaperone-like protein, is also located in the periplasm and is  
17  
18 required for optimal export of FasG and possibly for other subunits (Edwards *et al.*, 1996).  
19  
20  
21  
22

23 Two gene clusters *fos* and *stf* that encode proteins for expression and assembly of the F1C  
24  
25 pili of *E. coli* (Riegman *et al.*, 1990) and Stf fimbriae of *S. typhimurium* (Emmerth *et al.*, 1999)  
26  
27 and they encode three structural and one adhesin subunit exposed on the tip of fimbriae.  
28  
29

30 A group of gene clusters *fim*, *sfp*, *sfa* and *mrp* that encodes proteins for expression and  
31  
32 assembly of the type 1 pili of *E. coli* (Jones *et al.*, 1993), Sfp fimbriae of *E. coli* (Brunner *et al.*,  
33  
34 2001), S pili of *E. coli* (Dobrindt *et al.*, 2001) and mannose-resistant/Proteus-like MR/P pili of *P.*  
35  
36 *mirabilis* (Bahrani & Mobley, 1994). They encode four structural subunits and one adhesin  
37  
38 subunit which is exposed on the tip of fimbriae.  
39  
40  
41

42 The gene clusters *fan*, *lda*, *fae* and *ral* encode proteins for expression and assembly of the F4  
43  
44 (K88), Lda and F5 (K99) thin flexible pili and REPEC fimbriae of *E. coli*, respectively (Adams  
45  
46 *et al.*, 1997; Bakker *et al.*, 1991; Scaletsky *et al.*, 2005). These pili/fimbriae consist of four or  
47  
48 five subunits. However F4 (K88), F5 (K99) and Lda pili do not display specialized adhesive  
49  
50 domains on the tip of the pilus, but carry binding sites on their main structural subunit (FanH,  
51  
52 FaeH and LdaH) (Bakker *et al.*, 1991; Scaletsky *et al.*, 2005). The overall arrangement of the *ral*  
53  
54 gene cluster closely resembles that of the *fae* cluster with homologous genes occupying the same  
55  
56 relative position in each cluster. The *ral* cluster also has some of the more specific features of the  
57  
58 *fae* cluster such as the overlapping reading frames of the genes encoded chaperone and usher and  
59  
60

1  
2 the apparent absence of promoters within the region carrying the structural genes (Adams *et al.*,  
3  
4 1997). This general similarity together with the significant levels of homology exhibited by  
5  
6 individual genes makes it reasonable to propose functions for the *ral* gene products based on the  
7  
8 known roles of their Fae counterparts. Thus, Adams *et al.* (1997) proposed that RalC, RalF, and  
9  
10 RalH are minor fimbrial subunits of the fimbrial structure which is primarily composed of RalG,  
11  
12 the major fimbrial subunit. The gene cluster *afr* encodes proteins for expression and assembly of  
13  
14 the *E. coli* AF/R1 pili (Cantey *et al.*, 1999). The subunits encoded by *afr* gene cluster have the  
15  
16 highest percentage amino acid identity with the subunits encoded by *ral* cluster (Adams *et al.*,  
17  
18 1997).  
19  
20  
21  
22

23 The *mrf* and *pap* gene clusters that encode proteins for expression and assembly of mannose-  
24  
25 resistant fimbriae of *Ph. temperata* (Meslet-Cladiere *et al.*, 2004) and P pili of *E. coli* (Marklund  
26  
27 *et al.*, 1992) have the most complex composition: they encode six structural and one adhesin  
28  
29 subunit that is exposed on the tip of fimbriae.  
30  
31  
32

33 Fig. 1 shows the general organization of gene clusters for which the expression has been  
34  
35 experimentally confirmed.  
36  
37  
38  
39

## 40 STRUCTURE AND MECHANISM OF FUNCTION OF CHAPERONE/USHER

### 41 MACHINERY

#### 42 Molecular Functions

43  
44  
45  
46  
47  
48  
49  
50  
51 Periplasmic chaperones and outer membrane molecular usher proteins function in co-  
52  
53 operation as the chaperone/usher machinery that drives the assembly of surface-exposed fimbrial  
54  
55 adhesins (Fig. 2).  
56  
57

58  
59 Periplasmic chaperones possess the following main functions (Hung *et al.*, 1996; Knight *et*  
60  
*al.*, 2000; Remaut *et al.*, 2006; Sauer *et al.*, 2000, 2004; Thanassi *et al.*, 1998; Verger *et al.*,

1  
2 2007; Zavialov *et al.*, 2001, 2003, 2005, 2007; Zavialov & Knight, 2007; Zav'yalov *et al.*,  
3  
4 1995b):

- 5  
6  
7 (1) Binding to nascent subunits as they enter the periplasm via the Sec pathway;  
8  
9 (2) Protection of subunits from non-productive aggregation and proteolytic degradation by  
10 capping their assembly surfaces;  
11  
12 (3) Transport of subunits to an outer membrane molecular usher.  
13  
14

15  
16 Periplasmic chaperones either form stable complexes with subunits emerging to the  
17 periplasm or form dimers (PapD) (Hung *et al.*, 1999) or tetramers (Caf1M) (Zavialov & Knight,  
18 2007), where the subunit-binding sequences are protected against proteolysis and unspecific  
19 binding (see the chapter "3D structures of chaperones").  
20  
21

22  
23  
24  
25  
26 Outer membrane molecular ushers possess the following main functions (Fronzes *et al.*,  
27 2008; Nishiyama *et al.*, 2005; Remaut *et al.*, 2006, 2008; Yu *et al.*, 2009):

- 28  
29 (1) Release of subunit from the chaperone;  
30  
31 (2) Formation of assembly platform for polymerization of subunits in linear fibers;  
32  
33 (3) Formation of twinned-pore translocation machinery for secretion of linear fibers on the cell  
34 surface.  
35  
36

37  
38  
39 The recently decoded structure and proposed mechanism of the function of molecular usher  
40 proteins are described in the chapters "Structure of outer membrane molecular usher proteins"  
41 and "Mechanism of function of chaperone/usher machinery".  
42  
43  
44  
45  
46  
47  
48  
49

## 50 Structures of Chaperones

51  
52  
53  
54 **3D structure of chaperones.** For a long time the PapD chaperone has been serving as a  
55 prototype protein for the superfamily of periplasmic chaperones (Holmgren & Branden, 1989)  
56 and was the first structure of a molecular chaperones in general. The PapD chaperone structure  
57 consists of two domains joined at approximately right angle with a large cleft between the  
58  
59  
60

1 domains (Fig. 3). Both domains are 7-stranded  $\beta$ -sandwiches with immunoglobulin-like  
2 topology (Holmgren & Branden, 1989). The F1 and G1  $\beta$ -strands in the N-terminal domain of  
3 PapD are connected by a long and flexible loop that protrudes like a handle from the body of the  
4 domain.  
5  
6  
7  
8  
9  
10

11 Two families of the periplasmic chaperones were suggested with sequence analysis, FGS  
12 (having a short F1-G1 loop) and FGL (having a long F1-G1 loop) (Hung *et al.*, 1996; Zav'yalov  
13 *et al.*, 1995a) (Fig. 4). PapD chaperone represents the FGS class of chaperones. High resolution  
14 crystal structures for two FGL chaperones, Caf1M from *Y. pestis* and SafB from *S. typhimurium*,  
15 in complex with corresponding subunits, Caf1 of the F1 capsular antigen and SafA of atypical  
16 fimbriae Saf, have been determined (Remaut *et al.*, 2006; Zavialov *et al.*, 2003, 2005). As FGS  
17 chaperones (Choudhury *et al.*, 1999; Holmgren & Branden, 1989; Knight *et al.*, 2000; Sauer *et al.*,  
18 1999, 2002; Verger *et al.*, 2007), FGL chaperones consist of two domains joined at  
19 approximately right angle with a large cleft between the domains (Fig. 3). Both domains are 7-  
20 stranded  $\beta$ -sandwiches with immunoglobulin-like topology (Remaut *et al.*, 2006; Zavialov *et al.*,  
21 2003, 2005). The F1 and G1  $\beta$ -strands in the N-terminal domain of Caf1M and SafB are  
22 connected by a flexible loop that is much longer than in PapD chaperone (Fig. 4).  
23  
24  
25  
26  
27  
28  
29  
30  
31  
32  
33  
34  
35  
36  
37  
38  
39  
40

41 When PapD is not engaged in binding to subunits, it is capable of interacting transiently with  
42 itself to form a weakly but specifically bound dimer (Hung *et al.*, 1999). The crystal structures of  
43 two dimeric forms of PapD were solved to gain insight into the molecular basis of PapD dimer  
44 formation (Hung *et al.*, 1999). The structure–function analysis revealed that PapD interacts with  
45 itself by means of the same interactive surfaces that it uses to bind subunits, possibly  
46 representing a self-capping mechanism that protects the subunit-binding sequences against  
47 proteolysis and unspecific binding.  
48  
49  
50  
51  
52  
53  
54  
55  
56

57 Zavialov & Knight (2007) found that typical representative of FGL chaperones, subunit-free  
58 Caf1M, exists predominantly as a tetramer. A 2.9 Å resolution crystal structure of the Caf1M  
59 tetramer revealed that each of the four molecules contribute to its subunit binding sequences (the  
60

1  
2 A1 and G1 strands) to form an eight-stranded hetero-sandwich with a well-packed  
3  
4 phenylalanine-rich hydrophobic core (Zavialov & Knight, 2007). Tetramerization protects  
5  
6 chaperone molecules against enzymatic proteolysis. Deletions in the subunit binding motifs  
7  
8 completely abolish tetramer assembly, suggesting that the hetero-sandwich is the main structural  
9  
10 feature holding the tetramer together. Deletions in the VGVFVQFAI motif abolish both tetramer  
11  
12 assembly and aggregation, consistent with the predicted high  $\beta$ -aggregation propensity for this  
13  
14 motif. Such a packing of the aggregation-prone subunit binding sequences into the hetero-  
15  
16 domain is a novel molecular mechanism preventing unspecific aggregation of free chaperones.  
17  
18  
19

20  
21  
22 Assembly of F4 fimbriae of enterotoxigenic *E. coli*, indicate that self-capping of the pilin-  
23  
24 interactive interfaces is not the mechanism that is conservedly applied by all periplasmic  
25  
26 chaperones, but is rather a case-specific solution to cap aggregation-prone surfaces (Van Molle  
27  
28 *et al.*, 2009). FaeE crystal structure shows a dimer formed by interaction between pilin-binding  
29  
30 interfaces of two monomers. Thermodynamic and biochemical data show that FaeE occurs as a  
31  
32 stable monomer in solution (Van Molle *et al.*, 2009).  
33  
34  
35

36  
37 **Characteristic features of FGL and FGS chaperones.** Comparison of structures of FGS  
38  
39 and FGL chaperones reveals differences, which appear to locate in the functionally important  
40  
41 segments. These class-specific differences were correctly predicted earlier based on sequence  
42  
43 comparison and modelling using known structure of the FGS chaperone PapD (Chapman *et al.*,  
44  
45 1999; Hung *et al.*, 1996; Zav'yalov *et al.*, 1995b), and functional studies (Chapman *et al.*, 1999;  
46  
47 MacIntyre *et al.*, 2001; Zav'yalov *et al.*, 1997):  
48  
49  
50

51  
52 (1) FGL chaperones contain a significantly longer binding motif in the F1-G1 loop and G1  $\beta$ -  
53  
54 strand than FGS chaperones, due to the extension of this motif into the F1-G1 loop region  
55  
56 (typically by two hydrophobic alternating residues) (Fig. 4) (Hung *et al.*, 1996; MacIntyre *et al.*,  
57  
58 2001; Remaut *et al.*, 2006; Zavialov *et al.*, 2003, 2005; Zav'yalov *et al.*, 1995b);  
59  
60



1  
2 (2) FGL chaperones also contain a longer binding motif at the N-terminus with three alternating  
3 bulky hydrophobic residues than in FGS chaperones (two), which extends to A1 strand in FGL  
4 chaperones (at least 3 residues) (Chapman *et al.*, 1999; Remaut *et al.*, 2006; Zavialov *et al.*,  
5  
6  
7  
8  
9 2003, 2005; 2007).

10  
11 (3) In contrast to FGS chaperones, the massive subunit binding hairpin, F1 strand-loop-G1 strand  
12 of FGL chaperones is stabilized by a disulphide bridge between two conserved Cys-residues, one  
13 of which is localized in F1  $\beta$ -strand, and the other in G1  $\beta$ -strand (Figs 3 and 4; C98 and C137 in  
14 Caf1M and C98 and C125 in SafB) (Remaut *et al.*, 2006; Zavialov *et al.*, 2003, 2005).  
15  
16  
17  
18  
19

20  
21 Biochemical and mutagenesis studies showed that the unique structural features of FGL  
22 chaperones are crucial for function (see below).  
23  
24  
25

26 ***Importance of the disulphide bond in provision of FGL chaperone functions in vitro and***  
27 ***in vivo.*** Reduction of the disulphide bond and alkylation of the cysteine residues in a FGL  
28 chaperone considerably increase dissociation constant for Caf1M–Caf1 complex (Zav'yalov *et*  
29 *al.*, 1997). Later on, it was also showed that cysteine residues of FGL chaperone DraB form a  
30 disulfide bond and are crucial for the formation of the DraB–DraE binary complex (Piątek *et al.*,  
31  
32  
33  
34  
35  
36  
37  
38  
39  
40  
41  
42  
43  
44  
45  
46  
47  
48  
49  
50  
51  
52  
53  
54  
55  
56  
57  
58  
59  
60  
disulfide bond and are crucial for the formation of the DraB–DraE binary complex (Piątek *et al.*,  
2005). Probing the conformation and stability of Caf1M at different temperatures, pH, and  
concentration of urea by measurements of circular dichroism and fluorescence suggested that  
disulphide bond does not affect the general conformation, but induces changes in the local  
structure around the bond (Zav'yalov *et al.*, 1997). However, the level of expression of Caf1M in  
*E. coli* was clearly affected by disulphide isomerase DsbA. Caf1M accumulated in considerably  
larger quantities in DsbA<sup>+</sup> rather than in DsbA<sup>-</sup> strain, suggesting an important role of the  
disulphide bond in provision of Caf1M functions *in vivo* (MacIntyre *et al.*, 2001).

54  
55  
56  
57  
58  
59  
60  
***G1 and A1  $\beta$ -strands are crucial for chaperone function.*** The studies of MacIntyre *et al.*  
(2001) had highlighted the importance of G1  $\beta$ -strand hydrophobic residues in protecting newly  
secreted Caf1 from proteolytic degradation. This could be explained in part by the observed  
importance of some residues (F132) in stabilizing chaperone–subunit complex. The mutation,

1  
2 Caf1MV128A, which also resulted in subunit degradation, however, enhanced chaperone-  
3 subunit stability (communicated by A. Zavialov). Contrary to FGS chaperones, the A1  $\beta$ -strand  
4 of Caf1M also significantly adds to the binding contact in this region (Figs 3 and 6). Deletion of  
5 the sequence 10-15 of Caf1M in A1  $\beta$ -strand (communicated by A. Zavialov) led to complete  
6 loss of the chaperone function. Structure of the Caf1M–Caf1 complex suggests that the  
7 chaperone A1 and G1 strands are likely to form a binding platform, which is rigid enough to  
8 prevent collapse of the open subunit conformation in this very unstable region (Fig. 3).

9  
10  
11  
12  
13  
14  
15  
16  
17  
18  
19 ***Correlation between the length of FG loop and the number of different types of subunits***  
20 ***operated by a chaperone.*** Fig. 5 shows the plot of correlation between the number of deleted  
21 residues in a F1-G1 loop of chaperones (in comparison with the longest F1-G1 loop of the  
22 Caf1M chaperone) and the number of different types of subunits operating by the chaperones.  
23 These parameters show a strong correlation, but the slopes of the plots of correlation for FGL  
24 and FGS chaperones are different. That may be explained by an influence of the disulfide bond  
25 connecting F1 and G1 strands in FGLs. The coefficient of correlation for FGL chaperones is  
26 equal to 0.80 and for FGS chaperones it is equal to 0.72. The longer F1-G1 sequence creates a  
27 longer subunit recognition motif for a more specific binding of one or two subunits forming FGL  
28 chaperone-assembled fimbrial polyadhesins (Zavialov *et al.*, 2003, 2007). Probably, the shorter  
29 F1-G1 sequence in FGS chaperones was evolved as a consequence of a need in less specific  
30 binding of subunits because monoadhesive fimbriae/pili are composed of up to 7 different  
31 subunits.  
32  
33  
34  
35  
36  
37  
38  
39  
40  
41  
42  
43  
44  
45  
46  
47  
48  
49  
50

## 51 **Structure of Subunits and Molecular Architecture of Adhesive Organelles**

52  
53  
54  
55  
56 **3D structure of chaperone-complemented subunits.** Chaperone-free subunits of fimbrial  
57 polyadhesins (Zavialov *et al.*, 2005; Zav'yalov *et al.*, 1997) and mono-adhesive fimbriae/pili  
58 (Bann *et al.*, 2004; Nishiyama *et al.*, 2003) are highly unstable and prone to form aggregates.  
59  
60

1  
2 Hence, structural information on many subunits of these organelles was obtained by studying  
3  
4 chaperone-subunit complexes (Choudhury *et al.*, 1999; Remaut *et al.*, 2006; Sauer *et al.*, 1999,  
5  
6 2002; Verger *et al.*, 2007; Zavialov *et al.*, 2003, 2005).  
7  
8

9 The crystal structures of the type-1 pilus FimC–FimH (Choudhury *et al.*, 1999) and of the P  
10  
11 pilus PapD–PapK, PapD–PapE and PapD–PapA (Sauer *et al.*, 1999, 2002; Verger *et al.*, 2007)  
12  
13 chaperone–subunit complexes show that pilus subunits (pilins), like chaperones, have  
14  
15 immunoglobulin-like folds (Figs 3 and 6). However, the C-terminal (G)  $\beta$ -strand of the fold is  
16  
17 missing, creating a deep hydrophobic groove on the surface of the subunit (Figs 3 and 6).  
18  
19 Chaperones bind pilins by inserting their G1  $\beta$ -strand into this groove in a process called donor  
20  
21 strand complementation (Choudhury *et al.*, 1999; Sauer *et al.*, 1999, 2002; Verger *et al.*, 2007)  
22  
23 (Figs 3 and 6). Three hydrophobic side chains in the conserved G1 motif are inserted into the  
24  
25 hydrophobic acceptor groove and become an integral part of the subunit hydrophobic core.  
26  
27  
28  
29

30 The crystal structures of the Caf1M-Caf1 and SafB-SafA chaperone-subunit complexes  
31  
32 reveal the chaperone bound conformation of FGL chaperone-assembled polyadhesin subunits  
33  
34 (Remaut *et al.*, 2006; Zavialov *et al.*, 2003, 2005). As pilins, the polyadhesin subunits Caf1 and  
35  
36 SafA have an incomplete immunoglobulin-like fold (Figs 3 and 6). Despite the lack of  
37  
38 significant sequence similarity, polyadhesin subunits and pilins display similar organization of  
39  
40 the B, C, E, and F  $\beta$ -strands (Fig. 6a), which are known to form a common structural core of the  
41  
42 immunoglobulin-like fold (Bork *et al.*, 1994). However the  $\beta$ -strand A has different structures. In  
43  
44 pilins, the  $\beta$ -strand A starts hydrogen bonding to the  $\beta$ -strand B, participating in formation of  
45  
46 the ABED  $\beta$ -sheet, then it makes a switch in the middle and continues as part of the A'G1FC  $\beta$ -  
47  
48 sheet (Fig. 6a). In polyadhesin subunits the A  $\beta$ -strand either switches very late (in Caf1) or  
49  
50 becomes disordered (in SafA). A region between C and E  $\beta$ -strands shows a large structural  
51  
52 variability for both pilus and polyadhesin subunits (Fig. 6a). Pilins tend to have larger loop  
53  
54 between the  $\beta$ -strands D'' and E. Polyadhesin subunits have considerably longer sequences  
55  
56 which are involved in the region between the  $\beta$ -strands C and D''. This region is clearly more  
57  
58  
59  
60

1  
2 structurally variable in polyadhesin subunits than in pilins and potentially it might participate in  
3  
4 formation of binding sites and organelle-specific epitopes (see the chapter “Binding of FGL  
5  
6 chaperone-assembled polyadhesins to host cell receptors”).  
7

8  
9 The major differences between the two classes of subunits and corresponding chaperones are  
10  
11 found in the chaperone-subunit interactive area. Fig. 3 shows ribbon diagrams of the PapD–PapA  
12  
13 (Verger *et al.*, 2007), SafB–SafA (Remaut *et al.*, 2006) and Caf1M–Caf1 (Zavialov *et al.*, 2003,  
14  
15 2005) complexes. The end of the F1-G1 loop and the beginning of G1  $\beta$ -strand in PapD harbour  
16  
17 a four-residue subunit binding motif of one small hydrophilic (N101) and three alternating bulky  
18  
19 hydrophobic residues (L107, I105 and L103) (Verger *et al.*, 2007). The same region in SafB  
20  
21 molecule harbours a similar five-residue motif of one small hydrophobic (A114) and four bulky  
22  
23 hydrophobic residues (L116, L118, L120, and I122) (Remaut *et al.*, 2006). The end of F1-G1  
24  
25 loop and the beginning of G1  $\beta$ -strand in Caf1M harbour a subunit binding motif of five  
26  
27 alternating bulky hydrophobic residues (V126, V128, V130, F132, and I134) (Zavialov *et al.*,  
28  
29 2003, 2005). The rest of F1-G1 loop (residues 96-102 in PapD, 104-113 in SafB and 104-123 in  
30  
31 Caf1M) is disordered in the crystal structures. Another subunit binding motif in FGL chaperones  
32  
33 of three alternating hydrophobic residues (Y12 in Caf1M/F12 in SafB, V14, and I16) is localized  
34  
35 in a long N-terminal sequence, which forms A1 strand. A1 and G1  $\beta$ -strands are the edge strands  
36  
37 of the  $\beta$ -sandwich fold of the N-terminal domain. In the complex A1 and G1  $\beta$ -strands are  
38  
39 extended due to the partial ordering of the N-terminal sequence and F1-G1 loop, respectively, to  
40  
41 form a binding platform, exposing the hydrophobic residues of the binding motifs. In addition to  
42  
43 this binding structure, PapD, Caf1M and SafB chaperones apply a pair of conserved positively  
44  
45 charged residues (R8 and K112 in PapD, R20 and K127 in SafB, R20 and K139 in Caf1M) to  
46  
47 bind subunits by anchoring their C-terminal carboxyl groups.  
48  
49  
50  
51  
52  
53  
54  
55

56  
57 Fig. 6a illustrates how Caf1 subunit is complemented by Caf1M chaperone (Zavialov *et al.*,  
58  
59 2003, 2005). The absence of the 7th (G) strand results in a 6-stranded  $\beta$ -sandwich where the  
60  
hydrophobic core of Caf1 is partially exposed in a long and deep hydrophobic groove. Caf1

1  
2 interacts mainly with N-terminal domain in Caf1M (Fig. 3). These two proteins bind via edge  
3  
4 strands in Caf1 and in the N-terminal domain of Caf1M to form closed barrel with a common  
5  
6 core (Zavialov *et al.*, 2003). Strand G1 in Caf1M is hydrogen bonded to strand F in Caf1.  
7  
8 Chaperone A1 strand is hydrogen bonded to subunit strand A. As in FGS chaperone–pilin  
9  
10 complexes (Choudhury *et al.*, 1999; Sauer *et al.*, 1999, 2002; Verger *et al.*, 2007), hydrophobic  
11  
12 residues from Caf1M chaperone G1 strand are donated to Caf1 subunit to compensate for the  
13  
14 missing G strand (Figs 3 and 6). The longer G1 donor strand of the Caf1M chaperone inserts  
15  
16 motif of five bulky hydrophobic residues (P1 to P5 residues; see Figs 3 and 4) into five binding  
17  
18 pockets in the hydrophobic groove of the Caf1 subunit (P1 to P5 binding pockets). As a result,  
19  
20 the acceptor groove of Caf1 subunit is significantly longer than in the pilus subunits (Fig. 6a).  
21  
22 The longer A1 strand in Caf1M also interacts more extensively with the subunit than the A1  
23  
24 strand in FGS chaperone–pilin complexes.  
25  
26  
27  
28  
29

30 The crystal structure of the SafB–SafA complex also shows a considerably larger interactive  
31  
32 area between the chaperone and subunit than that in the FGS chaperone–pilin complexes (Fig. 3).  
33  
34 As in the Caf1M–Caf1 complex, this is a result from the presence of a more extended  
35  
36 hydrophobic groove in the SafA subunit than in pilus subunits, which is complemented by  
37  
38 subunit binding motifs of SafB containing the additional FGL specific sequences. However, the  
39  
40 major F1–G1–loop–G1  $\beta$ -strand binding motif of SafB contains four rather than five bulky  
41  
42 hydrophobic residues (L116, L118, L120, and I122), interacting with the hydrophobic P4–P1  
43  
44 pockets of the subunit's groove. The fifth donor residue inserting to the pocket P5 is a small  
45  
46 A114. It was observed two crystal forms of the SafB–SafA complex that differ in the extent of  
47  
48 ordering around A114 (Fig. 3) (Remaut *et al.*, 2006). In type I crystals, A114 is ordered and is  
49  
50 inserted into the P5 pocket of the SafA subunit (Fig. 3). In type II crystals this residue is  
51  
52 disordered and does not insert into the P5 pocket (Fig. 3). As a result, the loops and secondary  
53  
54 structure elements in the SafA subunit that form this P5 pocket are also disordered and are not  
55  
56 observed in the electron density map. These two structures suggest equilibrium between the two  
57  
58  
59  
60

1  
2 states of the SafB–SafA complex as a result of a weak binding of chaperone G1 donor strand at  
3  
4 P5 site of the SafA binding groove (Remaut *et al.*, 2006).  
5

6  
7 **3D structure of fiber subunits.** Elucidation of the crystal structure of *Y. pestis* F1 minimal  
8  
9 fiber Caf1M–Caf1'–Caf1'' (ternary complex) made an important step in understanding general  
10  
11 principles of subunit assembly via the chaperone/usher pathway, revealing the fiber  
12  
13 conformation of the organelle subunit (Caf1'') and subunit-subunit interactions in fibers  
14  
15 (Zavialov *et al.*, 2003, 2005). The structure of Caf1M and the chaperone-bound Caf1' subunit is  
16  
17 virtually the same as in the Caf1M–Caf1 binary pre-assembling complex. However, in contrast  
18  
19 to the disordered N-terminal region of Caf1 in binary complex, the N-terminal region of Caf1' is  
20  
21 ordered and forms an antiparallel donor  $\beta$ -strand interaction with the last (F)  $\beta$ -strand of the  
22  
23 chaperone free Caf1'' subunit (Fig. 6b). The donated strand produces a bona fide  
24  
25 immunoglobulin-like topology in the fibre subunit. The N-terminal donor strand was denoted as  
26  
27 “Gd” (d for donor) because it plays in the fibre the same structural role as the (C-terminal) G  
28  
29 strand of the canonical immunoglobulin fold (Zavialov *et al.*, 2003). Thus, the release of the  
30  
31 subunit from the chaperone-subunit complex and its incorporation into a growing fiber involves  
32  
33 an exchange of G1 and A1 donor strands of the chaperone to Gd strand of the neighboring  
34  
35 subunit in the fiber. The replacement of G1 strand by Gd strand also involves the change of  
36  
37 direction of the donor strand from parallel to anti-parallel to F  $\beta$ -strand of the subunit. This  
38  
39 process was predicted earlier for FGS chaperone-assembled adhesive pili (Choudhury *et al.*,  
40  
41 1999; Sauer *et al.*, 1999) and for FGL chaperone-assembled polyadhesins (Zavialov *et al.*, 2002)  
42  
43 and was termed “donor strand exchange”. A similar “topological transition” (Sauer *et al.*, 2002)  
44  
45 was also observed for the P pilus subunit PapE bound to a peptide designed to have sequence of  
46  
47 the proposed donor strand of the PapK subunit, suggesting that the donor strand exchange takes  
48  
49 place during assembly of both types of organelles.  
50  
51  
52  
53  
54  
55  
56  
57  
58

59  
60 Recently, the structure of a ternary complex of PapD bound to PapA (through donor–strand  
complementation) was solved (Verger *et al.*, 2007). The structure of this complex is shown in



1  
2 Fig. 6b. The structure provides a snapshot of PapA before and after donor strand exchange.  
3  
4 PapD–PapA'–PapA'' complex is similar to the one obtained for the Caf system (Zavialov *et al.*,  
5  
6 2003, 2005). The core sheet structure of donor strand-exchanged PapA is in a closer  
7  
8 conformation than that of donor strand complemented PapA, as the  $\beta$ -strands on each side of the  
9  
10 groove of donor strand exchanged PapA are nearer to each other. Also, the “63–74” loop is  
11  
12 ordered in donor strand exchanged PapA and not in donor strand complemented PapA, as this  
13  
14 molecule is missing residues 70 to 73 in this region.  
15  
16  
17

18  
19 High resolution structures of several other subunits of fimbrial polyadhesins AfaE/DraE,  
20  
21 DaaE and SafA have been determined (Anderson *et al.*, 2004a, b; Korotkova *et al.*, 2006b;  
22  
23 Pettigrew *et al.*, 2004; Remaut *et al.*, 2006). Artificially engineered constructs were made to  
24  
25 facilitate the structure determination in each of these studies. Structural information on the DaaE  
26  
27 and AfaE/DraE subunits was obtained by structure determination of cytoplasm-assembled  
28  
29 trimers of these subunits (Anderson *et al.*, 2004a; Korotkova *et al.*, 2006b; Pettigrew *et al.*, 2004;  
30  
31 Remaut *et al.*, 2006). The crystal structures revealed that the trimers are connected together by  $\beta$ -  
32  
33 strand swapping mechanism. Although non-native, the  $\beta$ -strand swapping is similar to the donor  
34  
35 strand complementation. A different approach was chosen to determine an NMR structure of a  
36  
37 circularly permuted self-complemented AfaE subunit (Anderson *et al.*, 2004b). This construct  
38  
39 contains the donor sequence fused at the C-terminus, rather than at N-terminus, which allows  
40  
41 insertion of this self-complementing Gd strand in the acceptor groove, restoring classical  
42  
43 immunoglobulin-like fold. To determine structure of the fiber form of the SafA subunit, the  
44  
45 group of Gabriel Waksman (Remaut *et al.*, 2006) employed the same technique, which they used  
46  
47 earlier for structure determination of PapE (Sauer *et al.*, 2002). SafA was co-crystallized with a  
48  
49 peptide corresponding to the N-terminal sequence, which was predicted to form to the donor  
50  
51 strand. Biological relevance of the constructs used by (Anderson *et al.*, 2004b; Remaut *et al.*,  
52  
53 2006) in their structural studies rely on the correctness of the prediction of the donor sequence,  
54  
55 which is not easy to prove. Hence, these structures potentially may contain errors. The self-  
56  
57  
58  
59  
60



1  
2 complemented AfaE (Anderson *et al.*, 2004b) has slightly distorted structure at the beginning of  
3  
4 the donor strand, which makes it dissimilar to Caf1 and SafA subunits (authors' observation).  
5  
6 Comparison with the crystal structure of the cytoplasm assembled trimers of the same subunit  
7  
8 suggests that this could be a result of changes introduced by the artificially engineered linker  
9  
10 connecting the donor strand to the C-terminus of the subunit. Nevertheless, all these structures  
11  
12 show a similar incomplete immunoglobulin-like fold for the subunits and suggest that subunit-  
13  
14 subunit interactions in polyadhesins fibers involve N-terminal Gd donor-strand  
15  
16 complementation.  
17  
18  
19

20  
21 The Caf1 polyadhesin subunit (Zavialov *et al.*, 2003, 2005) has a longer acceptor groove,  
22  
23 which accommodates longer Gd donor strand than the P pilus subunit PapA (Verger *et al.*,  
24  
25 2007) (Fig. 6b). This is in agreement with the observation of a more extended contact area  
26  
27 between FGL chaperone and polyadhesin subunit in structures of Caf1M–Caf1 and SafB–SafA  
28  
29 complexes than that between FGS chaperone and pilus subunit in structures of FimC–FimH,  
30  
31 PapD–PapK, PapD–PapE and PapD–PapA complexes (Choudhury *et al.*, 1999; Sauer *et al.*,  
32  
33 1999, 2002; Verger *et al.*, 2007; Zavialov *et al.*, 2003, 2005).  
34  
35  
36

37  
38 **Chaperone preserves folding energy of subunit for driving fiber assembly.** No energy  
39  
40 input from external sources is required to convert periplasmic chaperone–subunit pre-assembly  
41  
42 complexes to free chaperone and secreted fibers (Jacob-Dubuisson *et al.*, 1994), in spite of a  
43  
44 much more extensive interface between chaperone and subunit than between fiber subunits  
45  
46 (Zavialov *et al.*, 2003). Some clues as to how the process can be energetically driven have been  
47  
48 provided by structural studies (Sauer *et al.*, 2002; Verger *et al.*, 2007; Zavialov *et al.*, 2003,  
49  
50 2005). Comparison of chaperone complemented (Caf1') with fiber subunit (Caf1'') revealed a  
51  
52 large conformational difference (Zavialov *et al.*, 2003, 2005). The fiber conformation was  
53  
54 referred to as the “closed” or “condensed” conformation (Zavialov *et al.*, 2005). The observed  
55  
56 difference between open and closed conformations, involving a rearrangement and condensation  
57  
58 of the subunit hydrophobic core, suggested that periplasmic chaperones might trap subunits in a  
59  
60

1 high-energy molten globule-like folding-intermediate state (Zavialov *et al.*, 2003). A model was  
2 proposed in which release of the subunit followed by Gd donor strand complementation allows  
3 folding to be completed, driving fiber formation (Zavialov *et al.*, 2003). In contrast to the bulky  
4 hydrophobic donor residues in the chaperone G1 donor strand, much smaller donor residues in  
5 the subunit N-terminal Gd donor segment do not intercalate between the two sheets of the  
6 subunit  $\beta$ -sandwich, allowing close contact between the two sheets (Zavialov *et al.*, 2003, 2005).  
7  
8  
9  
10  
11  
12  
13  
14  
15

16 A significant stabilizing contribution from the final fine packing of the subunit hydrophobic  
17 core is suggested by the melting of the native ternary complex. The structurally observed  
18 complete collapse of the Gd complemented fiber Caf1" subunit results in a dramatic increase in  
19 the enthalpy and transition temperature for the melting of the fiber module. The thermodynamic  
20 studies provide strong evidence for the hypothesis that collapse of the subunit hydrophobic core  
21 shifts the equilibrium towards fiber formation (Zavialov *et al.*, 2005).  
22  
23  
24  
25  
26  
27  
28  
29

30 **Zip-in-zip-out mechanism of the donor strand exchange.** Zavialov *et al.* (2003) proposed  
31 a model for the usher-catalyzed fiber assembly involving a sequential concerted donor strand  
32 exchange in which G1 is gradually replaced by Gd with a zip-in-zip-out mechanism. Remaut *et*  
33 *al.* (2006) using real-time electrospray ionization mass spectrometry detected a transient ternary  
34 complex between the chaperone-subunit complex and a peptide mimicking the donor strand of  
35 the subunit, providing an experimental support to the hypothesis. Exchange of the donor strand  
36 of the chaperone to the peptide was highly dependent on the interactions at the P5 pocket of the  
37 subunit (Fig. 7). This site may recruit the incoming subunit donor strand. Indeed, the observation  
38 of two crystal forms with SafB–SafA complex (Fig. 3) (Remaut *et al.*, 2006) suggests that the  
39 acceptor cleft of SafA subunit could be easily uncapped at this site, providing a starting point for  
40 the donor strand exchange.  
41  
42  
43  
44  
45  
46  
47  
48  
49  
50  
51  
52  
53  
54  
55

56 Recently, Verger *et al.* (2008) solved the structure of the PapD: PapF complex in order to  
57 understand why PapF undergoes slow donor strand exchange. The structure reveals that the PapF  
58 P5 pocket is partially obstructed. Molecular dynamics simulations show that this region of PapF  
59  
60

1  
2 is flexible compared with its equivalent in PapH, a subunit that also has an obstructed P5 pocket  
3  
4 and is unable to undergo donor strand exchange. Using electro spray-ionization mass  
5  
6 spectrometry, Verger *et al.* (2008) showed that mutations in the P5 region result in increased  
7  
8 donor strand exchange rates. Thus, the partial obstruction of the P5 pocket serves as a  
9  
10 modulating mechanism of donor strand exchange.  
11  
12

13  
14 Rose *et al.* (2008) used molecular dynamics simulations to probe the donor strand exchange  
15  
16 mechanism during formation of the Saf pilus from *S. enterica* at the atomic level, allowing the  
17  
18 direct investigation of the zip-in–zip-out hypothesis. The simulations provide an explanation of  
19  
20 how the incoming Gd is able to dock and initiate donor strand exchange due to inherent dynamic  
21  
22 fluctuations within the chaperone–subunit complex. In the simulations, the chaperone donor  
23  
24 strand was seen to unbind from the pilus subunit, residue by residue, in direct support of the zip-  
25  
26 in–zip-out hypothesis. In addition, an interaction of a residue towards the N-terminus of the Gd  
27  
28 with a specific binding pocket on the adjacent pilus subunit was seen to stabilise the donor strand  
29  
30 exchange product against unbinding, which also proceeded in the simulations by a zippering  
31  
32 mechanism. The study provides an in-depth picture of donor strand exchange, including the first  
33  
34 atomistic insights into the molecular events occurring during the zip-in–zip-out mechanism. Fig.  
35  
36 7 schematically presents the donor strand exchange mechanism *in vivo* based on the  
37  
38 experimental data obtained *in vitro* by Remaut *et al.* (2006).  
39  
40  
41  
42  
43

44  
45 Zavialov *et al.* (2005) and Vitagliano *et al.* (2008) reported molecular dynamics  
46  
47 characterizations of *Y. pestis* Caf1 subunit in its monomeric-unbound and dimeric states. Data on  
48  
49 properties of the monomeric form show that it is highly reactive and tends to evolve toward  
50  
51 compact states, which likely hamper subunit–subunit association. The chaperone release and  
52  
53 subunit–subunit association evidently take place concerted.  
54  
55

56  
57 **Molecular architecture of adhesive organelles.** The final architecture and morphology of  
58  
59 linear fibres depend on subunit composition and mode of subunit–subunit interactions. These  
60  
factors determine the coiling of secreted linear fibres into different structures such as FGS

1  
2 chaperone-assembled thick rigid mono-adhesive pili with a diameter of 7-8 nm (Fig. 8a),  
3  
4 reviewed in Knight *et al.* (2000); Sauer *et al.* (2000, 2004); Soto & Hultgren (1999) and Thanassi  
5  
6 *et al.* (1998), FGS chaperone-assembled thin flexible hetero-polyadhesins with a diameter 2-4  
7  
8 nm (Fig. 8b), reviewed in van den Broeck *et al.* (2000), FGS chaperone-assembled homo-  
9  
10 polyadhesins with a diameter about 2 nm (Fig. 8c) (Chessa *et al.*, 2008) and FGL chaperone-  
11  
12 assembled polyadhesins with a diameter about 2 nm (Fig. 8d) (Zavialov *et al.*, 2007). The latter  
13  
14 polyadhesins can aggregate to form amorphous masses or capsules, e.g. the F1 capsular antigen  
15  
16 (Chen & Elberg, 1977), nonfimbrial adhesin I (NFA-I) (Ahrens *et al.*, 1993), NFA-I-like, Dr-II  
17  
18 (Pham *et al.*, 1997), or afimbrial adhesins, III, VII, and VIII (Jouve *et al.*, 1997; Lalioui *et al.*,  
19  
20 1999).

21  
22  
23  
24  
25  
26 In the case of FGS chaperone-assembled mono-adhesive fimbriae/pili, the specialized  
27  
28 adhesive subunit always occurs at the tip of fimbriae, either as the distal end of thin (~2.5 nm)  
29  
30 and flexible fimbriae (e.g. F17G from F17 fimbriae), or at the edge of a thin (~2.5 nm) tip  
31  
32 fibrillum that is stuck onto a relatively rigid, 1–2 μm long and ~7.5 nm wide right-handed  
33  
34 helical pilus rod (e.g. PapG of P pili and FimH of type 1 pili) (Fig. 8a) (de Greve *et al.*, 2007).  
35  
36 This specialized subunit is called as adhesin.  
37  
38

39  
40 All adhesive subunits of mono-adhesive fimbriae/pili are two-domain adhesins (Choudhury  
41  
42 *et al.*, 1999; Bouckaert *et al.*, 2005, 2006; de Greve *et al.*, 2007; Li *et al.*, 2007; Westerlund-  
43  
44 Wikström & Korhonen, 2005). A two-domain adhesin consists of N-terminal receptor-binding  
45  
46 domain that can be stably expressed on its own, and a rather conserved C-terminal pilin domain.  
47  
48 Both domains have an immunoglobulin-like fold and are joined via a short interdomain linker.  
49  
50 The few known crystal structures of tip-located receptor-binding N-terminal adhesin domains of  
51  
52 mono-adhesive fimbriae/pili, PapGII, FimH, F17G/GafD, show that, despite little or no sequence  
53  
54 identity, common to them all is an elongated beta-barrel jelly roll fold that contains the receptor-  
55  
56 binding groove (Fig. 9) (Choudhury *et al.*, 1999; Bouckaert *et al.*, 2005, 2006; de Greve *et al.*,  
57  
58 2007; Li *et al.*, 2007; Westerlund-Wikström & Korhonen, 2005). The adhesin domains differ in  
59  
60

1  
2 disulfide patterns, in size and location of the ligand-binding groove, as well as in mechanism of  
3  
4 receptor binding. In particular, their glycan-binding sites have evolved in different locations onto  
5  
6 this similar scaffold, and with distinct, highly specific binding properties.  
7  
8

9 Subunits of mono-adhesive fimbriae are called as pilins. In particular, P fimbriae are  
10  
11 composed of ~1000 copies of the major subunit protein, PapA, which polymerize to form a rigid  
12  
13 stalk connected to a flexible tip consisting of limited copies of the minor subunit proteins, PapE  
14  
15 and PapF, and receptor-binding adhesin, PapG, at the distal end (Kuehn *et al.*, 1992; Lindberg *et*  
16  
17 *al.*, 1987). Type 1 pili is composed of up to 3000 copies of the subunit FimA, which form a stiff,  
18  
19 helical pilus rod, and subunits FimF, FimG, and FimH, which form the linear tip fibrillum. All  
20  
21 subunits in the pilus interact via the donor strand complementation, in which the incomplete  
22  
23 immunoglobulin-like fold of each subunit is complemented by insertion of an N-terminal  
24  
25 extension from the following subunit. Gossert *et al.* (2007) determined the NMR structure of a  
26  
27 monomeric, self-complemented variant of FimF, FimFF, which has a second FimF donor strand  
28  
29 segment fused to its C-terminus that enables intramolecular complementation of the FimF fold.  
30  
31 NMR studies on bimolecular complexes between FimFF and donor strand-depleted variants of  
32  
33 FimF and FimG support for the intrinsic flexibility of the tip fibrillum and that this flexibility  
34  
35 would significantly increase the probability that the adhesin at the distal end of the fibrillum  
36  
37 successfully targets host cell receptors. To understand whether the mechanical properties of the  
38  
39 fimbrial rod regulate the stability of the FimH–mannose bond, Forero *et al.* (2006) pulled the  
40  
41 fimbriae via a mannosylated tip of an atomic force microscope. Individual fimbriae rapidly  
42  
43 elongate for up to 10  $\mu\text{m}$  at forces above 60 pN and rapidly contract again at forces below 25 pN.  
44  
45 At intermediate forces, fimbriae change length more slowly, and discrete  $5.0 \pm 0.3$ -nm changes in  
46  
47 length can be observed, consistent with uncoiling and coiling of the helical quaternary structure  
48  
49 of one FimA subunit at a time. The force range at which fimbriae are relatively stable in length is  
50  
51 the same as the optimal force range at which FimH–mannose bonds live longest. Higher or lower  
52  
53 forces, which cause shorter bond lifetimes, cause rapid length changes in the fimbria that help  
54  
55  
56  
57  
58  
59  
60

1  
2 maintain force at the optimal range for sustaining the FimH–mannose interaction. The  
3  
4 modulation of force and the rate at which it is transmitted from the bacterial cell to the adhesive  
5  
6 catch bond present a novel physiological role for the fimbrial rod in bacterial host cell adhesion.  
7  
8 This suggests that the mechanical properties of the fimbrial shaft have co-developed to optimize  
9  
10 the stability of the terminal adhesion under flow.  
11  
12

13  
14 In the case of FGL chaperone-assembled polyadhesins, all subunits may possess two  
15  
16 independent binding sites specific to different host cell receptors (Fig. 9; Anderson *et al.*,  
17  
18 2004a,b; Korotkova *et al.*, 2006a,b, 2008; Pettigrew *et al.*, 2004). Dimensions of the bacterial  
19  
20 poly-adhesive fibres Dr, assembling of which is assisted with FGL chaperone, were investigated  
21  
22 with negative-stain electron microscopy (Anderson *et al.*, 2004a). Thin flexible fibers (2 nm  
23  
24 diameter) were observed. The results are entirely consistent with the model with end-to-end  
25  
26 contact between each subunit (Fig. 9) (Anderson *et al.*, 2004a) and are reminiscent of the model  
27  
28 of capsular F1 antigen from *Y. pestis*, Caf1 (Zavialov *et al.*, 2003). Similar thin fibres have been  
29  
30 observed for pH6 antigen (Lindler & Tall, 1993). In addition to the predominance of thin fibers  
31  
32 Dr, the electron microscopy also revealed thicker morphology with overall dimensions larger  
33  
34 than the linear model suggested (Anderson *et al.*, 2004a). Thick fibers are not consistent with  
35  
36 end-to-end contact and imply that more extensive intersubunit interactions also exist. This would  
37  
38 rigidify the resulting rod by the tighter coiling of a single fiber or formation of a trimeric coiled-  
39  
40 coil arrangement of fibers.  
41  
42  
43  
44  
45

46  
47 Recently Runco *et al.* (2008) examined the ultrastructure of the *Y. pestis* capsule with whole  
48  
49 bacteria and negative-stain transmission electron microscopy. Bacteria were grown to  
50  
51 logarithmic phase at 37°C, pH 7.4. The appearance of the capsule was more clearly visible than  
52  
53 reported in previous studies, in which the capsule generally appeared as an amorphous haze or  
54  
55 dense mass surrounding the bacteria (Chen & Elberg, 1977; Du *et al.*, 2002; Liu *et al.*, 2006).  
56  
57 The *Y. pestis* KIM6<sup>+</sup> strain consistently produced an extended halo composed of thin fibrils and  
58  
59 denser aggregates. This denser capsular material, likely composed of aggregates of the thin  
60

1  
2 fibrils, sometimes extended out from the bacterial surface in long strands. The thin, fibrillar  
3  
4 appearance of the F1 capsule resembles structures previously reported for other members of the  
5  
6 FGL family of chaperone/usher pathways, including the pH6 antigen of *Yersinia* (Iriarte *et al.*,  
7  
8 1993; Lindler & Tall, 1993), and the CS3 and CS6 pili of enterotoxigenic *E. coli* (Knutton *et al.*,  
9  
10 1989; Levine *et al.*, 1984). This supports a common structure and assembly mechanism for  
11  
12 members of the FGL family.  
13  
14

15  
16 Salih *et al.* (2008) used negative-stain electron microscopy and single-particle image analysis  
17  
18 to determine the three-dimensional structure of the *S. typhimurium* Saf polyadhesin. Saf  
19  
20 polyadhesin comprises of highly flexible linear multi-subunit fibers that are formed by globular  
21  
22 subunits connected to each other by short links giving a “beads on a string”-like appearance.  
23  
24 Quantitative fitting of the atomic structure of the SafA polyadhesin subunit into the electron  
25  
26 density maps, in combination with linker modelling and energy minimization, has enabled  
27  
28 analysis of subunit arrangement and intersubunit interactions in the Saf polyadhesin. Short  
29  
30 intersubunit linker regions provide means for flexibility of the Saf polyadhesin by acting as  
31  
32 molecular hinges allowing a large range of movement between consecutive subunits in the fibre.  
33  
34  
35  
36  
37  
38  
39

### 40 Structure of Outer Membrane Molecular Usher Proteins

41  
42  
43  
44  
45 **3D structure of outer membrane molecular usher protein.** Recently, the 3.4 Å crystal  
46  
47 structure of the 130-640 amino acid fragment of the PapC usher was solved. The results help to  
48  
49 understand adhesive fiber biogenesis at the outer membrane (Fronzes *et al.*, 2008; Remaut *et al.*,  
50  
51 2008). It encompasses the full translocation pore consisting of a kidney-shaped, 24-stranded β-  
52  
53 barrel (residues 146–635), 45 Å in height and with outer and inner dimensions of 65 - 45 Å and  
54  
55 45 - 25 Å, respectively (Figs 10a and b). The β-barrel closes in an end-to-end fashion and  
56  
57 positions the N- and C-termini on the periplasmic side of the outer membrane. The N- and C-  
58  
59 terminal globular domains will thus be juxtaposed and reside in the periplasm, consistent with  
60



1  
2 their role in chaperone-subunit recruitment and adhesin-induced pore activation (Ng *et al.*, 2004;  
3  
4 Nishiyama *et al.*, 2003; Saulino *et al.*, 1998; Thanassi *et al.*, 2002). The predicted middle domain  
5  
6 (residues 257–332) (Capitani *et al.* 2006) is formed by a long sequence between strands  $\beta 6$  and  
7  
8  $\beta 7$  and consists of a six-stranded,  $\beta$  sandwich fold (strands  $\beta A$ – $\beta F$ ). The domain is positioned  
9  
10 laterally inside the  $\beta$ -barrel pore (Figs 10a and b). As a result, the middle domain, referred to as  
11  
12 the plug domain, completely occludes the luminal volume of the translocation pore, preventing  
13  
14 passage of solutes or periplasmic proteins across the channel in its non-activated form. The PapC  
15  
16 plug domain is inserted into the loop connecting two  $\beta$  strands (strands 6 and 7). The plug  
17  
18 domain is held in place by a  $\beta$ -hairpin (strands  $\beta 5$  and  $\beta 6$ , hereafter referred to as the  $\beta 5$ -6  
19  
20 hairpin) that is folded in from the barrel wall into the channel lumen. The inward curvature of the  
21  
22  $\beta 5$ -6 hairpin creates a large gap in the side of the  $\beta$ -barrel extending well into the part submerged  
23  
24 in the outer membrane bilayer (Figs 10a and b). The luminal part of the  $\beta 5$ -6 hairpin is capped  
25  
26 from the extracellular side by the only helix in the structure, the  $\alpha 1$  helix (residues 448–465).  
27  
28 Inside the  $\beta$ -barrel, the  $\beta 5$ -6 hairpin interacts with the inner surface of the channel and helix  $\alpha 1$   
29  
30 through a patch of hydrophobic interactions. In addition, the  $\beta 5$ -6 hairpin forms two electrostatic  
31  
32 interaction networks that bridge the plug domain with the channel wall and  $\alpha 1$  helix and help  
33  
34 position the plug domain laterally inside the translocation channel (Figs 10a and b).  
35  
36  
37  
38  
39  
40  
41

42 **Mechanism of channel gating.** In its non-activated form, the PapC channel is obstructed by  
43  
44 the plug domain (Figs 2 and 10). Therefore, the adhesive subunit-induced activation of the usher  
45  
46 (Saulino *et al.*, 1998) must include the displacement of the plug domain from the translocation  
47  
48 channel. A rotation of the plug domain out of the pore lumen and into the periplasm would create  
49  
50 a channel of  $37\text{\AA} \times 25\text{\AA}$  or  $45\text{\AA} \times 25\text{\AA}$  when the  $\beta 5$ -6 hairpin and  $\alpha 1$  helix are displaced from the  
51  
52 channel as well (Fig. 2, position P'). Alternatively, a conformational change in the  $\beta 5$ -6 hairpin  
53  
54 and  $\alpha 1$  helix could allow an upward rotation of the plug domain inside the pore, thereby  
55  
56 liberating a translocation channel of approximately  $27\text{\AA} \times 25\text{\AA}$  (Fig. 2, position P''). Outer  
57  
58 membrane ushers function independently of a hydrolyzable energy source or a proton gradient  
59  
60

1  
2 (Jacob-Dubuisson *et al.*, 1994). Gating of the plug domain in the usher therefore relies solely on  
3  
4 conformational changes induced by the binding of the chaperone-adhesin complex. Powering the  
5  
6 large conformational rotation of the plug domain must therefore come from the energy  
7  
8 emanating from the binding of the chaperone-adhesive subunit complex and/or must be stored as  
9  
10 structural strains in the non-activated PapC channel. One such area of apparent structural strain is  
11  
12 seen in the  $\beta$ 5-6 hairpin that breaks out of the  $\beta$ -barrel lining. The exposed part of the adjacent  
13  
14 strand  $\beta$ 4 represents a large open-edged  $\beta$  sheet structure. Such exposed edges form highly  
15  
16 aggregative surfaces for the edge-to-edge docking of  $\beta$  strands or  $\beta$  sheets (Richardson &  
17  
18 Richardson, 2002). As part of the activation process, the  $\beta$ 5-6 hairpin could line up with  $\beta$ 4 into  
19  
20 the barrel wall. This would break the interaction with the plug domain and allow its upward  
21  
22 rotation or displacement out of the barrel lumen. Another area of structural strain could reside in  
23  
24 the interaction of the plug domain with the barrel lumen, which includes a number of like-charge  
25  
26 residues. It seems plausible that during activation, these repulsive forces will aid in expelling the  
27  
28 plug domain from the barrel lumen.  
29  
30  
31  
32  
33

34  
35 **Comparison of isolated Caf1A plug domain with the structure of the corresponding**  
36  
37 **domain of PapC usher.** Yu *et al.* (2009) reported isolation and structural-functional  
38  
39 characterization of the plug domain of Caf1A usher from *Y. pestis*. The isolated Caf1A plug  
40  
41 domain is a highly soluble monomeric protein capable of autonomous folding. A 2.8 Å  
42  
43 resolution crystal structure of the Caf1A plug domain reveals that this domain has an  
44  
45 immunoglobulin-like fold similar to that of donor strand complemented Caf1 fibre subunit.  
46  
47 Moreover these proteins display significant structural similarity. Although the Caf1A plug  
48  
49 domain is in the middle of the predicted amphipathic  $\beta$ -barrel of Caf1A, the usher is still  
50  
51 assembled in the membrane in the absence of this domain. The Caf1A plug domain does not bind  
52  
53 Caf1M-Caf1 complexes, but its presence shows to be essential for Caf1-fibre secretion. The  
54  
55 study suggests that Caf1A plug domain may play the role of a subunit-substituting protein  
56  
57 (dummy subunit), plugging or priming secretion through the channel in the Caf1A usher.  
58  
59  
60

1  
2 Comparison of isolated Caf1A plug domain with the structure of the corresponding domain of  
3  
4 PapC usher (Fig. 10c) shows a high similarity of the core structures suggesting a universal  
5  
6 adaptation of FGL and FGS chaperone/usher pathways for the secretion of different types of  
7  
8 fibres.  
9

### 10 11 12 13 14 **Mechanism of Function of Chaperone/Usher Machinery** 15 16 17

#### 18 19 **N-terminal periplasmic domain of the usher protein binds chaperone-subunit complex.**

20 Nishiyama *et al.* (2003) identified N-terminal periplasmic domain of FimD usher protein  
21  
22 (FimD<sub>N</sub>) comprising the N-terminal 139 residues of mature FimD. Purified FimD<sub>N</sub> usher domain  
23  
24 is a monomeric, soluble protein that specifically recognizes complexes between FimC chaperone  
25  
26 and individual Type 1 pilus subunits, but does not bind the isolated FimC chaperone, or isolated  
27  
28 subunits. In addition, FimD<sub>N</sub> usher domain retains the ability of FimD usher protein to recognize  
29  
30 different chaperone-subunit complexes with different affinities, and has the highest affinity  
31  
32 towards the chaperone FimC–FimH adhesion complex. Overexpression of FimD<sub>N</sub> usher domain  
33  
34 in the periplasm of wild-type *E. coli* cells diminished incorporation of FimH adhesion at the tip  
35  
36 of Type 1 pili, while pilus assembly itself was not affected. Nishiyama *et al.* (2003) reported  
37  
38 nuclear magnetic resonance and X-ray protein structures of the FimD<sub>N</sub> usher domain before and  
39  
40 after binding of a chaperone FimC–FimH<sub>P</sub> pilin domain complex. FimD<sub>N</sub> usher domain consists  
41  
42 of a flexible N-terminal segment of 24 residues (N-terminal "tail"), a structured core with a novel  
43  
44 fold, and a C-terminal hinge segment (Fig. 11). In the ternary complex, residues 1–24 of FimD<sub>N</sub>  
45  
46 usher domain specifically interact with both FimC chaperone and the FimH<sub>P</sub> pilin domain. The  
47  
48 structures of FimC chaperone and FimH<sub>P</sub> pilin domain in the ternary complex are closely similar  
49  
50 to those in the previously published chaperone FimC–FimH adhesion binary complex  
51  
52 (Choudhury *et al.*, 1999). The residues 1–24 of the N-terminal tail, which are completely  
53  
54 unstructured in free FimD<sub>N</sub> usher domain, become ordered upon complex formation and  
55  
56  
57  
58  
59  
60

1 specifically interact with both FimC chaperone and the bound FimH<sub>P</sub> pilin domain (Fig. 11;  
2 Nishiyama *et al.*, 2005). The interactions formed by the N-terminal FimD<sub>N</sub> usher domain tail  
3  
4 comprise 60% of the total interface area of 1260Å<sup>2</sup> between FimD<sub>N</sub> (1–125) usher domain and  
5  
6 the chaperone FimC–FimH<sub>P</sub> pilin domain complex. The other 40% of the contact area is  
7  
8 contributed by the folded core FimD<sub>N</sub> (25–125) usher domain, which exhibits a complementary  
9  
10 surface to FimC chaperone. The N-terminal tail 1–24 of FimD<sub>N</sub> usher domain thus serves as a  
11  
12 sensor that selectively detects loaded FimC chaperone molecules. As the tail is the only FimD<sub>N</sub>  
13  
14 usher domain region that forms contacts with the chaperone-bound subunit, it may be  
15  
16 exclusively responsible for the discrimination of the different chaperone FimC–subunit  
17  
18 complexes by the assembly platform (Saulino *et al.*, 1998). FimD usher protein binds to different  
19  
20 chaperone FimC–subunit complexes with different affinities, which is a key element for correct  
21  
22 initiation of pilus assembly and for the correct ordering of the subunit incorporation into the pilus  
23  
24 (Saulino *et al.*, 1998; Nishiyama *et al.*, 2003). In the case of the chaperone FimC–FimH adhesion  
25  
26 complex, which is bound by FimD usher protein with highest affinity (Saulino *et al.*, 1998),  
27  
28 additional contacts between the FimH lectin domain and other FimD usher regions could  
29  
30 contribute to binding, as FimD usher protein has been shown to recognize the isolated FimH  
31  
32 lectin domain (Barnhart *et al.*, 2003), which is not bound by FimD<sub>N</sub> usher domain (Nishiyama *et*  
33  
34 *al.*, 2003). The X-ray structure of the FimD<sub>N</sub> (1–125) usher domain–FimC chaperone–FimH<sub>P</sub>  
35  
36 pilin domain complex thus predicts that the common element of the interactions of FimD<sub>N</sub> usher  
37  
38 domain with the four different chaperone FimC–subunit complexes is the contact area between  
39  
40 the N-terminal FimC chaperone domain and the structured FimD<sub>N</sub> (25–125) usher domain.  
41  
42 Nishiyama *et al.* (2005) assumed that this contact area alone is, however, neither sufficient for  
43  
44 binding of chaperone FimC–subunit complexes to FimD<sub>N</sub> usher domain, nor for stable binding of  
45  
46 the free chaperone to the assembly platform (Saulino *et al.*, 1998; Nishiyama *et al.*, 2003). The  
47  
48 fact that FimC chaperone alone is not bound by FimD usher ensures that FimC chaperone is  
49  
50  
51  
52  
53  
54  
55  
56  
57  
58  
59  
60

1 released to the periplasm for another reaction cycle as soon as the bound subunit dissociates from  
2  
3  
4 the ternary complex and is delivered to the translocation pore.  
5

6  
7 **Twinned-pore model of the translocation machinery functioning.** The Type 1 pilus tip  
8  
9 complex was analyzed by cryo-electron microscopy (Fronzes *et al.*, 2008; Remaut *et al.*, 2008).  
10  
11 The available structural and biochemical data on the purified Type 1 tip complex and PapC  
12  
13 firmly establish the outer membrane ushers function as dimers organized in twinned pores that is  
14  
15 the functional unit for chaperone/usher pilus biogenesis (Li *et al.*, 2004; So & Thanassi, 2006).  
16  
17 The dimer interface in the 3D crystals is formed by the flat side of the kidney-shaped  $\beta$ -barrel,  
18  
19 encompassing strands  $\beta 11$ – $\beta 20$  (residues 397–573; Fig. 10). The 3D cryo-electron microscopy  
20  
21 reconstruction reveals translocation of the polymerized subunits occurs asymmetrically and  
22  
23 through only a single pore (usher 1; Fig. 2). The usher mediates the translocation of folded,  
24  
25 polymerized protein units across the outer membrane (Sauer *et al.*, 2002; Remaut *et al.*, 2006;  
26  
27 Vetsch *et al.*, 2006). The width of the PapC translocation pore (inner diameter of  $45\text{\AA} \times 25\text{\AA}$ )  
28  
29 corresponds well with the passage of P pilus subunits in an upright orientation, along the length  
30  
31 of the polymer (P pilus subunit dimensions are  $55\text{\AA} \times 30\text{\AA} \times 25\text{\AA}$ ,  $57\text{\AA} \times 32\text{\AA} \times 23\text{\AA}$  and  
32  
33  $60\text{\AA} \times 27\text{\AA} \times 22\text{\AA}$  for PapE (Protein Data Bank accession number 1N12), PapK (Protein Data Bank  
34  
35 accession number 1PDK), and PapA (Protein Data Bank accession number 2UY6), respectively  
36  
37 (Sauer *et al.*, 1999, 2002; Verger *et al.*, 2007).  
38  
39  
40  
41  
42  
43

44 **Integrated model for fiber assembly at the outer membrane molecular usher protein.** Based  
45  
46 on the cryo-electron microscopy data, Remaut *et al.* (2008) proposed a mechanism where the  
47  
48 two ushers in the twin pores cooperate in pilus polymerization by alternately recruiting new  
49  
50 chaperone-subunit complexes through their N-terminal domains (Fig. 2). This mechanism  
51  
52 provides a rationale for the known requirement of a dimeric usher complex: one usher provides  
53  
54 the secretion channel, but two ushers are needed for successive rounds of subunit binding and  
55  
56 fiber assembly. The structural information presented and the available biochemical background  
57  
58 can be combined into an integrated model for subunit recruitment, subunit polymerization, and  
59  
60

1  
2 fiber translocation during pilus biogenesis at the outer membrane usher (Fig. 2). The structure of  
3  
4 the Fim(D×2):C:F:G:H tip complex captures the fiber assembly process after FimH, FimG, and  
5  
6 FimF have assembled into a pilus tip. In this complex, the last incorporated chaperone-subunit  
7  
8 complex (FimC:F) is bound to the N-terminal domain of usher pore 1. In the model, the next  
9  
10 subunit to be incorporated into the fiber is recruited to the twinned pores through the N-terminal  
11  
12 domain of usher 2 (step 1; Fig. 2). The N-terminal domain of the usher resides in the periplasm,  
13  
14 tethered by a 20-residue flexible linker to the translocation pore. This spacer between the usher  
15  
16 translocation pore and its N-terminal domain allows reorientation of the chaperone-subunit  
17  
18 complex to a position where the N-terminal donor strand Gd of the newly recruited subunit is in  
19  
20 proximity with the pilin domain of the previously recruited chaperone-subunit complex (bound  
21  
22 to usher 1). This strand exchange reaction results in the release of the chaperone from the  
23  
24 previously recruited chaperone-subunit complex and its dissociation from the N-terminal domain  
25  
26 of usher 1 (the usher lacks any detectable affinity for the chaperone when not in complex with  
27  
28 the adhesin or a pilus subunit [Dodson *et al.*, 1993; Nishiyama *et al.*, 2003; Saulino *et al.*, 1998])  
29  
30 (step 3; Fig. 2). Upon release of the chaperone, the subunit can now enter the translocating pore  
31  
32 of usher 1 and the N-terminal domain of usher 1 is free to bind a new chaperone-subunit  
33  
34 complex from the periplasmic pool and bring it within proximity of the previously recruited  
35  
36 chaperone-subunit complex for donor strand exchange (steps 4 and 5; Fig. 2). In this way,  
37  
38 iterations of the alternating recruitments of new chaperone-subunit complexes at either usher's  
39  
40 N-terminal domain, followed by donor strand exchange with the previously assembled subunit,  
41  
42 allow the stepwise polymerization and translocation of the pilus fiber (steps 5 and 6; Fig. 2).  
43  
44  
45  
46  
47  
48  
49  
50

51  
52 The model for chaperone/usher pilus assembly presented above incorporates all available  
53  
54 biochemical data into the new structural framework. It does, however, lack the usher C-terminal  
55  
56 domain. Earlier studies in the P pilus system showed that the C-terminal domain of PapC is  
57  
58 involved in the activation of the usher (So and Thanassi, 2006). From studies in type 1 pili, it is  
59  
60 known that FimH recruitment triggers a conformational change in the usher required for its

1  
2 activation (Saulino *et al.*, 1998). This activation step depends on the presence of the FimH  
3  
4 adhesin domain (Munera *et al.*, 2007). Remaut *et al.* (2008) proposed that, in its inactive state,  
5  
6 the C-terminal domain (not shown in Fig. 2) is positioned at least partially under the PapC or  
7  
8 FimD channel and is in contact with the  $\beta$ 5-6 hairpin and plug domain. This is consistent with  
9  
10 cryo-electron microscopy data showing that in the absence of the C-terminal domain, the  
11  
12 electron density within the channel is weaker (Li *et al.*, 2004). When the chaperone-adhesive  
13  
14 subunit complex is recruited to the usher via the usher's N-terminal domain, a putative additional  
15  
16 interaction between the adhesive subunit and the usher's C-terminal domain may relay a  
17  
18 conformational change to the plug domain and the  $\beta$ 5-6 hairpin and result in opening of the  
19  
20 channel. Such an interaction has been observed between the PapC C-terminal domain and the  
21  
22 PapD:G chaperone-adhesive subunit complex (So & Thanassi, 2006). As the FimD:tip complex  
23  
24 captures a later stage of pilus biogenesis, a stage at which the twinned pores are already activated  
25  
26 and the C-terminal domains may no longer be involved, it is not surprising that the C-terminal  
27  
28 domains should not be seen. The C-terminal domains may lay idle, possibly tethered to a long  
29  
30 linker (as for the N-terminal domain). However, further functional and structural work is needed  
31  
32 to elucidate the role of the usher C-terminal domain and the mechanism of channel gating.  
33  
34  
35  
36  
37  
38  
39  
40  
41

## 42 **FUNCTIONS OF ADHESIVE ORGANELLES ASSEMBLED WITH**

### 43 **CHAPERONE/USHER MACHINERY**

#### 44 **Binding of Bacterial Adhesive Organelles to Host Cell Receptors and Serum Proteins**

#### 45 **Binding of polyadhesins to host cell receptors and serum proteins. *Afa/Dr polyadhesins.***

46  
47  
48  
49  
50 Dr, F1845 (DaaE), NFA-I, and AfaE-III adhesins allow binding to the Dr<sup>a</sup> blood-group antigen  
51  
52 presented on the CD55/decay-accelerating factor (DAF), a complement regulatory and signaling  
53  
54 molecule (Nowicki *et al.*, 1988). Under physiological conditions, CD55/DAF plays a central role  
55  
56  
57  
58  
59  
60



1  
2 in preventing the amplification of the complement cascade on host cell surfaces (Fujita *et al.*,  
3  
4 1987; Lublin & Atkinson, 1989). CD55/DAF interacts directly with membrane-bound C3b or  
5  
6 C4b and prevents the subsequent uptake of C2 and factor B.  
7  
8

9 Human CD55/DAF is a cell-associated protein with *Mr* of 55,000 to 70,000, depending on its  
10 glycosylation level. Membrane-bound CD55/DAF is attached to the cell surface membrane by a  
11 glycosylphosphatidylinositol anchor (Caras *et al.*, 1987; Davitz *et al.*, 1986), attached to a serine-  
12 threonine-proline-rich region followed by four repeating domains (Carroll *et al.*, 1988; Rey-  
13 Campos *et al.*, 1988). They are currently named complement control protein repeat (CCP)  
14 domains, originally known as short consensus repeats (Le Bouguéneq & Servin, 2006; Servin,  
15 2005). Removal of CCP-1 has no effect on CD55/DAF function, but individual deletion of CCP-  
16 2 and CCP-3 or CCP-4 totally abolished it (Brodbeck *et al.*, 1996; Coyne *et al.*, 1992). Afa/Dr  
17 adhesins recognize CCP-3 on CD55/DAF (Nowicki *et al.*, 1993). Indeed, a single point  
18 substitution in CCP-3 (Ser155 to Leu) causes complete abolition of adhesin binding to  
19  
20 CD55/DAF (Nowicki *et al.*, 1993). Dr adhesin-binding and complement-regulating epitopes of  
21 CD55/DAF appear to be distinct and are approximately 20Å apart (Hasan *et al.*, 2002). The  
22 amino acids Gly159, Tyr160, and Leu162 also aid in binding adhesin Dr, while residues Phe123  
23 and Phe148 at the interface of CCP-2 and CCP-3, and also Phe154 in CCP-3 cavity, are  
24 important in complement regulation.  
25  
26  
27  
28  
29  
30  
31  
32  
33  
34  
35  
36  
37  
38  
39  
40  
41  
42  
43

44 An atomic resolution model for functions of AfaE-III adhesin reveals the pivotal role of CCP-  
45 2 and CCP-3 in binding of adhesins onto CD55/DAF (Anderson *et al.*, 2004a). Simultaneously  
46 the residues of AfaE-III adhesin involved in CD55/DAF binding were localized (Fig. 9;  
47 Anderson *et al.*, 2004a). Like DraE, AfaE-III binds to CCP-2 and CCP-3, but CCP-3 contributes  
48 most to the free energy of binding. The binding regions for AfaE-III and the complement  
49 pathway convertases lie in close proximity to each others on CD55/DAF.  
50  
51  
52  
53  
54  
55  
56  
57  
58

59 Binding of adhesin Dr to CD55/DAF is inhibited by chloramphenicol, whereas binding of  
60 AfaE-III is unaffected (Nowicki *et al.*, 1988; Westerlund *et al.*, 1989). This was used for

1  
2 localization of DraE adhesive site. 3-D structure of strand-swapped trimer of wild-type DraE in  
3  
4 complex with chloramphenicol was solved. NMR data supported the binding position of  
5  
6 chloramphenicol within the crystal (Anderson *et al.*, 2004b; Pettigrew *et al.*, 2004).  
7

8  
9 Chloramphenicol binds to a surface pocket between the N-terminal portion of strand B and C-  
10  
11 terminal portion of strand E and lies within the recently identified CD55/DAF-binding site (Fig.  
12  
13 9; Anderson *et al.*, 2004a). Recently Pettigrew *et al.* (2009) reported X-ray structures of DraE  
14  
15 bound to two chloramphenicol derivatives: chloramphenicol succinate (CLS) and  
16  
17 bromamphenicol (BRM). The CLS structure demonstrates that acylation of the 3-hydroxyl group  
18  
19 of CLM with succinyl does not significantly perturb the mode of binding while the BRM  
20  
21 structure implies that the binding pocket is able to accommodate bulkier substituents on the N-  
22  
23 acyl group. It is concluded that modifications of the 3-hydroxyl group would generate a potent  
24  
25 haemagglutinin Dr inhibitor that would not cause the toxic side effects that are associated with  
26  
27 the normal bacteriostatic activity of CLM. Korotkova *et al.* (2006b) solved the 3D structure of  
28  
29 DaaE at resolution 1.48 Å. Trimers of the protein were found in the crystal, as has been the case  
30  
31 for other adhesins Dr. Naturally occurring variants and directed mutations in DaaE have been  
32  
33 generated and analyzed for their ability to bind CD55/DAF. Mapping of the mutation sites onto  
34  
35 the DaaE molecular structure shows that several of them contribute to a contiguous surface that  
36  
37 is likely the primary CD55/DAF binding site (Fig. 9).  
38  
39  
40  
41  
42  
43

44 Dr, F1845 (DaaE), and AfaE-III adhesins interacts also with carcinoembryonic antigen  
45  
46 (CEA)-related cellular adhesion molecules, CEACAM1, CEACAM5, and CEACAM6 (Berger *et*  
47  
48 *al.*, 2004). This recognition is followed by activation of CEACAMS-associated signaling by  
49  
50 pathogens triggering the cellular events. CEACAM1, CEACAM5, and CEACAM6 belong to the  
51  
52 immunoglobulin superfamily of adhesion molecules (Grunert & Kuroki, 1998; Hammarstrom,  
53  
54 1999; Öbrink, 1997; Thompson *et al.*, 1991). They share a conserved N-terminal  
55  
56 immunoglobulin variable-like domain that is followed by 3, 6 and 2 immunoglobulin constant-  
57  
58 like domains, respectively. CEACAM1 is inserted into the cellular membrane via C-terminal  
59  
60

1  
2 transmembrane and cytoplasmic domains, whereas CEACAM5 and CEACAM6 have a  
3  
4 glycosylphosphatidylinositol anchor. CEACAMS family generally functions as intercellular  
5  
6 adhesion molecules (Benchimol *et al.*, 1989), and could play a role in innate immunity (Fahlgren  
7  
8 *et al.*, 2003). CEACAM1 has been shown to be expressed in leukocytes, including granulocytes,  
9  
10 activated T cells, B cells, and natural killer cells (Grunert & Kuroki, 1998). CEACAM1 acts as a  
11  
12 novel class of immunoreceptor tyrosine-based inhibition motif-bearing regulatory molecules on  
13  
14 T cells that are active during the early phases of the immune response in mice (Benchimol *et al.*,  
15  
16 1989; Fahlgren *et al.*, 2003; Kammerer *et al.*, 1998, 2001; Nakajima *et al.*, 2002). The  
17  
18 intracytoplasmic domain, which contains two immunoreceptor tyrosine-based inhibition motif-  
19  
20 like domains, is required for activation of a fraction of T cells in *Lamina propria* that express  
21  
22 CEACAM1 by IL-7 and IL-15, indicating that CEACAM1 amplifies T-cell activation and thus  
23  
24 could facilitate cross talk between epithelial cells and T lymphocytes in the intestinal immune  
25  
26 response (Donda *et al.*, 2002). The particular role of CEACAM1 in *Neisseria* pathogenicity has  
27  
28 been documented. *N. gonorrhoeae* evades host immunity by switching off T lymphocytes  
29  
30 (Bradbury, 2002). In *N. gonorrhoeae*, the Opa<sub>52</sub> protein is able to bind CEACAM1 expressed by  
31  
32 primary CD4<sup>+</sup> T lymphocytes and to suppress their activation and proliferation after the Opa  
33  
34 gonococcal protein associates with the tyrosine phosphatases SHP-1 and SHP-2 in the ITIM of  
35  
36 CEACAM1 (Boulton & Gray-Owen, 2002; Chen *et al.*, 2001). Rougeaux *et al.* (2008) found  
37  
38 that, as Opa, the adhesin Dr induces the Tyr-phosphorylation of ITIM and ITSM and the  
39  
40 recruitment of Shp-2. The recent review by Nouvion & Beauchemin (2009) summarized multiple  
41  
42 functions of CEACAM1. It was shown that this multifunctional protein plays a role in  
43  
44 intercellular adhesion, as an inhibitor of tumor development, as a bacterial adhesin, and as a  
45  
46 receptor for the mouse hepatitis virus. Moreover, CEACAM1 is an active regulator of cell  
47  
48 signaling, modulating the insulin or EGF receptor pathways in epithelial cells or the Zap-70  
49  
50 pathway in hematopoietic cells. The recent development of genetically modified mouse models  
51  
52 altering the *Ceacam1* gene corroborates most of these data, but also highlights CEACAM1's  
53  
54  
55  
56  
57  
58  
59  
60

1 functional complexity. Thus, in addition to the functions identified previously, CEACAM1 is an  
2 important regulator of lipid metabolism, of tumor progression as a regulator of the Wnt signaling  
3 pathway, of normal and tumor neo-angiogenesis and of immunity (Nouvion & Beauchemin,  
4 2009).

5  
6  
7  
8  
9  
10  
11 Random mutagenesis with functional analysis and chemical shift mapping by NMR show a  
12 clear-cut CEACAMS binding site located primarily in the A, B, E and D strands of adhesin Dr  
13 subunit (Fig. 9; Korotkova *et al.*, 2006a). This site is located opposite to the  $\beta$ -sheet  
14 encompassing the previously determined binding-site for CD55/DAF, which implies that the  
15 polyadhesin Dr can bind simultaneously to both receptors on the epithelial cell surface. Recently,  
16 the structure of the CEA/Dr adhesin complex was proposed based on NMR spectroscopy and  
17 mutagenesis data in combination with biochemical characterization (Korotkova *et al.*, 2008). The  
18 Dr adhesin/CEA interface overlaps appreciably with the region responsible for CEA  
19 dimerization. Binding kinetics, mutational analysis and spectroscopic examination of CEA  
20 dimers suggest that adhesins Dr can dissociate CEA dimers prior to the binding of monomeric  
21 forms (Korotkova *et al.*, 2008).  
22  
23  
24  
25  
26  
27  
28  
29  
30  
31  
32  
33  
34  
35  
36

37 Hemagglutinin Dr is unique in Afa/Dr adhesin family since it binds specifically to the 7S  
38 domain (tetramer) of the basement membrane protein type IV collagen that is inhibited by the  
39 presence of chloramphenicol (Nowicki *et al.*, 1988; Westerlund *et al.*, 1989; Westerlund &  
40 Korhonen, 1993). Site-directed mutagenesis has been used to show that a negatively charged  
41 amino acid is required at position 54 of adhesive subunit Dr to confer chloramphenicol  
42 sensitivity of binding and that mutations at positions 32, 40, 54, 90, and 113 have different  
43 effects on type IV collagen binding and the chloramphenicol sensitivity of binding (Carnoy &  
44 Moseley, 1997). In particular, replacement of a single amino acid at position 113 of the DraE  
45 subunit results in loss of type IV collagen binding. Moreover, the two conserved Cys of the  
46 Afa/Dr family structural subunits form a disulfide bond, and mutations of these residues abolish  
47 both hemagglutination and binding to type IV collagen. Together with fibronectin, laminin,  
48  
49  
50  
51  
52  
53  
54  
55  
56  
57  
58  
59  
60

1  
2 tenascin, and heparin sulfate proteoglycans, type IV collagen is a component of the basement  
3 membrane, which is involved in complex interactions at the epithelial-mesenchymal interface. In  
4 particular, type IV collagen interacts with integrins expressed at the basal domain of polarized  
5 cells (Beaulieu, 1999), to form a link between the basement membrane and epithelial cells  
6 (Louvard *et al.*, 1992). However, during inflammation, deregulated expression of membrane-  
7 bound molecules that are normally segregated in the basolateral domain of polarized intestinal  
8 cells occurs, and it is possible that in this context type IV collagen binding may contribute to the  
9 pathogenic action of Afa/Dr adhesins (Selvarangan *et al.*, 2004; Servin, 2005).

10  
11  
12  
13  
14  
15  
16  
17  
18  
19  
20  
21 **pH6 antigen.** It was found that pH6 antigen of *Y. pestis* is a novel bacterial IgG-binding  
22 receptor (Zav'yalov *et al.*, 1996). A pseudo-immune complex with human IgG1, IgG2 and IgG3  
23 was formed. No binding to human IgG4, rabbit, mouse and sheep IgG was found. Antigen pH6  
24 binds human IgG1 Fc subunit and does not bind Fab and pFc' subunits. This finding may be  
25 explained by pH6 antigen binding to  $\beta$ 1-linked galactosyl residue (Payne *et al.*, 1998) in a  
26 carbohydrate moiety of human IgG1, IgG2 and IgG3 that is linked to C<sub>H</sub>2 domains of their Fc  
27 subunit (Deisenhofer, 1981).

28  
29  
30  
31  
32  
33  
34  
35  
36  
37  
38 Binding of purified recombinant pH6 antigen to gangliotetraosylceramide,  
39 gangliotriaosylceramide, and lactosylceramide was indicated by an enzyme-linked  
40 immunosorbent assay (Payne *et al.*, 1998). The binding was saturable, with 50% of maximal  
41 binding occurring at 498, 390, and 196 nM, respectively. Intact *E. coli* cells that expressed pH6  
42 antigen had specificity similar to purified pH6 antigen of *Y. pestis* on a thin-layer  
43 chromatography, except that nonhydroxylated galactosylceramide was also bound. The binding  
44 pattern indicates that the presence of  $\beta$ 1-linked galactosyl residue in glycosphingolipids is the  
45 minimum determinant required for binding of pH6 antigen.

46  
47  
48  
49  
50  
51  
52  
53  
54  
55  
56  
57 Purified pH6 antigen selectively binds to apolipoprotein B-containing lipoproteins (low  
58 density lipoproteins) in human plasma (Makoveichuk *et al.*, 2003). Low density lipoproteins at  
59 normal physiological concentration in human blood (equal to ~250  $\mu$ g/ml) nearly abolish the  
60

1  
2 interaction of purified pH6 antigen with macrophages. This process could prevent recognition of  
3  
4 a pathogen by the host immune defense system (Makoveichuk *et al.*, 2003). Such immune  
5  
6 masking might be important for the ability of the pathogen to cause the disease (Makoveichuk *et*  
7  
8 *al.*, 2003).  
9

10  
11 Liu *et al.* (2006) found by flow cytometry that individual *Y. pestis* cells can express the  
12  
13 capsular F1 antigen concomitantly with pH6 antigen (Psa) on their surface when analyzed. To  
14  
15 better evaluate the separate effects of F1 and Psa on the adhesive and invasive properties of *Y.*  
16  
17 *pestis*, isogenic  $\Delta caf$  (F1 genes),  $\Delta psa$ , and  $\Delta caf \Delta psa$  mutants were constructed and studied with  
18  
19 the three respiratory tract epithelial cells. The  $\Delta psa$  mutant bound significantly less to all three  
20  
21 epithelial cells compared to the parental wild-type strain and the  $\Delta caf$  and  $\Delta caf \Delta psa$  mutants,  
22  
23 indicating that pH6 antigen acts as an adhesin for respiratory tract epithelial cells. An anti-  
24  
25 adhesive effect of F1 antigen was clearly detectable only in the absence of pH6 antigen,  
26  
27 underlining the dominance of the Psa<sup>+</sup> phenotype. Both F1 and pH6 antigens inhibited the  
28  
29 intracellular uptake of *Y. pestis*. Thus, F1 inhibits bacterial uptake by inhibiting bacterial  
30  
31 adhesion to epithelial cells, whereas pH6 antigen seems to block bacterial uptake by interacting  
32  
33 with a host receptor which controls the direct internalization. The  $\Delta caf \Delta psa$  double mutant  
34  
35 bound and invaded all three epithelial cell types well, indicating to the presence of undefined  
36  
37 adhesin(s) and invasin(s).  
38  
39  
40  
41  
42  
43  
44

45  
46 It was found that pH6 antigen (Psa) fimbriae mediate bacterial binding to human alveolar  
47  
48 epithelial cells (Galván *et al.*, 2006). The pH6 fimbriae bound mostly to one component present  
49  
50 in the total lipid extract from type II alveolar epithelial cells A549. Receptor of pH6 antigen was  
51  
52 identified as phosphatidylcholine with thin-layer chromatography, molybdenum blue staining  
53  
54 and pH6 antigen overlays. The pH6 antigen fimbriae bound to phosphatidylcholine in a dose-  
55  
56 dependent manner while the binding was inhibited with phosphorylcholine and choline. Antigen  
57  
58 pH6 also bound to pulmonary surfactant, which covers the alveolar surface as a product of type  
59  
60 II alveolar epithelial cells and includes phosphatidylcholine as the major component. The



1  
2 observed dose-dependent interaction of pH6 antigen with pulmonary surfactant was blocked by  
3 phosphorylcholine. Interestingly, surfactant did not inhibit pH6 antigen-mediated bacterial  
4 binding to alveolar cells, suggesting that both surfactant and cell membrane phosphatidylcholine  
5 retain pH6 antigen -fimbriated bacteria on the alveolar surface. Altogether, the results indicate  
6 that pH6 antigen uses the phosphorylcholine moiety of phosphatidylcholine as a receptor to  
7 mediate bacterial binding to pulmonary surfactant and alveolar epithelial cells.  
8  
9

10  
11  
12  
13  
14  
15  
16  
17 **F1 antigen.** It was found that human IL-1 $\beta$  specifically binds to a protein of *caf* operon,  
18 expressed on the surface of recombinant *E. coli* strain (Zav'yalov *et al.*, 1995a). The binding was  
19 specifically inhibited by the Caf1M–Caf1 complex but not by the free Caf1M chaperone.  
20 Partially purified Caf1A also demonstrated binding with human IL-1 $\beta$ . The contradiction  
21 between the results can be explained by a presence of an admixture of Caf1M–Caf1 complex in  
22 Caf1A sample. Indeed, it has been demonstrated that chaperone-subunit complex is co-purifying  
23 in complex with usher protein (Nishiyama *et al.*, 2005). A surprise is the absence of IL-1 $\beta$   
24 binding with the fragments of F1 antigen that are scattering into cultural media (Chen & Elberg,  
25 1977). This implies that only short non-aggregated F1 fibers, expressed during the early stages of  
26 cultivation/infection, possess the IL-1 $\beta$  binding activity.  
27  
28  
29  
30  
31  
32  
33  
34  
35  
36  
37  
38  
39  
40  
41  
42

43 **Binding of monoadhesins to host cell receptors and serum host proteins.** FGS chaperone-  
44 assembled mono-adhesive fimbriae or pili are cell-surface fibers that project a specialized  
45 bacterial lectin, or adhesin subunit, away from the bacterial surface, to reach out for specific  
46 glycan receptors on the host cell (De Greve *et al.*, 2007). Mono-adhesive fimbriae/pili can also  
47 mediate interbacterial interactions, thereby facilitating biofilm formation (De Greve *et al.*, 2007).  
48 Monoadhesins are important virulence factors that exploit the diversity and virtually unlimited  
49 combinatorial potential of their carbohydrate receptors to ensure selective and fine-tuned  
50 pathogen–host interactions (De Greve *et al.*, 2007). In recent years, it was shown that mono-  
51 adhesive fimbriae/pili allow bacterial pathogens to colonize, multiply, disseminate, and, in some  
52  
53  
54  
55  
56  
57  
58  
59  
60



1 cases, persist for weeks to months within their animal hosts (Bower *et al.*, 2005). Among these  
2  
3  
4  
5  
6  
7  
8  
9  
10  
11  
12  
13  
14  
15  
16  
17  
18  
19  
20  
21  
22  
23  
24  
25  
26  
27  
28  
29  
30  
31  
32  
33  
34  
35  
36  
37  
38  
39  
40  
41  
42  
43  
44  
45  
46  
47  
48  
49  
50  
51  
52  
53  
54  
55  
56  
57  
58  
59  
60  
cases, persist for weeks to months within their animal hosts (Bower *et al.*, 2005). Among these  
invasive bacteria, there are strains of uropathogenic *E. coli* which were previously characterized  
as strictly extracellular microbes but have been now shown to behave as opportunistic  
intracellular pathogens. Worldwide, uropathogenic *E. coli* account for the majority of urinary  
tract infections, including both cystitis (bladder infection) and pyelonephritis (kidney infection)  
(Foxman & Brown, 2003). These infections are exceedingly common in females, suffered by  
11% of women each year (Foxman *et al.*, 2000).

***FimH adhesin.*** Uropathogenic *E. coli* typically expresses filamentous adhesive organelles,  
called Type 1 pili, which mediate both bacterial attachment to and invasion of bladder urothelial  
cells. Type 1 pili or fimbriae possess a lectin-like component, FimH that is commonly thought to  
cause binding to mannose-containing oligosaccharides of host receptors. Since adhesion of Type  
1 fimbriated organisms are inhibited by mannose, the reactions are described as mannose  
sensitive.

Sokurenko *et al.* (1992) studied the adhesion of the Type 1 fimbriated CSH-50 strain of *E.*  
*coli* (which expresses only Type 1 fimbriae) to fibronectin (FN). *E. coli* CSH-50 does not bind  
detectable amounts of soluble FN but adheres well to immobilized plasma or cellular FN. This  
adhesion was inhibited by mannose-containing saccharides. By using purified domains of FN, it  
was found that *E. coli* CSH-50 adheres primarily to the N-terminal and gelatin-binding domains,  
only one of which is glycosylated, in mannose sensitive (MS) way. Binding of the mannose-  
specific lectin concanavalin A to FN and ovalbumin was eliminated or reduced, respectively, by  
incubation with periodate or endoglycosidase. Adhesion of *E. coli* CSH-50 to ovalbumin was  
reduced by these treatments, but adhesion to FN was unaffected. *E. coli* CSH-50 also adheres in  
an MS way to a synthetic peptide copying a portion of the amino-terminal FN domain (FNspl).  
Purified CSH-50 fimbriae bound to immobilized FN and FNspl in an MS way and inhibited  
adhesion of intact organisms. However, fimbriae purified from HB101(pPKL4), a recombinant  
strain harboring the entire Type 1 *fim* gene locus and expressing functional Type 1 fimbriae,

1  
2 neither bound to FN or FNspl, nor inhibited *E. coil* adhesion to immobilized FN or FNspl. These  
3  
4 findings suggest that there are two forms of Type 1 MS fimbriae. One form exhibits only the  
5  
6 well-known MS lectin-like activity that requires mannose-containing glycoproteins. The other  
7  
8 form exhibits not only the MS lectin-like activity but also binds to nonglycosylated regions of  
9  
10 proteins in an MS manner. Sokurenko *et al.* (1994) provided evidence that this functional  
11  
12 heterogeneity is due to variations in the *fimH* genes. They also investigated functional  
13  
14 heterogeneity among clinical isolates and whether variation in *fimH* genes accounts for  
15  
16 differences in receptor specificity. Twelve isolates obtained from human urine were tested for  
17  
18 their ability to adhere to mannan, fibronectin, periodate-treated fibronectin, and a synthetic  
19  
20 peptide copying 30 amino-terminal residues of fibronectin. CSH-50 and HB101 (pPKLA) were  
21  
22 tested for comparison. Selected isolates were also tested for adhesion to purified fragments  
23  
24 spanning the entire fibronectin molecule. Three distinct functional classes, designated M, MF,  
25  
26 and MFP, were observed. The *fimH* genes were amplified by PCR from chromosomal DNA  
27  
28 obtained from representative strains and expressed in a *fim<sup>-</sup>* strain (AAEC191A) transformed  
29  
30 with a recombinant plasmid containing the entire *fim* gene cluster but with a translational stop-  
31  
32 linker inserted into the *fimH* gene (pPKL114). Cloned *fimH* genes conferred on AAEC191A  
33  
34 (pPKL114) receptor specificities mimicking those of the parent strains from which the *fimH*  
35  
36 genes were obtained, demonstrating that the FimH subunits are responsible for the functional  
37  
38 heterogeneity. Representative *fimH* genes were sequenced, and the deduced amino acid  
39  
40 sequences were compared with the previously published FimH sequence. Allelic variants  
41  
42 exhibiting >98% homology and encoding proteins differing by as little as a single amino acid  
43  
44 substitution confer distinct adhesive phenotypes. This unexpected adhesive diversity within the  
45  
46 FimH family broadens the scope of potential receptors for enterobacterial adhesion and may lead  
47  
48 to a fundamental change in the understanding of the role(s) that Type 1 fimbriae may play in  
49  
50 enterobacterial ecology or pathogenesis.  
51  
52  
53  
54  
55  
56  
57  
58  
59  
60

1  
2 To further study the relationship between allelic variation of the *fimH* gene and adhesive  
3 properties of Type 1 fimbriae, Sokurenko *et al.* (1995) cloned the *fimH* genes from five strains  
4 and used to complement the FimH deletion in *E. coli* KB18. The parental and recombinant  
5 strains showed a wide quantitative range in the ability of bacteria to adhere to immobilized  
6 mannan. The differences in adhesion are due to differences in the levels of fimbriation or relative  
7 levels of incorporation of FimH, because these parameters were similar in low-adhesion and  
8 high-adhesion strains. The nucleotide sequence for each of the *fimH* genes was determined.  
9 Analysis of deduced FimH sequences showed two sequence homology groups, based on the  
10 presence of Asn70 and Ser78 or Ser70 and Asn78 residues. The consensus sequences for each  
11 group conferred very low adhesion activity, and this low-adhesion phenotype predominated  
12 among a group of 43 fecal isolates. Strains isolated from different host niches in the urinary tract,  
13 expressed Type 1 fimbriae which conferred an increased level of adhesion. The results suggest  
14 that the quantitative variations in MS adhesion are primarily due to structural differences in the  
15 FimH adhesin.

16  
17  
18  
19  
20  
21  
22  
23  
24  
25  
26  
27  
28  
29  
30  
31  
32  
33  
34  
35 The differences in MS adhesion among of *E. coli* isolates makes possible that phenotypic  
36 variants of FimH play a functional role in population dynamics. Sokurenko *et al.* (1997)  
37 analyzed in more detail the ability of isogenic, recombinant strains of *E. coli* expressing *fimH*  
38 genes of the predominant fecal and urinary tract infection (UTI) phenotypes to adhere to  
39 glycoproteins and to uroepithelial cells. Type 1 fimbriae differ in their ability to recognize  
40 various mannosides by utilizing at least two different mechanisms. All FimH subunits studied to  
41 date are capable of mediating adhesion via trimannosyl residues, but only certain variants are  
42 capable of mediating high levels of adhesion via monomannosyl residues. The ability of the  
43 FimH lectins to interact with monomannosyl residues strongly correlates with their ability to  
44 mediate *E. coli* adhesion to uroepithelial cells. It would be possible for certain phenotypic  
45 variants of Type 1 fimbriae to contribute more than others to virulence of *E. coli* in the urinary  
46  
47  
48  
49  
50  
51  
52  
53  
54  
55  
56  
57  
58  
59  
60

1  
2 tract. Sokurenko *et al.* (1998) showed that genetic variation in FimH lectin of Type 1 fimbriae,  
3  
4 can change the tropism of *E. coli*, shifting it toward the urovirulent phenotype.  
5

6  
7 Random point mutations in *fimH* genes that increase binding of an adhesin to mono-mannose  
8  
9 residues, structures abundant in the oligosaccharide moieties of urothelial glycoproteins, confer  
10  
11 increased virulence. These mutant FimH variants, however, owe increased sensitivity to soluble  
12  
13 inhibitors bathing the oropharyngeal mucosa, the physiological portal of *E. coli*. This functional  
14  
15 trade-off seems to be detrimental for the intestinal ecology of the urovirulent *E. coli*. Thus,  
16  
17 bacterial virulence can be increased by random functional mutations in a commensal trait that are  
18  
19 adaptive for a pathologic environment, even at the cost of reduced physiological fitness in the  
20  
21 nonpathologic habitat. Schembri *et al.* (2000) used random mutagenesis to specifically identify  
22  
23 nonselective mutations in the FimH adhesin which modify its binding phenotype. Isogenic *E.*  
24  
25 *coli* clones expressing FimH variants were tested for their ability to bind yeast cells and model  
26  
27 glycoproteins which contain oligosaccharide moieties rich in either terminal monomannose,  
28  
29 oligomannose, or nonmannose residues. Type 1 fimbriae were altered for amino acids in the  
30  
31 FimH protein. The monomannose-binding phenotype was particularly sensitive to the changes,  
32  
33 with extensive differences in binding being observed in comparison to wild-type FimH levels.  
34  
35 Different structural alterations caused similar functional changes in FimH, suggesting to a high  
36  
37 degree of flexibility to target recognition by this adhesin. Alteration of residue Pro49 of the  
38  
39 carbohydrate-binding pocket of FimH, completely abolished its function. Amino acid changes  
40  
41 which increased the binding capacity of FimH were located outside receptor-interacting residues,  
42  
43 indicating that functional changes relevant to pathogenicity are likely to be due to  
44  
45 conformational changes of the adhesin.  
46  
47  
48  
49  
50  
51  
52

53  
54 Weissman *et al.* (2006) analysed the variability of *fimA* and *fimH* in strains of *E. coli* O1:K1-,  
55  
56 O2:K1- and O18:K1 serotypes. Multiple locus sequence typing (MLST) of this group revealed  
57  
58 that the strains are identical at eight housekeeping loci around the genome and belong to the  
59  
60 ST95 complex. Multiple highly diverse *fimA* alleles have been introduced into the ST95 clonal

1  
2 complex via horizontal transfer, at a frequency comparable to that of genes defining the major O-  
3 and H-antigens. However, no further significant FimA diversification occurred via point  
4 and H-antigens. However, no further significant FimA diversification occurred via point  
5 mutation after the transfers. In contrast, while *fimH* alleles also move horizontally (along with  
6 the *fimA* loci), they acquire point amino acid replacements at a higher rate than either  
7 housekeeping genes or *fimA*. These FimH mutations enhance binding to monomannose receptors  
8 and bacterial tropism for human vaginal epithelium. A similar pattern of rapid within-clonal  
9 structural evolution of the adhesive, but not pilin, subunit is also seen, respectively, in *papG* and  
10 *papA* alleles of the di-galactose-specific P-fimbriae. Thus, while structurally diverse pilin  
11 subunits of *E. coli* fimbriae are under selective pressure for frequent horizontal transfer between  
12 clones, the adhesive subunits of extraintestinal *E. coli* are under strong positive selection ( $D_n/D_s$   
13  $> 1$  for *fimH* and *papG*) for functionally adaptive amino acid replacements. Thomas *et al.*  
14 (2002) showed that bacterial attachment to target cells switches from loose to firm upon a 10-  
15 fold increase when a shear stress is applied. Steered molecular dynamics simulations of tertiary  
16 structure of the FimH receptor binding domain and subsequent site-directed mutagenesis studies  
17 indicate that shear-enhancement of the FimH-receptor interactions involves extension of the  
18 interdomain linker chain under mechanical force. The ability of FimH to function as a force  
19 sensor provides a molecular mechanism for discrimination between surface-exposed and soluble  
20 receptor molecules. Thomas *et al.* (2004) demonstrated that raising the shear stress (within the  
21 physiologically relevant range) increased accumulation of Type 1 fimbriated bacteria on  
22 monomannose surfaces by up to two orders of magnitude, and reducing the shear stress caused  
23 them to detach. In contrast, bacterial binding to anti-FimH antibody-coated surfaces showed  
24 essentially the opposite behaviour, detaching when the shear stress was increased. These results  
25 can be explained if FimH is force-activated; that is, that FimH mediates 'catch-bonds' with  
26 mannose that are strengthened by tensile mechanical force. As a result, on monomannose-coated  
27 surfaces, bacteria displayed a complex 'stick-and-roll' adhesion in which they tend to roll over  
28 the surface at low shear but increasingly halted to stick firmly as the shear was increased.  
29  
30  
31  
32  
33  
34  
35  
36  
37  
38  
39  
40  
41  
42  
43  
44  
45  
46  
47  
48  
49  
50  
51  
52  
53  
54  
55  
56  
57  
58  
59  
60

1  
2 Mutations in FimH that were predicted earlier to increase or decrease force-induced  
3  
4 conformational changes in FimH were furthermore shown to increase or decrease the probability  
5  
6 that bacteria exhibited the stationary versus the rolling mode of adhesion. This 'stick-and-roll'  
7  
8 adhesion could allow Type 1 fimbriated bacteria to move along mannosylated surfaces under  
9  
10 relatively low flow conditions and to accumulate preferentially in high shear regions.  
11  
12

13  
14 Nilsson *et al.* (2008) described two distinctively different conformations of the mannose-  
15  
16 bound FimH binding site. Force-induced dissociation was slowed when the mannose ring rotated  
17  
18 such that additional force-bearing hydrogen bonds formed with the base of the FimH binding  
19  
20 pocket. The lifetime of the complex was further significantly enhanced by rigidifying this base.  
21  
22 It was shown how even sub-Å spatial alterations of the hydrogen bonding pattern within the base  
23  
24 can lead to significantly decreased bond lifetimes (Nilsson *et al.*, 2008). Pereverzev *et al.* (2005)  
25  
26 developed a physical model that explains how the ligand escapes the receptor binding site via  
27  
28 two alternative routes, a catch-pathway that is opposed by the applied force and a slip-pathway  
29  
30 that is promoted by force. The model predicts under what conditions and at what critical force  
31  
32 the catch-to-slip transition would be observed, as well as the degree to which the bond lifetime is  
33  
34 enhanced at the critical force. Nilsson *et al.* (2006) discovered that when surface adhesion is  
35  
36 mediated by catch bonds, whose bond life increases with increased applied force, shear stress  
37  
38 may dramatically increase the ability of bacteria to withstand detachment by soluble competitive  
39  
40 inhibitors. This shear stress-induced protection against inhibitor-mediated detachment was  
41  
42 shown for the fimbrial FimH-mannose-mediated surface adhesion of *E. coli*. Shear stress-  
43  
44 enhanced reduction of bacterial detachment has major physiological and therapeutic implications  
45  
46 and needs to be considered when developing and screening drugs.  
47  
48  
49  
50  
51  
52

53  
54 Nilsson *et al.* (2006) showed that the oligosaccharide-specific interaction of FimH with  
55  
56 trimannose (3M), lacks a shear threshold for binding, since the number of bacteria bind under  
57  
58 static conditions stronger than under any flow. However, similar to 1M, the binding strength of  
59  
60 surface-interacting bacteria is enhanced by shear. Bacteria change from rolling into firm

1 stationary surface adhesion as the shear increases. The shear-enhanced bacterial binding on 3M  
2 is mediated by catch bond properties of the 1M-binding subsite within the extended  
3  
4 is mediated by catch bond properties of the 1M-binding subsite within the extended  
5  
6 oligosaccharide-binding pocket of FimH, since structural mutations in the putative force-  
7  
8 responsive region and in the binding site affect 1M- and 3M-specific binding in an identical  
9  
10 manner. A shear-dependent conversion of the adhesion mode is also exhibited by P-fimbriated *E.*  
11  
12 *coli* adhering to digalactose surfaces.  
13  
14

15  
16 Anderson *et al.* (2007) compared levels of surface colonization by *E. coli* strains that differ in  
17  
18 the strength of adhesion as a result of flow conditions or point mutations in FimH. They showed  
19  
20 that the weak rolling mode of surface adhesion allows a more rapid spreading during growth on a  
21  
22 surface in the presence of fluid flow. An attempt to inhibit the adhesion of strongly adherent  
23  
24 bacteria by blocking mannose receptors with a soluble inhibitor actually increased the rate of  
25  
26 surface colonization by allowing the bacteria to roll. This work suggests that (i) an advantage of  
27  
28 a weak adhesion is a rapid surface colonization and (ii) antiadhesive therapies intended to  
29  
30 prevent biofilm formation can have unintended effect of enhancing the rate of surface  
31  
32 colonization.  
33  
34  
35

36  
37 Nilsson *et al.* (2007) showed that removal of the cysteine bond in the mannose-binding  
38  
39 domain of FimH did not affect FimH-mannose binding under static or low shear conditions ( $<$  or  
40  
41  $= 0.2 \text{ dyne cm}^{-2}$ ). However, the adhesion level was substantially decreased under increased fluid  
42  
43 flow. Under intermediate shear ( $2 \text{ dynes cm}^{-2}$ ), the ON-rate of bacterial attachment was  
44  
45 significantly decreased for disulphide-free mutants. Molecular dynamics simulations  
46  
47 demonstrated that the lower ON-rate of cysteine bond-free FimH could be due to destabilization  
48  
49 of the mannose-free binding pocket of FimH. In contrast, mutant and wild-type FimH had  
50  
51 similar conformation when bound to mannose, explaining their similar binding strength to  
52  
53 mannose under intermediate shear. The stabilizing effect of mannose on disulphide-free FimH  
54  
55 was also confirmed by protection of the FimH from thermal and chemical inactivation in the  
56  
57 presence of mannose. However, this stabilizing effect could not protect the integrity of FimH  
58  
59  
60



1  
2 structure under high shear ( $> 20$  dynes  $\text{cm}^{-2}$ ), where lack of the disulphide significantly  
3  
4 increased adhesion OFF-rates. Thus, the cysteine bonds in bacterial adhesins could be adapted to  
5  
6 enable bacteria to bind target surfaces under increased shear conditions.  
7

8  
9 Yakovenko *et al.* (2008) applied force to single isolated FimH bonds with an atomic force  
10  
11 microscope in order to test this directly. If force was loaded slowly, most of the bonds broke up  
12  
13 at low force ( $<60$  pN of rupture force). However, when force was loaded rapidly, all bonds  
14  
15 survived until much higher force (140-180 pN of rupture force), behavior that indicates to a  
16  
17 catch bond. Structural mutations or pretreatment with a monoclonal antibody both of which  
18  
19 allosterically stabilize a high affinity conformation of FimH cause all bonds to survive until high  
20  
21 forces regardless of the rate at which force is applied. Pretreatment of FimH bonds with  
22  
23 intermediate force has the same strengthening effect on the bonds. This demonstrates that FimH  
24  
25 forms catch bonds and that tensile force induces an allosteric switch to the high affinity, strong  
26  
27 binding conformation of the adhesin. The catch bond behavior of FimH, the amount of force  
28  
29 needed to regulate FimH, and the allosteric mechanism, all provide insight into how bacteria  
30  
31 bind and form biofilms in fluid flow. Additionally, these observations may provide a means for  
32  
33 designing antiadhesive mechanisms.  
34  
35  
36  
37  
38

39  
40 Thomas *et al.* (2008) reviewed experimental data and biophysical theory to analyze why  
41  
42 mechanical force prolongs the lifetime of these bonds rather than shortens the lifetime by pulling  
43  
44 the ligand out of the binding pocket. Although many mathematical models can explain catch  
45  
46 bonds, experiments using structural variants have been more helpful in determining how catch  
47  
48 bonds work. The underlying mechanism has been worked out so far only for the bacterial  
49  
50 adhesive protein FimH. This protein forms catch bonds because it is allosterically activated when  
51  
52 mechanical force pulls an inhibitory domain away from the ligand-binding domain. Other catch  
53  
54 bond-forming proteins, including blood cell adhesion proteins called selectins and the motor  
55  
56 protein myosin, show evidence of allosteric regulation between two domains, but it remains  
57  
58 unclear if this is related to their catch bond behavior.  
59  
60

1  
2 FimH adhesin consists of a fimbria-associated pilin domain and a mannose-binding lectin or  
3  
4 adhesin domain, with the binding pocket positioned opposite the interdomain interface (Fig. 9;  
5  
6 Choudhury *et al.*, 1999). By using the yeast two-hybrid system, purified lectin and pilin domains,  
7  
8 and docking simulations, it was showed that the FimH domains interact with one another  
9  
10 (Aprikian *et al.*, 2007). The affinity for mannose is greatly enhanced (up to 300-fold) in FimH  
11  
12 variants in which the interdomain interaction is disrupted by structural mutations in either the  
13  
14 pilin or lectin domains. Also, affinity to mannose is dramatically enhanced in isolated lectin  
15  
16 domains or in FimH complexed with the chaperone molecule that is wedged between the  
17  
18 domains. Furthermore, FimH with native structure mediates weak binding at low shear stress but  
19  
20 shifts to strong binding at high shear, whereas FimH with disrupted interdomain contacts (or the  
21  
22 isolated lectin domain) mediates strong binding to mannose-coated surfaces even under low  
23  
24 shear. Interactions between lectin and pilin domains decrease the affinity of the mannose-binding  
25  
26 pocket via an allosteric mechanism (Choudhury *et al.*, 1999). Mechanical force at high shear  
27  
28 separates the two domains, allowing the lectin domain to switch from a low affinity to a high  
29  
30 affinity state. This shift provides a mechanism for FimH-mediated shear-enhanced adhesion by  
31  
32 enabling the adhesin to form catch bond-like interactions that are longer lived at high tensile  
33  
34 force. FimH lectin domain possesses a ligand-induced binding site - a type of allosterically  
35  
36 regulated epitopes characterized in integrins (Tchesnokova *et al.*, 2008). Analogous to integrins,  
37  
38 in FimH the ligand-induced binding site epitope becomes exposed in the presence of the ligand  
39  
40 (or 'activating' mutations) and is located far from the ligand-binding site, close to the interdomain  
41  
42 interface. Also, the antibody binding to the ligand-induced binding site shifts adhesin from the  
43  
44 low- to high-affinity state. Binding of streptavidin to the biotinylated residue within the ligand-  
45  
46 induced binding site also locks FimH in the high-affinity state, suggesting that the allosteric  
47  
48 perturbations in FimH are sustained by the interdomain wedging. In the presence of antibodies,  
49  
50 the strength of bacterial adhesion to mannose is increased similar to the increase observed under  
51  
52 shear force, suggesting the same allosteric mechanism - a shift in the interdomain configuration.  
53  
54  
55  
56  
57  
58  
59  
60

1  
2 Thus, an integrin-like allosteric link between the binding pocket and the interdomain  
3  
4 conformation can serve as the basis for the catch bond property of FimH and, possibly, of other  
5  
6 adhesive proteins. Pereverzev *et al.* (2009) found that the Type 1 fimbrial adhesive protein  
7  
8 (FimH)/mannose bond is governed by the interface between the lectin and pilin domains of  
9  
10 FimH. Catch-binding occurs in these systems when the external force stretches the receptor  
11  
12 proteins and increases the interdomain distance. The proposed model accurately describes the  
13  
14 experimentally observed anomalous behavior of the lifetimes of the FimH/mannose complexes  
15  
16 as a function of applied force and provides valuable insights into the mechanism of catch-  
17  
18 binding.  
19  
20  
21  
22

23 Recently Pereverzev *et al.* (2009) reviewed the proposed model that demonstrates the  
24  
25 allosteric role of the two-domain region of the receptor protein in the increased lifetimes of  
26  
27 biological receptor/ligand bonds subjected to an external force. Interaction between the domains  
28  
29 is represented by a bounded potential, containing two minima corresponding to the attached and  
30  
31 separated conformations of the two protein domains. The dissociative potential with a single  
32  
33 minimum, describing receptor/ligand binding, fluctuates between deep and shallow states,  
34  
35 depending on whether the domains are attached or separated. A number of valuable analytic  
36  
37 expressions are derived and are used to interpret experimental data for two catch bonds.  
38  
39  
40  
41

42 Using overlay assays with FimH, the purified type 1 pilus adhesin, and mass spectroscopy,  
43  
44  $\beta 1$  and  $\alpha 3$  integrins were identified as key host receptors for uropathogenic *E. coli* (Eto *et al.*,  
45  
46 2007). FimH recognizes N-linked oligosaccharides on these receptors, which are expressed  
47  
48 throughout the urothelium. In a bladder cell culture system,  $\beta 1$  and  $\alpha 3$  integrin receptors co-  
49  
50 localize with invading type 1-piliated bacteria and F-actin. FimH-mediated bacterial invasion of  
51  
52 host bladder cells is inhibited by  $\beta 1$  and  $\alpha 3$  integrin-specific antibodies and by disruption of the  
53  
54  $\beta 1$  integrin gene in the GD25 fibroblast cell line. Phosphorylation site mutations within the  
55  
56 cytoplasmic tail of  $\beta 1$  integrin alter integrin signaling. They also variably affect uropathogenic *E.*  
57  
58 *coli* entry into host cells, by either attenuating or boosting invasion frequencies (Eto *et al.*, 2007).  
59  
60

1  
2 Furthermore, focal adhesion and Src family kinases, which propagate integrin-linked signalling  
3  
4 and downstream cytoskeletal rearrangements, are shown to be required for FimH-dependent  
5  
6 bacterial invasion of target host cells. Cumulatively, these results indicate that  $\beta 1$  and  $\alpha 3$   
7  
8 integrins are functionally important receptors for type 1 pili-expressing bacterium within the  
9  
10 urinary tract and possibly at other sites within the host (Eto *et al.*, 2007).  
11  
12

13  
14 GP2 is the major membrane protein present in the pancreatic zymogen granule, and is  
15  
16 cleaved and released into the pancreatic duct along with exocrine secretions. The function of  
17  
18 GP2 is unknown. GP2's closest homologue is uromodulin, a protein expressed by the kidney that  
19  
20 shows 52% identity and 67% conservation in amino acid sequence. Uromodulin is secreted into  
21  
22 the urine and binds *E. coli* with Type 1 fimbriae. A role in host defense has been proposed in  
23  
24 which uromodulin serves as a molecular decoy that prevents bacteria from binding to uroplakin,  
25  
26 the host receptor in uroepithelia (Mo *et al.*, 2004; Pak *et al.*, 2001). In addition, two independent  
27  
28 laboratories (Mo *et al.*, 2004; Pak *et al.*, 2001) have produced uromodulin *null* mice that showed  
29  
30 increase sensitivity to urinary tract infections. Yu S & Lowe (2009) examined whether GP2 also  
31  
32 shares similar binding properties to bacteria with Type 1 fimbria. Commensal and pathogenic  
33  
34 bacteria, including *E. coli* and *Salmonella*, express type 1 fimbria. An *in vitro* binding assay was  
35  
36 used to assay the binding of recombinant GP2 to defined strains of *E. coli* that differ in their  
37  
38 expression of Type 1 fimbria or its subunit protein, FimH. Studies were also performed to  
39  
40 determine whether GP2 binding is dependent on the presence of mannose residues, which is a  
41  
42 known determinant for FimH binding. It was demonstrated that GP2 binds *E. coli* which  
43  
44 expresses Type 1 fimbria. Binding is dependent on GP2 glycosylation, and specifically the  
45  
46 presence of mannose residues. Thus, GP2 binds to Type 1 fimbria, a bacterial adhesin that is  
47  
48 commonly expressed by members of the *Enterobacteriaceae* family.  
49  
50  
51  
52  
53  
54  
55

56  
57 **PapG adhesin.** The most extensively studied adhesin, and also the first virulence-associated  
58  
59 factor identified for uropathogenic *E. coli* is P fimbria (Lane & Mobley, 2007), encoded by the  
60  
61 *pap* (pyelonephritis-associated pili) genes. P fimbria are prevalent among strains of

1  
2 uropathogenic *E. coli* causing pyelonephritis<sup>4</sup> and are characterized by their mannose-resistant  
3  
4 adherence to Gal(a1–4)Galb moieties present in the globoseries of membrane glycolipids on  
5  
6 human erythrocytes of the P blood group and on uroepithelial cells (Johnson, 1991; Jones *et al.*,  
7  
8 1996; Leffler & Svanborg-Edén, 1980, 1981). Three major and well-studied classes of *papG*  
9  
10 alleles exist, which encode the molecular variants of adhesin PapGI, -II, and -III. Each PapG  
11  
12 variant is known to have a distinct isoreceptor specificity, which in turn results in altered host  
13  
14 tissue tropism. PapGII, which is clinically associated with acute pyelonephritis in humans, binds  
15  
16 preferentially globoside, or GbO<sub>4</sub>, the predominant glycolipid isoreceptor of the human kidney.  
17  
18

19  
20 Both the solution structure of the PapGII adhesin domain and the crystal structure of the  
21  
22 PapGII receptor bound to GbO<sub>4</sub> as well as the unbound form of the adhesin have been  
23  
24 determined using NMR and the multiwavelength anomalous dispersion phasing method (Fig. 9;  
25  
26 Dodson *et al.*, 2001; Sung *et al.*, 2001).  
27  
28

29  
30 ***F17G/GafD adhesin.*** Bacterial adhesion to intestinal surfaces is important for successful  
31  
32 colonization, and a number of fimbrial adhesins expressing differing receptor-binding  
33  
34 specificities and serological properties have been detected on enterotoxigenic *E. coli* from  
35  
36 different hosts (Nataro & Kaper, 1998). The G fimbria is most closely related to the F17c  
37  
38 fimbriae that are common on bovine septicemic and diarrhea-associated *E. coli* (Saarela *et al.*,  
39  
40 1995) and they occur in human *E. coli* infections as well (Le Bouguéneç & Bertin, 1999). The G  
41  
42 fimbriae bind to the terminal N-acetyl-D-glucosamine (GlcNAc) residues of glycoproteins at calf  
43  
44 intestinal brush borders as well as mammalian basement membrane (Saarela *et al.*, 1996; Sanchez  
45  
46 *et al.*, 1993). The latter is thought to potentiate translocation of the enterotoxigenic *E. coli* into  
47  
48 circulation. G fimbrial binding to GlcNAc receptors is mediated by the 321 amino acid residue  
49  
50 GafD lectin subunit (Saarela *et al.*, 1995) present mainly at the G-fimbrial tip (Saarela, 1999). The  
51  
52 structure of the ligand-binding domain, GafD1-178, has been determined at 1.7 Å resolution in  
53  
54 the presence of the receptor sugar N-acetyl-D-glucosamine (Fig. 9; Merckel *et al.*, 2003). As in  
55  
56 N-terminal adhesin PapG and FimH domains the overall fold of GafD1-178 is a β-barrel jelly-  
57  
58  
59  
60

roll fold. The ligand-binding site was identified and localized to the side of the molecule. Receptor binding is mediated by side-chain as well main-chain interactions. Ala43-Asn44, Ser116-Thr117 form the sugar acetamide specificity pocket, while Asp88 confers tight binding and Trp109 appears to position the ligand. There is a disulfide bond that rigidifies the acetamide specificity pocket.

**MrkD adhesin.** Li *et al.* (2009) expressed in *E. coli* and purified to homogeneity the recombinant adhesin MrkD of *K. pneumoniae*. The adhesive activity of MrkD was examined and the binding site was studied with the laser confocal microscopy. The adherent activity of *K. pneumoniae* was significantly inhibited by MrkD showing that MrkD putative adhesin contains adhesion epitopes.

### Anti-Immune and Pro-Inflammatory Activities of Adhesive Organelles

**Features of anti-immune and pro-inflammatory activities of poly- and mono-adhesive organelles.** In contrast to mono-adhesive pili, which possess only one binding domain on the tip of pilus (Fig. 12a), each poly-adhesive fiber potentially might (Fig. 12b):

- (1) Ensure a powerful polyvalent fastening of a bacterial pathogen to a host target cell (Galván *et al.*, 2006);
- (2) Aggregate host cell receptors and trigger transduction of signals causing immunosuppressive and pro-inflammatory responses (Galván *et al.*, 2006; Sharma *et al.*, 2005a,b; Sodhi *et al.*, 2004);
- (3) Pull a bacterium to a host cell by a zipper-like mechanism that increases tightness of the contact.

It was directly demonstrated that Psa fimbriae (pH6 antigen) of *Y. pestis* are functioning as polyadhesins (Galván *et al.*, 2006). The Psa fimbriae bound to phosphatidylcholine in a dose-dependent manner and binding was inhibited by phosphorylcholine and choline. Binding inhibition was dose-dependent, although only high concentrations of phosphorylcholine

1  
2 completely blocked Psa binding to phosphatidylcholine. In contrast, less than 1  $\mu\text{M}$  of a  
3  
4 phosphorylcholine-polylysine polymer inhibited specifically the adhesion of Psa-fimbriated *E.*  
5  
6  
7 *coli* to phosphatidylcholine, and type I (WI-26 VA4) and type II alveolar epithelial cells.  
8

9 A tight contact between interacting cells hampers diffusion of  $\text{Ca}^{+2}$  in the site of contact, and,  
10 consequently, triggers  $\text{Ca}^{+2}$ -dependent Type III secretion system (encoded by the pCD1  
11 virulence plasmid) that destroys defense activity of the host cell (Cornelis & Wolf-Watz, 1997;  
12 Viboud & Bliska, 2005). This is extremely important for the bacterial virulence. In particular, *Y.*  
13  
14 *pestis* appears to utilize the Type III secretion pathway to destroy cells with innate immune  
15 functions (macrophages, dendritic cells and neutrophils) that represent the first line of defence,  
16 thereby preventing adaptive responses and precipitating the fatal outcome of plague (Marketon *et*  
17  
18 *al.*, 2005). It was found that dendritic cells infected with *Y. pestis* failed to adhere to solid  
19 surfaces and to migrate toward the chemokine CCL19, in an *in vitro* transmembrane assay. Both  
20 effects were dependent on presence of a pCD1 plasmid, and on bacterial growth shift to 37°C,  
21 prior to infection (Velan *et al.*, 2006). Moreover, while instillation of a pCD1-cured *Y. pestis*  
22 strain into mice airways triggered effective transport of alveolar dendritic cells to the mediastinal  
23 lymph node, instillation of *Y. pestis* harboring the plasmid failed to do so. Taken together, these  
24 results suggest that pCD1 virulence-plasmid dependent impairment of dendritic cell migration is  
25 the major mechanism utilized by *Y. pestis* to subvert dendritic cell function.  
26  
27  
28  
29  
30  
31  
32  
33  
34  
35  
36  
37  
38  
39  
40  
41  
42  
43

44 **Contribution of polyadhesins to virulence and anti-immune activity of bacteria.** The  
45 most important structure-functional information by now was obtained for the Afa/Dr adhesins.  
46  
47

48 Nowicki *et al.* (1994) found gestational age-dependent distribution of *E. coli* fimbriae in  
49 pregnant patients with pyelonephritis. Later Hart *et al.* (1996) indicated that it is likely that *E.*  
50  
51 *coli* associated with acute pyelonephritis during different trimesters of pregnancy represents non-  
52 random closely related isolates, and some of these strains may be characteristic in pregnant  
53 patients only. Nowicki *et al.* (1997) demonstrated that the rate of uterine infection in pregnant  
54 rats was about 10-fold higher than in non-pregnant animals. It was proposed that infectious  
55  
56  
57  
58  
59  
60



1 complications of pregnancy may be related to gestation-dependent sensitivity to the pathogenic  
2 microorganism and the host nitric oxide, NO, status. Fang *et al.* (1999) with  
3 immunofluorescence studies indicated that macrophages and natural killer cells, located in the  
4 endometrial layer clustering around epithelial cells, expressed type II protein. They suggested  
5 that localized increase in type II NO synthase (NOS) expression and NO production occurs in  
6 response to intrauterine infection while the NO system may play a role in host response to  
7 restrict the infection. Moreover, Fang *et al.* (2001) demonstrated that intrauterine infection  
8 induced an elevated expression of tumor necrosis factor (TNF)- $\alpha$  in both non-pregnant and  
9 pregnant rats. The sequential stimulation of NOS expression, especially the inducible isoform,  
10 and generation of uterine NO may be lacking during pregnancy despite of an elevated TNF- $\alpha$   
11 after infection. Fang *et al.* (2001) indicated that NO synthesis response may be maximal at  
12 pregnancy, and infection may not further induce the NO system. These studies, together with the  
13 previous report (Fang *et al.*, 1999) suggest that intrauterine infection-induced lethality in  
14 pregnant rats is amplified with the inhibition of NO and that pregnancy is a state predisposed for  
15 increased complications associated with intrauterine infection. The constitutively elevated uterine  
16 NO during pregnancy may help reduce the risk of infection-related complications.

17 Kaul *et al.* (1999) reported that expression of CD55/DAF protein, recognized by adhesin Dr  
18 of diffusially adhering *E. coli* as the host tissue receptor, is increased during pregnancy.  
19 Induction of pathogenesis is a cumulative process of the host-pathogen relationship involving  
20 specific host factors and virulence characteristics of the invading organism. Kaul *et al.* (1999)  
21 developed an experimental model of chronic pyelonephritis with *E. coli* bearing adhesin Dr (*E.*  
22 *coli* Dr1) in non-pregnant lipopolysaccharide-hypo-responder C3H/HeJ mice. With this model the  
23 role of *E. coli* Dr1 was investigated on the outcome of pregnancy in C3H/HeJ mice. Groups of  
24 pregnant mice were infected with *E. coli* Dr1 or its isogenic mutant which does not bear the  
25 adhesin Dr (*E. coli* Dr2) by urethral catheterization. Nearly 90% of pregnant mice infected with  
26 *E. coli* Dr1 delivered preterm (before 90% gestation) compared to 10% of mice infected with *E.*  
27 *coli* Dr2.

1  
2 *coli* Dr2 but none of the mice treated with phosphate-buffered saline (PBS). There was a  
3  
4 significant reduction in fetal birth weight in the *E. coli* Dr1-infected group compared to the *E.*  
5  
6 *coli* Dr2- and PBS-treated groups ( $P = 0.003$ ) (Kaul *et al.*, 1999). Goluszko *et al.* (2001) used a  
7  
8 gentamycin protection assay to assess the ability of gestational pyelonephritis isolates of *E. coli*  
9  
10 to invade HeLa cells. The ability to enter HeLa cells was strongly associated with the presence of  
11  
12 *dra* gene clusters coding adhesins Dr. In contrast, the noninvasive isolates predominantly  
13  
14 expressed *papG*, coding P fimbriae. Hart *et al.* (2001) found significant increase of ampicillin  
15  
16 resistance among gestational pyelonephritis *E. coli* and the association with the *dra* gene cluster  
17  
18 encoding colonization and invasive capacity.  
19  
20  
21  
22

23  
24 It was found that the family of adhesins Dr, like Type 1 fimbriae, mediated concentration-  
25  
26 dependent adherence to human neutrophils (PMNs) (Johnson *et al.*, 1995). Adherence to human  
27  
28 neutrophils was mannose sensitive for Type 1 fimbriae but mannose resistant for Dr family  
29  
30 adhesins. Chloramphenicol inhibited PMNs adherence for the hemagglutinin Dr with the same  
31  
32 potency as that with which it inhibited hemagglutination, but it was inactive against PMN  
33  
34 adherence and hemagglutination mediated by other members of the adhesin Dr family. In  
35  
36 contrast to PMN adherence, mediated by type 1 fimbriae, the adherence, mediated by the  
37  
38 hemagglutinin Dr, did not lead to significantly increased bacterial killing. These data suggest that  
39  
40 family of adhesins Dr mediate a novel pattern of adherence to PMNs, probably by recognizing  
41  
42 CD55/DAF, with minimal consequent bacterial killing.  
43  
44  
45  
46

47  
48 Peiffer *et al.* (1998) studied F-actin rearrangements in the host cells expressing CD55/DAF  
49  
50 protein as a result of attachment of *E. coli* strain bearing adhesin Dr. Infection of INT407 cells  
51  
52 by the diffusely adhering strain *E. coli* C1845 (DAEC C1845) can provoke dramatic F-actin  
53  
54 rearrangements without cell entry. Clustering of phosphotyrosines was observed, revealing that  
55  
56 the DAEC C1845- CD55/DAF F interaction involves recruitment of signal transduction  
57  
58 molecules. DAEC C1845-induced F-actin rearrangements can be blocked dose dependently by  
59  
60 protein tyrosine kinase, phospholipase C $\gamma$ , phosphatidylinositol 3-kinase, protein kinase C, and

1  
2 Ca21 inhibitors. F-actin rearrangements and blocking by inhibitors were observed after infection  
3  
4 of the cells with two *E. coli* recombinants carrying the plasmids containing the fimbrial adhesin  
5  
6 F1845 or the fimbrial hemagglutinin Dr, belonging to the same family of adhesins. Thus, DAEC  
7  
8 Dr family of pathogens promotes alterations in the intestinal cell cytoskeleton by piracy of the  
9  
10 CD55/DAF -GPI signal cascade without bacterial cell entry. Later Peiffer *et al.* (2000a) provided  
11  
12 evidence that infection of the polarized human intestinal cell line Caco-2/TC7 by strain C1845 is  
13  
14 followed by an increase in the paracellular permeability for [<sup>3</sup>H]-mannitol without a decrease of  
15  
16 the transepithelial resistance of the monolayers. Alterations in the distribution of tight-junction-  
17  
18 associated occludin and ZO-1 protein were observed, whereas the distribution of the zonula  
19  
20 adherens-associated E-cadherin was not affected. Using the recombinant *E. coli* strains HB101-  
21  
22 (pSSS1) and - (pSSS1C) expressing the F1845 fimbrial adhesin, it was demonstrated that the  
23  
24 adhesin- CD55/DAF interaction is not sufficient for the induction of structural and functional  
25  
26 tight-junction lesions (Peiffer *et al.*, 2000). Moreover, using the actin filament-stabilizing agent  
27  
28 Jaspilakinolide, Peiffer *et al.*, 2000 demonstrated that the C1845-induced functional alterations in  
29  
30 tight-junctions are independent of the C1845-induced apical cytoskeleton rearrangements. The  
31  
32 results indicated that pathogenic factor(s) other than F1845 adhesin may be operant in Afa/Dr  
33  
34 DAEC C1845. Infection of human intestinal Caco-2/TC7 cells by the Afa/Dr DAEC strains  
35  
36 C1845 and IH11128 causes clustering of CD55/DAF around adhering bacteria (Guignot *et al.*,  
37  
38 2000). Mapping of CD55/DAF epitopes involved in CD55/DAF clustering by Afa/Dr DAEC  
39  
40 was conducted with CD55/DAF deletion mutants expressed by stable transfection in CHO cells.  
41  
42 Deletion in the short consensus repeat 1 (SCR1) domain abolished Afa/Dr DAEC-induced  
43  
44 CD55/DAF clustering. In contrast, deletion in the SCR4 domain does not modify Afa/Dr DAEC-  
45  
46 induced CD55/DAF clustering. It was shown that the brush border-associated  
47  
48 glycosylphosphatidylinositol (GPI)-anchored protein CD66e/CEA (carcinoembryonic antigen) is  
49  
50 recruited by the Afa/Dr DAEC strains C1845 and IH11128. This conclusion is based on the  
51  
52 observations that (i) infection of Caco-2/TC7 cells by Afa/Dr DAEC strains is followed by  
53  
54  
55  
56  
57  
58  
59  
60

1  
2 clustering of CD66e/CEA around adhering bacteria and (ii) Afa/Dr DAEC strains bound  
3  
4 efficiently to stably transfected HeLa cells expressing CD66e/CEA, accompanied by  
5  
6 CD66e/CEA clustering around adhering bacteria.  
7

8  
9 Inhibition assay with monoclonal antibodies directed against CD55/DAF SCR domains, and  
10  
11 polyclonal anti- CD55/DAF and anti- CD66e/CEA antibodies demonstrate that CD55/DAF and  
12  
13 CD66e/CEA function as receptors for the C1845 and IH11128 bacteria. Moreover, using  
14  
15 structural *draE* gene mutants, Guignot *et al.* (2000) found that a mutant in which cysteine  
16  
17 replaces aspartic acid at position 54 displayed conserved the binding capacity but failed to  
18  
19 induce CD55/DAF and CD66e/CEA clustering. Peiffer *et al.* (2000b) further characterized cell  
20  
21 injuries following the interaction of wild-type Afa/Dr DAEC strains C1845 and IH11128  
22  
23 expressing fimbrial F1845 adhesin and hemagglutinin Dr, respectively, with polarized, fully  
24  
25 differentiated Caco-2/TC7 cells. In both cases, bacterium-cell interaction was followed by  
26  
27 rearrangement of the major brush border-associated cytoskeletal proteins F-actin, villin, and  
28  
29 fimbrin; proteins which play a pivotal role in brush border assembly. In contrast, distribution of  
30  
31 G-actin, actin-depolymerizing factor, and tubulin was not modified. Peiffer *et al.* (2000b) found  
32  
33 that a mutant in which cysteine replaces aspartic acid at position 54 conserved the binding  
34  
35 capacity but failed to induce F-actin disassembly. Distribution of brush border-associated  
36  
37 functional proteins sucrase-isomaltase, dipeptidylpeptidase IV, glucose transporter SGLT1, and  
38  
39 fructose transporter GLUT5 was dramatically altered. In parallel, sucrase-isomaltase and  
40  
41 dipeptidylpeptidase IV enzyme activity decreased.  
42  
43  
44  
45  
46  
47  
48

49 Selvarangan *et al.* (2004) constructed an isogenic mutant in the DraE adhesin subunit that  
50  
51 was unable to bind type IV collagen but retained binding to CD55/DAF and examined its  
52  
53 virulence in the mouse model. The collagen-binding mutant DrI113T was eliminated from the  
54  
55 mouse renal tissues in 6 to 8 weeks, while the parent strain caused persistent renal infection  
56  
57 which lasted at least for 14 weeks. Trans-complementation with the intact operon *dra* restored  
58  
59 collagen-binding activity, interstitial tropism, and the ability to cause persistent renal infection. It  
60

1  
2 was concluded that type IV collagen binding mediated by DraE adhesin is a critical step for the  
3  
4 development of the infection in murine model of *E. coli* pyelonephritis.  
5

6  
7 Brest *et al.* (2004) found that infection of polymorphonuclear leukocytes by Afa/Dr DAEC  
8  
9 strains induced PMNL apoptosis characterized by morphological nuclear changes, DNA  
10  
11 fragmentation, caspase activation, and a high level of annexin V expression. PMNL apoptosis  
12  
13 depended on their agglutination, induced by Afa/Dr DAEC, and was still observed after  
14  
15 preincubation of PMNs with anti-CD55/DAF and/or anti-CD66e/CEA antibodies. Low levels of  
16  
17 phagocytosis of Afa/Dr DAEC strains were observed both in nontransmigrated and in  
18  
19 transmigrated polymorphonuclear leukocytes compared to that observed with the control *E. coli*  
20  
21 DH5 $\alpha$  strain. Interaction of Afa/Dr DAEC with polymorphonuclear leukocytes may increase the  
22  
23 bacterial virulence both by inducing apoptosis of polymorphonuclear leukocytes through an  
24  
25 agglutination process and by diminishing their phagocytic capacity.  
26  
27  
28  
29

30  
31 Wroblewska-Seniuk *et al.* (2005) investigated the role of the *afaE* and *afaD* genes in the  
32  
33 mortality of pregnant rats from intrauterine infection, using *afaE* and/or *afaD* mutants. The  
34  
35 highest maternal mortality was observed in the group infected with the *afaE*<sup>+</sup> *afaD*<sup>+</sup> strain,  
36  
37 followed by the group infected with the *afaE*<sup>+</sup> *afaD* strain. The *afaE* *afaD* double mutant did not  
38  
39 cause maternal mortality, even with the highest infection dose. The *in vivo* studies corresponded  
40  
41 with the invasion assay, where the *afaE*<sup>+</sup> strains were the most invasive (*afaE*<sup>+</sup> *afaD* strain >  
42  
43 *afaE*<sup>+</sup> *afaD*<sup>+</sup> strain), while the *afaE* mutant strains (*afaE* *afaD*<sup>+</sup> and *afaE* *afaD* strains) seemed to  
44  
45 be noninvasive. This study shows for the first time that the *afaE* gene coding the AfaE subunit of  
46  
47 Dr/Afa adhesin is involved in the lethal outcome of gestational infection in rats. This lethal effect  
48  
49 associated with AfaE correlates with the invasiveness of *afaE*<sup>+</sup> *E. coli* strains *in vitro*.  
50  
51  
52  
53

54  
55 Korotkova *et al.* (2008b) demonstrated that CD55/DAF or CEACAM receptors  
56  
57 independently promote DraE mediated internalization of *E. coli* by CHO cell transfectants  
58  
59 expressing these receptors. They also found that DraE-positive recombinant bacteria adhere to  
60  
and are internalized by primary human bladder epithelial cells which express CD55/DAF and

1  
2 CEACAMs. DraE-mediated bacterial internalization by bladder cells was inhibited by agents,  
3  
4 which disrupt lipid rafts, microtubules, and phosphatidylinositol 3-kinase (PI3K) activity.  
5  
6 Immunofluorescence confocal microscopic examination of epithelial cells detected considerable  
7  
8 caveolin,  $\beta$ 1 integrin, phosphorylated ezrin, phosphorylated PI3K, and tubulin, but not F-actin,  
9  
10 by cell-associated bacteria. DraD subunit, previously implicated as an “invasin,” is not required  
11  
12 for  $\beta$ 1 integrin recruitment or bacterial internalization. Guignot *et al.* (2009) also provided  
13  
14 evidence that AfaD or DraD putative invasins do not participate in the cell-association  
15  
16 and -entry of bacteria, whereas DraE or AfaE-III adhesin subunits are necessary and sufficient to  
17  
18 promote the receptor-mediated bacterial internalization into epithelial cells expressing  
19  
20 CD55/DAF, CEACAM1, CD66e/CEA, or CEACAM6. They confirmed independently data of  
21  
22 Korotkova *et al.* (2008b) that internalization of Dr fimbriae-positive *E. coli* within CHO-  
23  
24 CD55/DAF, -CEACAM1, -CD66e/CEA, or -CEACAM6 cells occurs through microtubule- and  
25  
26 lipid rafts-dependent mechanism. Wild-type Dr fimbriae-positive bacteria survived more than  
27  
28 within cells expressing CD55/DAF as compared with bacteria internalized within CHO-  
29  
30 CEACAM1, -CD66e/CEA, or -CEACAM6 cells (Guignot *et al.*, 2009).  
31  
32  
33  
34  
35  
36

37  
38 Korotkova *et al.* (2007) supposed that immune escape is considered to be the driving force  
39  
40 behind structural variability of major antigens on the surface of bacterial pathogens, such as  
41  
42 fimbriae. In the family Dr of *E. coli* adhesins, structural and adhesive functions are carried out by  
43  
44 the same subunit. Adhesins Dr have been shown to bind CD55/DAF, collagen IV, and  
45  
46 CEACAMs. They showed that genes encoding adhesins Dr from 100 *E. coli* strains form eight  
47  
48 structural groups with a high level of amino acid sequence diversity between them. However,  
49  
50 genes comprising each group differ from each other by only a small number of point mutations.  
51  
52 Out of 66 polymorphisms identified within the groups, only three were synonymous mutations,  
53  
54 indicating strong positive selection for amino acid replacements. Functional analysis of  
55  
56 intragroup variants comprising the haemagglutinin Dr (DraE) group revealed that the point  
57  
58 mutations result in distinctly different binding phenotypes, with a tendency of increased affinity  
59  
60



1  
2 to CD55/DAF, decreased sensitivity of CD55/DAF binding to inhibition by chloramphenicol,  
3  
4 and loss of binding capability to collagen, CEACAM3 and CEACAM6. Thus, variability by  
5  
6 point mutation of major antigenic proteins on the bacterial surface can be a signature of selection  
7  
8 for functional modification.  
9

10  
11  
12 **F1 antigen.** *Y. pestis* is the etiologic agent of bubonic and pneumonic plague, one of the most  
13  
14 deadly diseases known to man (Cleri *et al.*, 1997; Li *et al.*, 2009; Perry & Fetherston, 1997;  
15  
16 Smiley, 2008a, b). Electron micrographs of *Y. pestis* demonstrate that F1 antigen forming capsule  
17  
18 is maximally expressed at 37°C after 72 hours of cultivation *in vitro* (Chen & Elberg, 1977). The  
19  
20 expression of F1 antigen at 22°C is negligible (Chen & Elberg, 1977). During the early stages of  
21  
22 infection, when the F1 capsule is not yet formed, type III secretion system protects *Y. pestis* from  
23  
24 phagocytosis (Cornelis & Wolf-Watz, 1997; Viboud & Bliska, 2005). This system is encoded on  
25  
26 a virulence plasmid of 70 kb in size that is common to *Y. pestis*, *Y. pseudotuberculosis*, and *Y.*  
27  
28 *enterocolitica*. After 24-h of cultivation *in vitro* at 37°C, *Y. pestis* expresses enough large  
29  
30 capsule-like structure composed of aggregating F1 antigen (Chen & Elberg, 1977). The capsule  
31  
32 material is readily soluble and dissociates from the bacterium during *in vitro* cultivation.  
33  
34 Association of F1 antigen with virulence is evident from recent studies since all F1<sup>□</sup> mutants  
35  
36 were of low virulence to mice compared with the wild types (Welkos *et al.*, 2004). Similar to  
37  
38 other capsules or capsule-like antigens, F1 seems to be involved in the antiphagocytic activity  
39  
40 reported for *Y. pestis*, but the contribution of F1 to this activity was not understood until recently.  
41  
42 *Y. pestis* strain EV76 is highly resistant to uptake by J774 cells (Du *et al.*, 2002). *Y. pestis* strain  
43  
44 EV76 with an in-frame deletion of the *cafIM* gene fails to express F1 polymer on the bacterial  
45  
46 surface. This strain had somewhat lowered ability to prevent uptake by J774 cells. Strain EV76C,  
47  
48 cured with the virulence plasmids, was much reduced in its ability to resist uptake. A strain  
49  
50 lacking both the virulence plasmid and *cafIM* was almost totally phagocytosed (95%; Du *et al.*,  
51  
52 2002). It was concluded that F1 and the type III secretion system act in concert to make *Y. pestis*  
53  
54 highly resistant to phagocytosis. Type III secretion system of *Y. pestis* may function optimally  
55  
56  
57  
58  
59  
60



1  
2 only during early stages of infection, when the contact-dependent delivery of Yop effector  
3  
4 proteins is the highest. Later on, when the surface of *Y. pestis* is covered with the F1 capsule, the  
5  
6 delivery of Yop effector proteins may be lower. While the expression of F1 capsule reduces the  
7  
8 number of bacteria that interacts with the macrophages, it does not influence on the general  
9  
10 phagocytic ability of J774 cells (Du *et al.*, 2002). This suggests that F1 capsule prevents uptake  
11  
12 by interfering at the level of receptor interaction in the phagocytosis process. Sebbane *et al.*  
13  
14 (2009) found that a *caf*<sup>□</sup> *Y. pestis* mutant was neither impaired in flea colonization nor in  
15  
16 virulence in mice after intradermal inoculation of cultured bacteria. In contrast, absence of the  
17  
18 *caf* operon decreased bubonic plague incidence after fleabite. Successful development of plague  
19  
20 in mice infected by fleabite with the *caf*<sup>□</sup> mutant required a higher number of infective bites per  
21  
22 challenge. In addition, the mutant displayed a highly autoaggregative phenotype in infected liver  
23  
24 and spleen. The results suggest that acquisition of the *caf* locus via horizontal transfer by an  
25  
26 ancestral *Y. pestis* increased transmissibility and the potential for epidemic spread. Sebbane *et al.*  
27  
28 (2009) suggested a model in which atypical *caf*<sup>□</sup> strains could emerge during climatic conditions  
29  
30 that favor a high flea burden. Human infection with such strains would not be diagnosed by the  
31  
32 standard clinical tests that detect F1 antibody or antigen, suggesting that more comprehensive  
33  
34 surveillance for atypical *Y. pestis* strains in plague foci may be necessary.  
35  
36  
37  
38  
39  
40  
41  
42

43  
44 *Y. pestis* survives and replicates in phagosomes of murine macrophages. *Y. pestis* -containing  
45  
46 vacuoles (YCVs) acquire markers of late endosomes or lysosomes in naïve macrophages and that  
47  
48 this bacterium can survive in macrophages activated with IFN- $\gamma$ . An autophagic process known  
49  
50 as xenophagy, which destroys pathogens in acidic autophagolysosomes, can occur in naïve  
51  
52 macrophages and is upregulated in activated macrophages. Studies on mechanism of *Y. pestis*  
53  
54 survival in phagosomes of naïve and activated macrophages were undertaken to determine if the  
55  
56 pathogen avoids or co-opts autophagy. Colocalization of the YCV with markers of  
57  
58 autophagosomes or acidic lysosomes and the pH of the YCV were determined by microscopic  
59  
60 imaging of infected macrophages (Pujol *et al.* 2009). Some YCVs contained double membranes

1  
2 characteristic of autophagosomes, as determined by electron microscopy. Fluorescence  
3  
4 microscopy showed that approximately 40% of YCVs colocalized with green fluorescent protein  
5  
6 (GFP)-LC3, a marker of autophagic membranes, and that YCVs failed to acidify below pH 7 in  
7  
8 naïve macrophages. Replication of *Y. pestis* in naïve macrophages caused accumulation of LC3-  
9  
10 II, as determined by immunoblotting. While activation of infected macrophages increased LC3-II  
11  
12 accumulation, it decreased the percentage of GFP-LC3-positive YCVs (approximately 30%). A  
13  
14 viable count assay showed that *Y. pestis* survived equally well in macrophages proficient for  
15  
16 autophagy and macrophages rendered deficient for this process by Cre-mediated deletion of  
17  
18 ATG5, showing that this pathogen does not require autophagy for intracellular replication. Pujol  
19  
20 *et al.* (2009) concluded that although YCVs can acquire an autophagic membrane and  
21  
22 accumulate LC3-II, the pathogen avoids xenophagy by preventing vacuole acidification.  
23  
24  
25  
26  
27  
28

29 **pH6 antigen.** The pH6 antigen was first described more than 40 years ago and was initially  
30  
31 identified as an antigen expressed only at pH below 6 at 37°C (Ben-Efraim *et al.*, 1961). The  
32  
33 electron micrographs of highly virulent phenotype *Y. pestis* grown at 37°C, pH6, indicate the  
34  
35 expression both the F1 capsule and thin filaments of pH6 (PsaA) antigen on the bacterial surface  
36  
37 (Lindler & Tall, 1993). The pH6 antigen is essential for full virulence of *Y. pestis* (Lindler *et al.*,  
38  
39 1991; Lindler & Tall, 1993). A  $\Delta$ *psaA* mutant had a significant dissemination defect after  
40  
41 subcutaneous infection but only slight attenuation by the pneumonic-disease model indicating  
42  
43 different roles of the pH6 antigen in bubonic and pneumonic plague (Cathelyn *et al.*, 2006). The  
44  
45 expression of pH6 antigen adds to the antiphagocytic armament of the bacterium (Huang &  
46  
47 Lindler, 2004). *Y. pestis* *psaA* isogenic strains do not show any significant difference in their  
48  
49 association with mouse macrophage cells. However, expression of *psaA* appeared to reduce  
50  
51 significantly phagocytosis of both *Y. pestis* and *E. coli* by mouse macrophages ( $P < 0.05$ ).  
52  
53 Furthermore, complementation of *psaA* mutant of *Y. pestis* strains could completely restore the  
54  
55 bacterial resistance to phagocytosis. Fluorescence microscopy following differential labeling of  
56  
57 intracellular and extracellular portion of *Y. pestis* revealed that significantly lower numbers of  
58  
59  
60

1  
2 *psaA*-expressing bacteria were located inside the macrophages. Enhanced phagocytosis  
3  
4 resistance was specific for bacteria expressing *psaA* and did not influence the ability of the  
5  
6 macrophages to engulf other bacteria. This shows that *Y. pestis* pH6 antigen does not enhance  
7  
8 adhesion to macrophages but rather promotes resistance to phagocytosis helping the bacteria to  
9  
10 escape host immune defence mechanisms (Huang & Lindler, 2004). Recently Anisimov *et al.*  
11  
12 (2009) generated by site-directed mutagenesis of the *psa* operon and subsequent  
13  
14 complementation in trans two isogenic sets of *Y. pestis* strains, composed of wild-type strains  
15  
16 231 and I-1996, their non-polar pH6<sup>□</sup> mutants with deletions in the *psaA* gene or the whole  
17  
18 operon, as well as strains with restored ability for temperature- and pH-dependent synthesis of  
19  
20 adhesion fimbriae or constitutive production of pH6 antigen. It was shown that the loss of  
21  
22 synthesis or constitutive production of pH6 antigen did not influence *Y. pestis* virulence or the  
23  
24 average survival time of subcutaneously inoculated BALB/c naïve mice or animals immunized  
25  
26 with this antigen.  
27  
28  
29  
30  
31

32  
33 ***SefD putative invasin.*** The translocation of the minor putative invasin SefD subunit is a  
34  
35 prerequisite for the export of the major structural SefA subunit across the outer membrane and  
36  
37 formation of the SEF14 fimbriae (Edwards, Matlock & Maloy, unpublished observations); thus,  
38  
39 SefD is probably located at the tip of the fimbrial shaft (Edwards *et al.*, 2000). The LD50 values  
40  
41 for the wild-type strain and mutants lacking SefA are comparable, but both the oral and intra-  
42  
43 peritoneal virulence of mutants lacking SefD are greatly reduced. It means that major SEF14  
44  
45 subunit SefA is not required for the virulence of *S. enteritidis*, indicating that the tip of the  
46  
47 fimbrial structure composed of SefD subunits is probably sufficient for successful interactions  
48  
49 with phagocytes (Edwards *et al.*, 2000). SefD may bind to a receptor on the macrophage surface  
50  
51 and alter the uptake of *S. enteritidis* into the phagocyte so that *S. enteritidis* can survive in the  
52  
53 intracellular environment.  
54  
55  
56  
57

58  
59 ***Polyadhesin Ral.*** Hart *et al.* (2009) investigated the contribution of a fimbrial polyadhesin,  
60  
Ral, of rabbit-specific EPEC (REPEC) to host specificity by introducing Ral into derivatives of

1 human-specific EPEC (hEPEC) strain, E2348/69, in which expression of the fimbrial adhesin,  
2 Bfp, had been interrupted. Although unable to cause diarrhoeal disease in rabbits, Ral-bearing  
3 hEPEC strains colonised rabbit intestine more efficiently and showed altered intestinal  
4 localisation when compared to an isogenic Ral<sup>+</sup> strain. These findings suggest that Ral enhances  
5 the initial interaction between a  $\Delta bfpA$  mutant of hEPEC and rabbit intestine and may influence  
6 tissue specificity, but is not sufficient on its own to transform hEPEC into a rabbit pathogen.  
7  
8  
9  
10  
11  
12  
13  
14  
15

16 **Contribution of monoadhesins to virulence. Type 1 fimbriae.** Urinary tract infection is the  
17 second most common infectious disease and is caused predominantly by Type 1-fimbriated  
18 uropathogenic *E. coli* (UPEC). UPEC initiates infection by attaching to uroplakin (UP) Ia, its  
19 urothelial surface receptor, via the FimH adhesins capping the distal end of its fimbriae. UP Ia,  
20 together with UP Ib, UP II, and UP IIIa, forms a 16-nm receptor complex that is assembled into  
21 hexagonally packed, two-dimensional crystals (urothelial plaques) covering >90% of the  
22 urothelial apical surface. Recent studies indicate that FimH is the invasin of UPEC as its  
23 attachment to the urothelial surface can induce cellular signaling events including calcium  
24 elevation and the phosphorylation of the UP IIIa cytoplasmic tail, leading to cytoskeletal  
25 rearrangements and bacterial invasion. However, it remains unknown how the binding of FimH  
26 to the UP receptor triggers a signal that can be transmitted through the highly impermeable  
27 urothelial apical membrane. Wang et al. (2009) showed by cryo-electron microscopy that FimH  
28 binding to the extracellular domain of UP Ia induces global conformational changes in the entire  
29 UP receptor complex, including a coordinated movement of the tightly bundled transmembrane  
30 helices. This movement of the transmembrane helix bundles can cause a corresponding lateral  
31 translocation of the UP cytoplasmic tails, which can be sufficient to trigger downstream  
32 signaling events. The results suggest a novel pathogen-induced transmembrane signal  
33 transduction mechanism that plays a key role in the initial stages of UPEC invasion and receptor-  
34 mediated bacterial invasion in general.  
35  
36  
37  
38  
39  
40  
41  
42  
43  
44  
45  
46  
47  
48  
49  
50  
51  
52  
53  
54  
55  
56  
57  
58  
59  
60

1  
2 Enteropathogenic *E. coli* (EPEC) produce attaching/effacing (A/E) lesions on eukaryotic  
3 cells mediated by the outer membrane adhesin intimin. EPECs are sub-grouped into typical  
4 (tEPEC) and atypical (aEPEC). aEPEC strain 1551-2 (serotype O non-typable, non-motile)  
5  
6 (tEPEC) and atypical (aEPEC). aEPEC strain 1551-2 (serotype O non-typable, non-motile)  
7  
8 invades HeLa cells by a process dependent on the expression of intimin sub-type omicron.  
9  
10 Yamamoto *et al.* (2009) showed that invasion of HeLa cells by aEPEC 1551-2 depends on actin  
11  
12 filaments, but not on microtubules. In addition, disruption of tight junctions enhanced its  
13  
14 invasion efficiency in T84 cells, suggesting preferential invasion via a non-differentiated surface.  
15  
16 It was concluded that some aEPEC strains may invade intestinal cells *in vitro* with varying  
17  
18 efficiencies and independently of the intimin sub-type.  
19  
20  
21  
22

23 FimH, the mannose-specific, Type 1 fimbrial adhesin of *E. coli*, acquires amino acid  
24  
25 replacements adaptive in extraintestinal niches (the genitourinary tract) but detrimental in the  
26  
27 main habitat (the large intestine). This microevolutionary dynamics is reminiscent of an  
28  
29 ecological "source-sink" model of continuous species spread from a stable primary habitat  
30  
31 (source) into transient secondary niches (sink), with eventual extinction of the sink-evolved  
32  
33 populations. Chattopadhyay *et al.* (2007) adapted two ecological analytical tools - diversity  
34  
35 indexes DS and alpha - to compare size and frequency distributions of *fimH* haplotypes between  
36  
37 evolutionarily conserved FimH variants ("source" haplotypes) and FimH variants with adaptive  
38  
39 mutations (putative "sink" haplotypes). Both indexes show two- to three-fold increased diversity  
40  
41 of the sink *fimH* haplotypes relative to the source haplotypes, a pattern that ran opposite to those  
42  
43 seen with nonstructural fimbrial genes (*fimC* and *fimI*) and housekeeping loci (*adk* and *fumC*) but  
44  
45 similar to that seen with another fimbrial adhesin of *E. coli*, papG-II, also implicated in  
46  
47 extraintestinal infections. The increased diversity of the sink pool of adhesin genes is due to the  
48  
49 increased richness of the number of unique haplotypes, rather than their extent of similarity in  
50  
51 relative abundances. Taken together, this pattern supports a continuous emergence and extinction  
52  
53 of the gene alleles adaptive to virulence sink habitats of *E. coli*, rather than a one-time change in  
54  
55 the habitat conditions. Thus, ecological methods of species diversity analysis can be successfully  
56  
57  
58  
59  
60

1 adapted to characterize the emergence of microbial virulence in bacterial pathogens subject to  
2 source-sink dynamics.  
3  
4

5  
6 The enteric bacterium *K. pneumoniae* is an environmental organism that is also a frequent  
7 cause of sepsis, urinary tract infection (UTI) and liver abscess. Type 1 fimbriae have been shown  
8 to be critical for the ability of *K. pneumoniae* to cause UTI in a murine model. Stahlhut *et al.*  
9 (2009) showed that the *K. pneumoniae fimH* gene is found in 90% of strains from various  
10 environmental and clinical sources. The *fimH* alleles exhibit relatively low nucleotide and  
11 structural diversity, but are prone to frequent horizontal transfer events between different  
12 bacterial clones. Addition of the *fimH* locus to Multiple Locus Sequence Typing significantly  
13 improved resolution of the clonal structure of pathogenic strains, including the K1-encapsulated  
14 liver isolates. In addition, the *K. pneumoniae* FimH protein is targeted by adaptive point  
15 mutations, though not to the same extent as FimH from uropathogenic *E. coli* or TonB from the  
16 same *K. pneumoniae* strains. Such adaptive mutations include a single amino acid deletion from  
17 the signal peptide that might affect the length of the fimbrial rod by affecting FimH translocation  
18 into the periplasm. Another FimH mutation (S62A) occurred in the course of endemic circulation  
19 of a nosocomial uropathogenic clone of *K. pneumoniae*. This mutation is identical to one found  
20 in a highly virulent uropathogenic strain of *E. coli*, suggesting that the FimH mutations are  
21 pathoadaptive in nature. Considering the abundance of Type 1 fimbriae in *Enterobacteriaceae*,  
22 the finding, presented by Stahlhut *et al.* (2009), suggests that *fimH* genes are subject to adaptive  
23 microevolution substantiates and the importance of Type 1 fimbriae-mediated adhesion in *K.*  
24 *pneumoniae*.  
25  
26  
27  
28  
29  
30  
31  
32  
33  
34  
35  
36  
37  
38  
39  
40  
41  
42  
43  
44  
45  
46  
47  
48  
49  
50

51 **Long Polar Fimbriae.** The Long Polar Fimbriae (Lpf) is one of few adhesive factors of  
52 enterohemorrhagic *E. coli* O157:H7 associated with colonization of the intestine. *E. coli*  
53 O157:H7 strains possess two *lpf* loci encoding highly regulated fimbrial structures. Database  
54 analysis of the genes encoding the major fimbrial subunits demonstrated that they are present in  
55 pathogenic *E. coli* (including commensal as well as intestinal and extra-intestinal pathogenic *E.*  
56  
57  
58  
59  
60



1  
2 *coli* isolates), and *Salmonella* strains; and that the *lpfA1* and *lpfA2* genes are highly prevalent  
3  
4 among LEE-positive *E. coli* strains associated with severe and/or epidemic disease (Torres *et al.*,  
5  
6 2009). Further DNA sequence analysis of the *lpfA1* and *lpfA2* genes from different "Attaching  
7  
8 and Effacing" *E. coli* strains has led to the identification of several polymorphisms and the  
9  
10 classification of the major fimbrial subunits in distinct variants (Torres *et al.*, 2009). Using  
11  
12 collections of pathogenic *E. coli* isolates from Europe and Latin America, Torres *et al.* (2009)  
13  
14 demonstrated that the different *lpfA* types are associated with the presence of specific intimin  
15  
16 (eae) adhesin variants, and most importantly, they are found in specific *E. coli* pathotypes. Their  
17  
18 results showed that the use of these fimbrial genes as markers, in combination with the different  
19  
20 intimin types, resulted in a specific test to identify *E. coli* O157:H7 from other pathogenic *E. coli*  
21  
22 strains.  
23  
24  
25  
26  
27

28 **Induction of pro-inflammatory responses by polyadhesins. Afa/Dr polyadhesins.** Afa/Dr  
29  
30 diffusely adhering *E. coli* strains in polarized monolayers of intestinal T84 cells, were able to  
31  
32 promote the basolateral secretion of IL-8 through the activation of the mitogen-activated protein  
33  
34 kinases (MAP kinases), including ERK1/2, p38, and SAPK/JNK (stress-activated protein  
35  
36 kinase/c-Jun NH2-terminal kinases) kinases (Betis *et al.*, 2003a). IL-8 induced in turn the  
37  
38 transmigration across the epithelial monolayer of polymorphonuclear leukocytes (Betis *et al.*,  
39  
40 2003a). The polymorphonuclear leukocytes transepithelial migration induced epithelial synthesis  
41  
42 of TNF- $\alpha$  and IL-1 $\beta$ , which in turn promoted the upregulation of DAF, increasing the adhesion  
43  
44 of Afa/Dr diffusely adhering *E. coli* bacteria (Betis *et al.*, 2003b). Moreover, upregulation of the  
45  
46 inflammation-associated molecule, MICA, has been found in intestinal Caco-2 cells infected by  
47  
48 AfaE-III-positive bacteria, an effect mediated by the specific interaction between bacterial  
49  
50 adhesin and DAF (Tieng *et al.*, 2002).  
51  
52  
53  
54  
55

56  
57 Angiogenesis has been recently described as a novel component of inflammatory bowel  
58  
59 disease pathogenesis. The level of vascular endothelial growth factor has been found increased in  
60  
Crohn's disease and ulcerative colitis mucosa. To question whether a pro-inflammatory *E. coli*



1  
2 could regulate the expression of vascular endothelial growth factor in human intestinal epithelial  
3  
4 cells, Cane *et al.* (2007) examined the response of cultured human colonic T84 cells to infection  
5  
6 by *E. coli* strain C1845 that belongs to the typical Afa/Dr diffusely adhering *E. coli* family  
7  
8 (Afa/Dr DAEC). Vascular endothelial growth factor mRNA expression was examined by  
9  
10 Northern blotting and q-PCR. VEGF protein levels were assayed by ELISA and its bioactivity  
11  
12 was analysed in endothelial cells. The bacterial factor involved in vascular endothelial growth  
13  
14 factor induction was identified by recombinant *E. coli* expressing adhesin Dr, purified adhesin  
15  
16 Dr and lipopolysaccharide. The signaling pathway activated for the up-regulation of vascular  
17  
18 endothelial growth factor was identified by a blocking monoclonal anti-DAF antibody, Western  
19  
20 blot analysis and specific pharmacological inhibitors. C1845 bacteria induced the production of  
21  
22 vascular endothelial growth factor protein which is bioactive. Vascular endothelial growth factor  
23  
24 was induced by adhering C1845 in both a time- and bacteria concentration-dependent manner.  
25  
26 This phenomenon was not cell line dependent since Cane *et al.* (2007) reproduced this  
27  
28 observation in intestinal LS174, Caco2/TC7 and INT407 cells. Up-regulation of vascular  
29  
30 endothelial growth factor production requires:  
31  
32

- 33 (1) The interaction of the bacterial F1845 adhesin with the brush border-associated CD55/DAF  
34 acting as a bacterial receptor;
- 35 (2) The activation of a Src protein kinase upstream of the activation of the Erk and Akt signaling  
36 pathways.

37  
38 Results demonstrate that Afa/Dr diffusely adhering *E. coli* strain induces an adhesin-  
39  
40 dependent activation of CD55/DAF signaling that leads to the upregulation of bioactive vascular  
41  
42 endothelial growth factor in cultured human intestinal cells. Thus, these results suggest a link  
43  
44 between an enteroadherent, pro-inflammatory *E. coli* strain and angiogenesis which appeared  
45  
46 recently as a novel component of inflammatory bowel disease pathogenesis.  
47  
48

49  
50 Diard *et al.* (2006) showed that fragments of polyadhesin Dr are released in response to  
51  
52 multiple environmental signals. Production and secretion of fragments of polyadhesin Dr are  
53  
54  
55  
56  
57  
58  
59  
60

1  
2 clearly regulated by temperature. Secretion of fragments of polyadhesin Dr is drastically  
3  
4 increased during anaerobic growth in minimal medium. The secretion was maximal during the  
5  
6 logarithmic-phase growth and corresponded to 27 and 57% of total fimbriae Dr produced by  
7  
8 bacteria grown in mineral medium with glucose and LB broth, respectively. Controlled release of  
9  
10 fragments of polyadhesin Dr, which are carried out in the absence of cellular lysis, appears  
11  
12 independent of the action of proteases or process of maturation. The fragments of polyadhesin Dr  
13  
14 secreted into environmental medium by diffusely adhering *E. coli* strains can provoke  
15  
16 unproductive pro-inflammatory responses like the fragments of F1 capsule scattered into cultural  
17  
18 media by *Y. pestis* (see below the chapter "F1 antigen").  
19  
20  
21  
22

23 **F1 antigen.** Fragments of recombinant F1 capsule of *Y. pestis* scattered into cultural media  
24  
25 activate mice peritoneal macrophages *in vitro* (Sodhi *et al.*, 2004). The fragments of F1 capsule  
26  
27 induce the production of pro-inflammatory cytokines, TNF- $\alpha$ , IL-1 and IL-6. The activation  
28  
29 suggests the involvement of NF- $\kappa$ B and MAPK pathways (Sharma *et al.*, 2005a, b; Sodhi *et al.*,  
30  
31 2004). While IL-1 $\beta$  and F1 stimulate macrophages to produce various pro-inflammatory  
32  
33 mediators via the same pathway (Kida *et al.*, 2005), *Yersinia* virulence factor YopJ, that is  
34  
35 essential for the death of infected macrophages, can block host pro-inflammatory responses by  
36  
37 inhibiting both NF- $\kappa$ B and MAPK pathways (Zhou *et al.*, 2005). Lemaitre *et al.* (2006)  
38  
39 confirmed that YopJ suppresses TNF- $\alpha$  induction and contributes to apoptosis of immune cells  
40  
41 in the lymph node but is not required for virulence in a rat model of bubonic plague.  
42  
43  
44  
45  
46

47 Thus, during early stage of infection, the type III secretion system and short non-aggregated  
48  
49 F1 Ag act in concert: the former inhibits production of pro-inflammatory cytokines and the latter  
50  
51 inhibits binding of IL-1 $\beta$  to the host cell receptors. However, at the final stage of systemic  
52  
53 infection, fragments of F1 capsule from the disseminated bacteria can provoke unproductive pro-  
54  
55 inflammatory response contributing to a toxic shock and death of the host. Sebbane *et al.* (2006)  
56  
57 demonstrated that high NO levels induced during plague may also influence the developing  
58  
59 adaptive immune response and contribute to septic shock.  
60

1  
2 **Induction of pro-inflammatory responses by monoadhesins. *P pili*.** Bergsten *et al.* (2005)  
3  
4 uncovered a molecular crosstalk between innate immune Toll-like receptor 4 binds bacterial  
5 lipopolysaccharide signaling and P-fimbrial-mediated attachment, which is lipopolysaccharide-  
6  
7 independent. Upon P-fimbrial attachment to its glycosphingolipid receptor, ceramide is released  
8  
9 from the lipid part of the receptor; in particular, it has recently been shown that ceramide acts as  
10  
11 an agonist of Toll-like receptor 4 and potentially acts as a signaling intermediate between Toll-  
12  
13 like receptor 4 and the glycosphingolipid receptor (Fischer *et al.*, 2007). Activation of the Toll-  
14  
15 like receptor 4 receptor by P-fimbrial attachment subsequently leads to the production of pro-  
16  
17 inflammatory cytokines and chemokines (interleukin-6 and CXCL8, respectively) and  
18  
19 recruitment of neutrophils (Bergsten *et al.*, 2005). Although this proinflammatory response is  
20  
21 beneficial in initiating bacterial clearance, it also causes damage to the surrounding tissue and is  
22  
23 associated with renal complications. Since P fimbriae are implicated in triggering inflammation,  
24  
25 it can be deduced that they may also contribute to the pathology and symptoms of acute  
26  
27 pyelonephritis.  
28  
29  
30  
31  
32  
33  
34  
35  
36

### 37 **FUNCTION-STRUCTURAL CLASSIFICATION OF ADHESIVE ORGANELLES** 38 39 **ASSEMBLED WITH CHAPERONE-USHER MACHINERY** 40 41 42 43 44

45 In fact, the first classification of periplasmic chaperones and organelles assembled by them  
46  
47 was suggested by Zav'yalov *et al.* (1995b). For this aim the 3D structure of the CafIM chaperone  
48  
49 was reconstructed by computer modeling, using a primary structure homology between CafIM  
50  
51 and PapD proteins, and the atomic coordinates obtained by the X-ray crystallography for PapD  
52  
53 (Holmgren & Branden, 1989). In the 3D model of CafIM an accessory sequence between Fl and  
54  
55 Gl  $\beta$ -strands (as compared to PapD) was recognized. The sequences of 17 periplasmic  
56  
57 chaperones known at that time were aligned and two families with specific structural properties  
58  
59 were identified. It was found that the characteristic structural feature of the family of periplasmic  
60

1  
2 chaperones with the accessory sequence (CafIM family) is the existence of solvent exposed Cys  
3  
4 residues in F1 and G1  $\beta$ -strands which can form disulfide bond in the putative binding site for  
5  
6 organelle subunits. The specific functional property of CafIM family is the assisting in assembly  
7  
8 of nonfimbrial surface structures or thin fibrillae of a simple composition (i.e., F1 and pH6  
9  
10 antigens of *Y. pestis* consist of only one subunit) in comparison with the chaperones of PapD  
11  
12 family which assist in assembling of more complex thick fimbriae/pili (i.e., P pili are composed  
13  
14 of 7 different subunits).  
15  
16  
17

18  
19 Hung *et al.* (1996) studied 26 chaperones and defined proteins containing a relatively long  
20  
21 F1-G1 loop as the FGL chaperone family and proteins with a short F1-G1 loop as the FGS  
22  
23 chaperone family. Hung *et al.* (1996) also revealed that the FGL chaperone family assembles  
24  
25 nonfimbrial surface structures or thin fibrillae, composed of 1-2 subunits, while the FGS  
26  
27 chaperone family assembles thick fimbriae/ pili, composed of up to 7 subunits.  
28  
29

30  
31 Sequence comparison of 31 chaperones by the neighbor-joining method suggests that the  
32  
33 classical chaperone/usher superfamily can be divided into several clades, each including  
34  
35 members that apparently share a common ancestor that is not shared by another protein outside  
36  
37 of the clade (Bonci *et al.*, 1997). This phylogenetic tree suggests that members of the FGL  
38  
39 chaperone family (i.e., MyfB, PsaB, Caf1M, CS3-1, AggD, AfaB, NfaE, SefB, and CssC) share  
40  
41 a common ancestor. However, this analysis also shows that the FGS chaperone subfamily cannot  
42  
43 be defined by a single node or branch on the phylogenetic tree, suggesting that further  
44  
45 subdivision is needed to explicitly categorize the respective fimbriae into clades on the basis of  
46  
47 common ancestry.  
48  
49  
50

51  
52 The next principal step in development of function/structural nomenclature of adhesive  
53  
54 fimbrial organelles, assembled with the classical chaperone/usher machinery, was the discovery  
55  
56 that FGL chaperone-assembled organelles possess polyadhesive function (Zavialov *et al.*, 2007)  
57  
58 in distinction to FGS chaperone-assembled monoadhesive thick fimbriae/pili with one adhesive  
59  
60 domain on the tip of fibre.

1  
2 Analysis of the currently available data suggests that the classical chaperone/usher  
3  
4 machinery involves three distinct families and a few subfamilies of surface-exposed adhesive  
5  
6 organelles, which have unique functional and structural properties (Table 2).  
7  
8

9 The FGL chaperone-assembled adhesive organelles represent linear polymers of one or in  
10  
11 some cases two distinct types of protein subunits. The characteristic feature of the organelles is  
12  
13 that each protein subunit in the fiber possesses two independent binding sites, which are specific  
14  
15 to different receptors on cells of the host. Such architecture enables a single fiber to establish  
16  
17 polyvalent contacts with receptors on the host cells. The FGL chaperone-assembled polyadhesins  
18  
19 may be subdivided into three subfamilies (Table 2):  
20  
21

22  
23 (1) FGL chaperone-assembled polyadhesins-1-1 where the first numeral shows that organelles of  
24  
25 this subfamily are homopolymers composed of only one subunit. The second numeral displays  
26  
27 that assembly of the organelles is assisted by one chaperone;  
28  
29

30 (2) FGL chaperone-assembled polyadhesins-(1+1)-1 where the numerals in parentheses indicate  
31  
32 that organelles of this subfamily are heteropolymers composed of two distinct subunits secreted  
33  
34 via different pathways. One subunit is secreted with the classical chaperone/usher machinery,  
35  
36 and another subunit is displayed on the tip of fibre with type II secretion system. The numeral  
37  
38 out the parentheses indicates that assembly of the organelles is assisted with one chaperone;  
39  
40

41 (3) FGL chaperone-assembled polyadhesins-2-1 where the first numeral shows that organelles of  
42  
43 this subfamily are heteropolymers composed of two distinct subunits both of which are secreted  
44  
45 with the chaperone/usher machinery. The second numeral shows that assembly of the organelles  
46  
47 is assisted by one chaperone.  
48  
49

50  
51 The majority of FGS chaperone-assembled adhesive fimbriae/pili are monoadhesins, which  
52  
53 display only one adhesin domain on the tip of the pilus. The FGS chaperone-assembled  
54  
55 monoadhesins may be subdivided into six subfamilies (Table 2):  
56  
57

58 (1) The subfamily of FGS chaperone-assembled monoadhesins-2-1 collects the structurally  
59  
60 simplest mono-adhesive organelles composed of two subunits one of which is structural and

1  
2 another contains adhesive domain exposed on the tip of pili. Assembly of the organelles is  
3  
4 assisted with one chaperone.

5  
6 (2) The subfamily of FGS chaperone-assembled monoadhesins-3-1 includes the mono-adhesive  
7  
8 organelles composed of three subunits two of which are structural and one contains adhesive  
9  
10 domain exposed on the tip of pili. Assembly of the organelles also is assisted with one  
11  
12 chaperone.  
13

14  
15 (3) The subfamily of FGS chaperone-assembled monoadhesins-3-3 also represents the mono-  
16  
17 adhesive organelles composed of three subunits two of which are structural and one is specific  
18  
19 adhesin exposed on the tip of pili. However, assembly of these organelles is assisted by three  
20  
21 distinct chaperones.  
22  
23

24  
25 (4) The subfamily of FGS chaperone-assembled monoadhesins-4-1 collects the mono-adhesive  
26  
27 organelles composed of four subunits three of which are structural and one contains adhesive  
28  
29 domain exposed on the tip of pili. Assembly of the organelles is assisted with one chaperone.  
30  
31

32  
33 (5) The subfamily of FGS chaperone-assembled monoadhesins-5-1 represents the mono-  
34  
35 adhesive organelles composed of five subunits four of which are structural and one is  
36  
37 specialized adhesin exposed on the tip of pili. Assembly of the organelles is assisted with one  
38  
39 chaperone.  
40  
41

42  
43 (6) The subfamily of FGS chaperone-assembled monoadhesins-7-1 is the most complex  
44  
45 subfamily of mono-adhesive organelles composed of seven subunits six of which are structural  
46  
47 and one is specialized adhesin exposed on the tip of pili. Assembly of the organelles is assisted  
48  
49 by one chaperone.  
50

51  
52 The FGS chaperone-assembled thin flexible pili F4 (K88), F5 (K99) and Lda of *E. coli*, PE  
53  
54 (plasmid-encoded) fimbriae of *S. typhimurium*, atypical fimbriae ACIAD of *Acinetobacter* sp.  
55  
56 and ATF of *P. mirabilis*, however are an exception, as they do not display specialized adhesive  
57  
58 domains on the tip of the pilus, but carry binding site on their main structural subunit (FaeH,  
59  
60 FanH and LdaH) or are composed of only one structural subunit that is functioning as an

1  
2 adhesin subunit (ACIAD122, AtfA and PefA). Such architecture enables a single fiber to  
3  
4 establish polyvalent contacts with receptors on the host cells. Therefore we called this family as  
5  
6 FGS chaperone-assembled polyadhesins. These polyadhesins may be subdivided into five  
7  
8 subfamilies (Table 2):  
9

10  
11 (1) The subfamily of FGS chaperone-assembled polyadhesins-1-1 collects the poly-adhesive  
12  
13 homopolymers. Assembly of the organelles is assisted by one chaperone;  
14  
15

16  
17 (2) The subfamily of FGS chaperone-assembled polyadhesins-1-2 also represents the poly-  
18  
19 adhesive homopolymer. However, assembly of the fiber is assisted with two distinct  
20  
21 chaperones;  
22

23  
24 (3) The subfamily of FGS chaperone-assembled polyadhesins-3-1 includes the heteropolymer  
25  
26 composed of three distinct subunits. The organelle carries binding site on its main structural  
27  
28 subunit. Assembly of the polyadhesin is assisted by one chaperone;  
29

30  
31 (4) The subfamily of FGS chaperone-assembled polyadhesins-4-1 includes the heteropolymer  
32  
33 composed of four distinct subunits. The organelle carries binding site on its main structural  
34  
35 subunit. Assembly of the polyadhesin is assisted by one chaperone;  
36

37  
38 (5) The subfamily of FGS chaperone-assembled polyadhesins-5-1 includes the heteropolymers  
39  
40 composed of five distinct subunits. The organelles carry binding site on their main structural  
41  
42 subunit. Assembly of the polyadhesins is assisted with one chaperone.  
43  
44

#### 45 46 47 **PHYLOGENESIS OF THE CLASSICAL CHAPERONE/ USHER GENE CLUSTERS** 48

49  
50  
51 It is very interesting to compare the suggested function-structural nomenclature of adhesive  
52  
53 organelles, assembled with the classical chaperone/usher machinery, and their phylogenetic  
54  
55 classification.  
56  
57

58  
59 Sequence comparison of chaperones (Bonci *et al.*, 1997) may not be ideally suited for  
60  
developing of a phylogenetic subdivision because some fimbrial operons encode more than one



1  
2 chaperone, thus raising the question as to which protein should be used to assign the respective  
3  
4 operon to a phylogenetic group. Therefore comparison of usher sequences has been used to  
5  
6 derive phylogenetic trees of members of the chaperone/usher assembly class (Anantha *et al.*,  
7  
8 2004; Yen *et al.*, 2002). This approach has the advantage that the resulting definition of  
9  
10 phylogenetic groups is unambiguous, because all fimbrial operons belonging to the  
11  
12 chaperone/usher assembly class contain only a single usher gene. An initial comparison of 58  
13  
14 members of the fimbrial usher protein (FUP) superfamily distinguished 10 clusters on the basis  
15  
16 of common ancestry (Yen *et al.*, 2002). A revised phylogenetic tree of the FUP superfamily  
17  
18 constructed by comparing 189 proteins is shown in Fig. 13 (Nuccio & Bäumlér, 2007). The  
19  
20 phylogenetic analysis of 189 usher proteins suggests a classification into clades, which is similar  
21  
22 but not identical to that proposed based on analysis of 58 usher proteins (Yen *et al.*, 2002).  
23  
24 Nuccio & Bäumlér (2007) proposed a nomenclature using Greek letters to refer to individual  
25  
26 clades. Using a node-based definition, the FUP superfamily can be divided into six clades,  
27  
28 designated  $\alpha$ ,  $\beta$ ,  $\gamma$ ,  $\kappa$ ,  $\pi$ , and  $\sigma$ -fimbriae, each stemming from a common ancestor represented by  
29  
30 a node in the phylogenetic tree (Fig. 13). The  $\gamma$ -fimbrial clade is further subdivided into four  
31  
32 clades, termed  $\gamma_1$ ,  $\gamma_2$ ,  $\gamma_3$ , and  $\gamma_4$ -fimbriae. Nuccio & Bäumlér (2007) assigned arbitrarily  $\alpha$ ,  $\beta$ ,  $\gamma$ ,  
33  
34  $\kappa$ ,  $\pi$ , and  $\sigma$ -fimbrial clade names to recall a particular characteristic of the clade or a prominent  
35  
36 member as follows:  $\alpha$ -fimbriae, alternate chaperone/usher family;  $\kappa$ -fimbriae, K88 (F4) fimbriae;  
37  
38  $\pi$ -fimbriae, pyelonephritis-associated fimbriae (P fimbriae); and  $\sigma$ -fimbriae, spore coat protein U  
39  
40 from *Myxococcus xanthus*. The  $\beta$ - and  $\gamma$ -fimbriae were assigned names alphabetically. This  
41  
42 subdivision of the FUP superfamily largely confirms the subdivisions proposed initially (Yen *et*  
43  
44 *al.*, 2002), but former FUP clusters 4 and 5 now form a single clade ( $\gamma_3$ -fimbriae). The  
45  
46 subdivision of the chaperone/usher class into six FUP clades confirms that the alternate  
47  
48 chaperone/usher family ( $\alpha$ -fimbriae) (Anantha *et al.*, 2004) contains operons that stem from a  
49  
50 common ancestor (Fig. 13; Nuccio & Bäumlér, 2007). The FGL chaperone assembled family of  
51  
52 polyadhesins forms a monophyletic group ( $\gamma_3$ -fimbriae) within the classical chaperone/usher  
53  
54  
55  
56  
57  
58  
59  
60

1  
2 family (Hung *et al.*, 1996; Zav'yalov *et al.*, 1995b). However, the FGS chaperone assembled  
3  
4 family of adhesive organelles is composed of several clades ( $\beta$ -,  $\gamma$ 1-,  $\gamma$ 2-,  $\gamma$ 4-,  $\kappa$ -, and  $\pi$ -fimbriae)  
5  
6 that are not more closely related to each other than to the FGL chaperone assembled family of  
7  
8 polyadhesins ( $\gamma$ 3-fimbriae). The analysis also reveals the existence of a major FUP clade ( $\sigma$ -  
9  
10 fimbriae) that was represented only by two usher proteins in a previous analysis (Yen *et al.*,  
11  
12 2002) and whose members share limited or no sequence homology to members of the alternate  
13  
14 chaperone/usher family ( $\alpha$ -fimbriae) or the classical chaperone/usher family ( $\beta$ -,  $\gamma$ -,  $\kappa$ -, and  $\pi$  -  
15  
16 fimbriae).  
17  
18  
19

20  
21 The utility of delineating the genealogy of gene clusters that encode fimbrial adhesins lies in  
22  
23 its value for predicting their evolutionary relationship. For instance, gene clusters of the  $\gamma$ 3- and  
24  
25  $\kappa$ -fimbrial clades, identified by Nuccio & Bäumlner (2007), encode exclusively FGL and FGS  
26  
27 chaperone assembled polyadhesins, respectively, while gene clusters belonging to the  $\alpha$ -,  $\gamma$ 1-,  $\gamma$ 2-  
28  
29 ,  $\gamma$ 4-, and  $\pi$ -fimbrial clades exclusively encode monoadhesins. When the most common gene  
30  
31 clusters within each clade are placed at the end of each of the corresponding branches on the  
32  
33 FUP tree, an evolutionary scenario explaining the divergence of gene clusters from a common  
34  
35 precursor can be derived. The exact relationship between major clusters in the FUP tree (Fig. 13;  
36  
37 Nuccio & Bäumlner, 2007) is currently not clear, since the nodes connecting  $\alpha$ -,  $\beta$ -,  $\gamma$ -,  $\kappa$ -,  $\pi$ -, and  $\sigma$ -  
38  
39 fimbrial clades are supported by low bootstrapping values. However, the gene clusters of  $\kappa$ - and  
40  
41  $\pi$ -fimbriae are related to each other, as both share a core structure composed of genes encoding a  
42  
43 major subunit, an usher, and a chaperone. Furthermore, a close relationship of the  $\gamma$ -fimbriae to  
44  
45 the  $\kappa$ - and  $\pi$ -fimbriae is indicated by the presence of a PFAM00419 domain exclusively in  
46  
47 subunits of gene clusters belonging to these three clades (Nuccio & Bäumlner, 2007). These data  
48  
49 suggest that members of the  $\gamma$ -,  $\kappa$ -, and  $\pi$ -fimbrial clades form a monophyletic group, which will  
50  
51 be referred to as the  $\gamma\kappa\pi$  cluster from here on. The  $\gamma\kappa\pi$  cluster and the  $\beta$ -fimbriae together  
52  
53 comprise the previously defined classical chaperone/usher superfamily.  
54  
55  
56  
57  
58  
59  
60

1  
2 The FGL chaperone-assembled polyadhesins that correspond to  $\gamma$ 3-fimbriae (Fig. 14; Nuccio  
3 & Bäumlér, 2007) comprise the adhesive organelles, which consist of only one or two distinct  
4 types of subunits and at low resolution typically have non-pilus, amorphous or capsule-like  
5 morphology (Anderson *et al.*, 2004a,b; Hung *et al.*, 1996; Korotkova *et al.*, 2006a,b, 2008; Li *et*  
6 *al.*, 2007; Pettigrew *et al.*, 2004; Remaut *et al.*, 2006; Salih *et al.*, 2008; Soto & Hultgren, 1999;  
7 Verger *et al.*, 2007; Westerlund-Wikström & Korhonen, 2005; Zavialov *et al.*, 2003, 2005,  
8 2007). Their notable property is that all subunits possess two independent binding sites specific  
9 to different host cell receptors. In particular, DraE/AfaE/DaaE subunits of the Dr/Afa  
10 polyadhesins have two independent binding sites to CD55/DAF and CEACAMs (Fig. 9;  
11 Anderson *et al.*, 2004a, b; Korotkova *et al.*, 2006a, b; 2008a; Pettigrew *et al.*, 2004). The PsaA  
12 subunit of pH6 antigen binds to  $\beta$ 1-linked galactosyl residue of glycosphingolipids (Payne *et al.*,  
13 1998) and to phosphorylcholine moiety of phosphatidylcholine (Galván *et al.*, 2006) as the host  
14 cell receptors.

15  
16  
17  
18  
19  
20  
21  
22  
23  
24  
25  
26  
27  
28  
29  
30  
31  
32  
33 The  $\kappa$ -clade (Fig. 15; Nuccio & Bäumlér, 2007) comprises all subfamilies of the FGS  
34 chaperone-assembled polyadhesins, in particular, the FGS chaperone-assembled polyadhesins-1-  
35 1 (Pef pili), -3-1 (AF/R1 pili), -4-1 (K88 pili), and -5-1 (K99 pili, REPEC fimbriae, and afimbrial  
36 adhesin, encoded by the *locus for diffuse adherence, lda*). Like the FGL polyadhesive fibers, the  
37 FGS polyadhesins carry binding site on their main structural subunit (FaeH, FanH and LdaH) or  
38 are composed of only one structural subunit that is functioning as an adhesin subunit  
39 (ACIAD122 and PefA). In contrast to mono-adhesive pili, which possess only one binding  
40 domain on the tip of pilus (Fig. 12a), each poly-adhesive fiber potentially might (Fig. 12b)  
41 ensuring powerful polyvalent fastening of a bacterial pathogen to a host target cell (Galván *et al.*,  
42 2006), and aggregating host cell receptors by a zipper-like mechanism that trigger transduction  
43 of signals causing immunosuppressive and pro-inflammatory responses (Galván *et al.*, 2006;  
44 Sharma *et al.*, 2005a,b; Sodhi *et al.*, 2004).

1  
2 The  $\gamma$ 2-clade (Fig. 14; Nuccio & Bäumler, 2007), corresponds to the FGS chaperone-  
3 assembled monoadhesins-3-3 which are representing the mono-adhesive organelles composed of  
4 three subunits two of which are structural and one is specific adhesin exposed on the tip of pili.  
5  
6  
7  
8  
9  
10  
11  
12  
13  
14  
15  
16  
17  
18  
19  
20  
21  
22  
23  
24  
25  
26  
27  
28  
29  
30  
31  
32  
33  
34  
35  
36  
37  
38  
39  
40  
41  
42  
43  
44  
45  
46  
47  
48  
49  
50  
51  
52  
53  
54  
55  
56  
57  
58  
59  
60

The  $\gamma$ 1-clade (Fig. 14; Nuccio & Bäumler, 2007) comprises some of the members of the FGS  
chaperone-assembled monoadhesins-3-1, 4-1 and 5-1, however, the Ambient-temperature  
fimbriae (Atf) of *Pr. mirabilis* related to the FGS chaperone-assembled polyadhesins-1-1, is the  
exception. Like the most of FGL chaperone assembled polyadhesins, Atf fimbriae are  
polyadhesive homopolymers.

The  $\gamma$ 4-clade (Fig. 14; Nuccio & Bäumler, 2007) includes some of the members of the FGS  
chaperone-assembled monoadhesins-2-1, -3-1, 4-1 and 5-1.

The  $\pi$ -clade (Fig. 15; Nuccio & Bäumler, 2007) consists of some of the members of the FGS  
chaperone-assembled monoadhesins-3-1, -4-1, -5-1, and -7-1.

The remarkable feature of the  $\kappa$ - and  $\pi$ -gene clusters is the location of gene encoding  
chaperone after gene encoding usher, while in the  $\gamma$ -clusters gene encoding chaperone, precedes  
gene for usher. This finding underlines more close phylogenetic relationships between  $\kappa$ - and  $\pi$ -  
clusters of genes than with the  $\gamma$ -clusters.

## APPLICATIONS OF ADHESIVE ORGANELLES ASSEMBLED WITH CHAPERONE/USHER MACHINERY

### Applications of Polyadhesins

1  
2  
3  
4  
5  
6  
7  
8  
9  
10  
11  
12  
13  
14  
15  
16  
17  
18  
19  
20  
21  
22  
23  
24  
25  
26  
27  
28  
29  
30  
31  
32  
33  
34  
35  
36  
37  
38  
39  
40  
41  
42  
43  
44  
45  
46  
47  
48  
49  
50  
51  
52  
53  
54  
55  
56  
57  
58  
59  
60

**Applications of polyadhesins for vaccine design. *Anti-plague vaccines based on the recombinant F1 antigen or on peptides from the F1 antigen.*** *Y. pestis*, the causative agent of pneumonic plague, is a rapidly progressing and exceptionally virulent disease (reviewed by Cleri *et al.*, 1997; Perry & Fetherston, 1997; Smiley, 2008a, b). Extensively antibiotic-resistant strains of *Y. pestis* exist and a safe and effective pneumonic plague vaccine is currently absent (Smiley, 2008a, b). These facts raise concern that *Y. pestis* may be exploited as a biological weapon.

F1 antigen is the major or single protective component of the current human whole-cell vaccines against plague (Li *et al.*, 2005; Li & Yang, 2008; Smiley, 2008a, b). This vaccine is, however, ineffective against pneumonic plague caused by typical F1<sup>+</sup> strains of *Y. pestis* (Heath *et al.*, 1998). It is also ineffective against F1<sup>-</sup> *Y. pestis* strains, which have been isolated from one human patient and from several rodents. For these reasons, new recombinant plague vaccines comprising Caf1 and V antigens of *Y. pestis* are under development.

Heath *et al.* (1998) developed a recombinant vaccine composed of a fusion protein of F1 with a second protective immunogen, V antigen. V antigen is an essential virulence factor and mediator of immunity common for *Yersinia*. It plays a crucial role in the functioning of the type III secretion system. This protein forms a distinct structure at the tip of injectisome needle (Mueller *et al.*, 2005). Derewenda *et al.* (2004) solved the three-dimensional structure of V antigen with high resolution X-ray analysis. The developed recombinant F1-V fusion vaccine protected mice against pneumonic as well as bubonic plague produced by either an F1<sup>+</sup> or F1<sup>-</sup> strain of *Y. pestis* and provided a better protection than recombinant F1 or recombinant V alone against the F1<sup>+</sup> strain. Therefore, the recombinant proteins serve as the basis of an improved human anti-plague vaccine (Heath *et al.*, 1998).

Powell *et al.* (2005) re-engineered a two-component F1-V fusion protein antigen and tested as a medical countermeasure against the possible biological threat of aerosolized *Y. pestis*. As formulated with aluminum hydroxide adjuvant and administered in a single subcutaneous dose, this new F1-V fusion protein also protected mice from wild-type and non-encapsulated *Y. pestis*

1 challenge strains, modeling prophylaxis against pneumonic and bubonic plague. Jones *et al.*  
2  
3  
4 (2006) found that the rF1-V antigen given intramuscularly with Alhydrogel adjuvant protects  
5  
6 mice against the challenge, but is less effective in nonhuman primates against high-dose  
7  
8 aerosolized *Y. pestis*, perhaps because the antigen fails to induce respiratory immunity. Mice  
9  
10 immunized intranasally with rF1-V formulated with a proteosome-based adjuvant  
11  
12 (Protollin<sup>TM</sup>) were 100% protected against aerosol challenge with 170 LD<sub>50</sub> of *Y. pestis* and  
13  
14 80% protected against 255 LD<sub>50</sub> (Jones *et al.*, 2006). Indeed, the examination of different prime-  
15  
16 boost regimens with rF1-V demonstrated that inclusion of an appropriate adjuvant is critical for  
17  
18 nonparenteral immunization (Glynn *et al.*, 2005). In view of the extraordinary potency of  
19  
20 flagellin as an inducer of innate immunity and the contribution of innate responses to the  
21  
22 development of adaptive immunity, Honko *et al.* (2006) evaluated the efficacy of recombinant  
23  
24 *Salmonella* flagellin as an adjuvant in subunit antiplague vaccine. Mice immunized intranasally  
25  
26 or intratracheally with the F1 antigen and flagellin exhibited dramatic increases in anti-F1  
27  
28 plasma IgG titers that remained stable over time. Importantly, intranasal immunization with  
29  
30 flagellin and the F1 antigen was protective against intranasal challenge with virulent *Y. pestis*  
31  
32 CO92, with 93–100% survival of immunized mice. Vaccination of cynomolgus monkeys with  
33  
34 flagellin and the rF1-V fusion protein induced a robust antigen-specific IgG antibody response.  
35  
36 Alvarez *et al.* (2006) developed a novel production and delivery system for an anti-plague  
37  
38 vaccine of the rF1-V fusion protein expressed in tomato. The immunogenicity of the rF1-V  
39  
40 transgenic tomatoes was confirmed in mice that were primed subcutaneously with bacterially-  
41  
42 produced rF1-V and boosted orally with transgenic tomato fruit. Expression of the plague  
43  
44 antigens in fruit made it possible to produce an oral vaccine candidate without protein  
45  
46 purification and with minimal processing technology. The recombinant plague antigens F1, V,  
47  
48 and fusion protein F1-V were produced by transient expression in *Nicotiana benthamiana* using  
49  
50 a reconstructed tobacco mosaic virus-based system that allowed very rapid and extremely high  
51  
52 levels of expression (Santi *et al.*, 2006). All of the plant-derived purified antigens, administered  
53  
54  
55  
56  
57  
58  
59  
60

1  
2 subcutaneously to guinea pigs, generated systemic immune responses and provided protection  
3  
4 against an aerosol challenge of virulent *Y. pestis*. Chichester *et al.* (2009) reported a plague  
5  
6 vaccine consisting of the F1 and LcrV antigens fused to a single carrier molecule, the  
7  
8 thermostable enzyme lichenase from *Clostridium thermocellum*, and expressed in and purified  
9  
10 from *Nicotiana benthamiana* plants. When administered to *Cynomolgus Macaques* this purified  
11  
12 plant-produced vaccine induced high titers of serum IgG, mainly of the IgG1 isotype, against  
13  
14 both F1 and LcrV. These immunized animals were subsequently challenged and the LcrV-F1  
15  
16 plant-produced vaccine conferred complete protection against aerosolized *Y. pestis*. Del Prete *et*  
17  
18 *al.* (2009) produced in *Nicotiana benthamiana* F1 and V antigens, and F1-V fusion protein and  
19  
20 administered them to guinea pigs resulted in immunity and protection against an aerosol  
21  
22 challenge of virulent *Y. pestis*. They examined the effects of plant-derived F1, V, and F1-V on  
23  
24 human cells of the innate immunity. F1, V, and F1-V proteins engaged TLR2 signalling and  
25  
26 activated IL-6 and CXCL-8 production by monocytes, without affecting the expression of TNF-  
27  
28  $\alpha$ , IL-12, IL-10, IL-1 $\beta$ , and CXCL10. Native F1 antigen and plant-derived rF1 and rF1-V all  
29  
30 induced similar specific T-cell responses, as shown by their recognition by T-cells from subjects  
31  
32 who recovered from *Y. pestis* infection. Native F1 and rF1 were equally well recognized by  
33  
34 serum antibodies of *Y. pestis*-primed donors, whereas serological reactivity to rF1-V hybrid was  
35  
36 lower, and that to rV was virtually absent. In conclusion, plant-derived F1, V, and F1-V antigens  
37  
38 are weakly reactogenic for human monocytes and elicit cell-mediated and humoral responses  
39  
40 similar to those raised by *Y. pestis* infection.  
41  
42  
43  
44  
45  
46  
47  
48

49 The subunit vaccine involving a mixture of recombinant F1 and V antigens protects mice  
50  
51 against exposure to 4104 CFUs of virulent plague organisms (100 LD50 doses), whereas the  
52  
53 whole cell vaccine provided only 50% protection against 1.8-10<sup>3</sup> CFUs (Williamson *et al.*,  
54  
55 1997). The enhanced protective efficacy of this subunit vaccine over existing vaccines has been  
56  
57 demonstrated in an animal model of pneumonic plague. Bronchopulmonary administration of the  
58  
59 combined subunits (1 mg V plus 5 mg F1) entrapped within microspheres composed of a  
60



1  
2 biodegradable polyester (poly-L-lactide) elicits a similar level of protective immunity against  
3  
4 systemic plague infection as that evoked by injecting coencapsulated subunits into the muscle  
5  
6 (Eyles *et al.*, 2000). Such findings indicate that introduction of appropriately formulated F1 and  
7  
8 V subunits into the respiratory tract may be an alternative to parenteral immunization schedules  
9  
10 for protecting individuals from plague (Eyles *et al.*, 2000). Elvin *et al.* (2006) individually  
11  
12 encapsulated the recombinant F1 and V antigens in polymeric microspheres; the same antigen  
13  
14 was adsorbed to the surface of these microspheres. Virulent challenge experiments showed that  
15  
16 noninvasive immunization by intranasal instillation can provide strong systemic and local  
17  
18 immune responses and protect against high-level challenge. Recently Thomas *et al.* (2009)  
19  
20 reported that the pathogenesis patterns of plague infections caused by the deposition of 1- and  
21  
22 12- $\mu\text{m}$ -particle aerosols of *Y. pestis* in the lower and upper respiratory tracts (URTs) of mice are  
23  
24 different. The median lethal dose for 12- $\mu\text{m}$  particles was 4.9-fold higher than that for 1- $\mu\text{m}$   
25  
26 particles. The 12- $\mu\text{m}$ -particle infection resulted in the degradation of the nasal mucosa and nasal-  
27  
28 associated lymphoid tissue (NALT) plus cervical lymphadenopathy prior to bacteremic  
29  
30 dissemination. Lung involvement was limited to secondary pneumonia. In contrast, the 1- $\mu\text{m}$ -  
31  
32 particle infection resulted in primary pneumonia; in 40% of mice, the involvement of NALT and  
33  
34 cervical lymphadenopathy were observed, indicating entry via both URT lymphoid tissues and  
35  
36 lungs. Despite bacterial deposition in the gastrointestinal tract, the involvement of Peyer's  
37  
38 patches was not observed in either infection. Although there were major differences in  
39  
40 pathogenesis, the recombinant F1 and V antigen vaccine and ciprofloxacin protected against  
41  
42 plague infections caused by small- and large-particle aerosols.  
43  
44  
45  
46  
47  
48  
49  
50

51  
52 Human immune response to the recombinant plague vaccine comprising F1 and V antigens  
53  
54 was assessed during a phase 1 safety and immunogenicity trial in healthy volunteers (Williamson  
55  
56 *et al.*, 2005). All the subjects produced specific IgG in serum after the priming dose, which  
57  
58 peaked in value after the booster dose (day 21). However, no significant vaccination-related  
59  
60 change in activation of peripheral blood mononuclear cells was detected at any time. Thus, any

1  
2 evidence on the cell immune response to recombinant F1 and V antigens is missing. Williamson  
3  
4 *et al.* (2005) suppose that it may be associated with the immunosuppressive action of these  
5  
6 antigens. DeBord *et al.* (2006) therefore designed the recombinant V10 (rV10) variant lacking  
7  
8 residues 271–300. This variant does not suppress the release of proinflammatory cytokines by  
9  
10 immune cells. In contrast to *Y. pestis* LcrV, the immunization with rV10 generates robust  
11  
12 antibody-induced protective responses against bubonic plague and pneumonic plague, suggesting  
13  
14 that rV10 may serve as an improved component of anti-plague vaccine.  
15  
16  
17

18  
19 The antigen structure may critically influence on the protective immune responses (Watts,  
20  
21 2004). The data on the structural and thermodynamic properties of Caf1 (Zavialov *et al.*, 2003,  
22  
23 2005) can explain the failure to induce the cell immune response to this antigen. The structurally  
24  
25 observed complete collapse of the donor-strand-complemented fiber Caf1 subunit results in a  
26  
27 dramatic increase in the enthalpy and transition temperature for the melting of the fiber module  
28  
29 (Zavialov *et al.*, 2005). The collapse of the hydrophobic core of subunits shifts the equilibrium  
30  
31 towards fiber formation (Zavialov *et al.*, 2003, 2005). As a result, the temperature of melting of  
32  
33 the fiber subunit increases as high as to 90°C (Zavialov *et al.*, 2005). The subunit preserves  
34  
35 practically the same stability at pH 2.4 (Fooks *et al.*, personal communication). It can be deduced  
36  
37 that such a high stability can reduce the processing of Caf1 antigen in macrophages to CD4 T  
38  
39 cell epitopes and therefore abolish cellular immune responses. Indeed, Musson *et al.* (2006)  
40  
41 found that optimal T cell responses required significantly extended exposure of antigen  
42  
43 presenting cells to highly stable polymeric Caf1 compared with Caf1 that was depolymerized  
44  
45 and destabilized by heating. Destabilization of Caf1 caused a shift toward presentation by mature  
46  
47 MHC class II and toward independence of low pH and proteolytic processing.  
48  
49  
50  
51  
52  
53

54  
55 An overcoming of low proteolytic processing of highly stable native Caf1 may be the attempt  
56  
57 to develop an anti-plague vaccine based upon the peptide conjugates made between different B-  
58  
59 and T-cell epitopes of F1 antigen of *Y. pestis* (Sabhnani & Rao, 2000; Sabhnani *et al.*, 2003;  
60  
Tripathi *et al.*, 2006). Intranasal immunization generated consistently high titers and a

1  
2 longlasting immune response for both IgG and IgA in sera and secreted IgA in washes, whereas  
3  
4 the intramuscular route generated peak IgG levels in sera only. *In vivo* protective studies showed  
5  
6 that B1–T1 and B2–T1 peptide conjugates protected the mice till day 15.  
7  
8

9 ***Anti-plague passive immunization with monoclonal antibodies against the F1 antigen.*** The  
10  
11 newest anti-plague vaccines based on the F1 and V antigens provide a high degree of protection.  
12  
13 However, they must be administered several weeks before exposure to prevent plague. It is  
14  
15 unlikely that vaccines will provide post-exposure protection against plague. As an alternative to  
16  
17 vaccines, the passive immunization with monoclonal antibodies against the F1 protein has been  
18  
19 demonstrated to be effective in mice for protection from fatal bubonic and pneumonic plague  
20  
21 (Anderson *et al.*, 1997). Moreover, Hill *et al.* (2003) showed that intraperitoneal injection of  
22  
23 monoclonal antibodies that target the F1 and LcrV proteins protected mice in a synergistic  
24  
25 manner as either a pretreatment or a post-exposure therapy. Recently, Hill *et al.* (2006)  
26  
27 demonstrated that intratracheal delivery of aerosolized monoclonal antibodies with specificity  
28  
29 for LcrV and F1 antigens protected mice in a model of pneumonic plague. These data support the  
30  
31 utility of inhaled antibodies as a fast-acting post-exposure treatment for plague. The efficacy of  
32  
33 passive immunization with monoclonal IgG antibodies specific for Caf1 suggests that  
34  
35 opsonization is a major mechanism to overcome the resistance of *Y. pestis* to phagocytosis  
36  
37 conferred by the Caf1 capsule.  
38  
39  
40  
41  
42  
43

44 ***Application of polyadhesin Saf for design of Salmonella vaccine.*** Typhoid fever caused by  
45  
46 *S. enterica* serovar Typhi (*S. Typhi*), which is a predominantly human pathogen, remains a  
47  
48 burden problem in India and worldwide (Crump *et al.*, 2004; Hamid & Jain, 2007). The mortality  
49  
50 rates in untreated typhoid fever infections can be 10–15%. There are estimated 20 million cases  
51  
52 and 200,000 deaths worldwide each year (Crump *et al.*, 2004). In some instances patients  
53  
54 recover but remain carriers of the bacteria for many years. Another clinical syndrome associated  
55  
56 with *Salmonella* infection is nontyphoidal salmonellosis – a gastrointestinal disease also known  
57  
58 as enteritis. Components of the *Salmonella* atypical fimbriae (Saf) were investigated for  
59  
60

1  
2 inclusion in a vaccine (Strindelius *et al.*, 2004). A complex of recombinant SafB chaperone with  
3  
4 SafD adhesin was expressed in *E. coli* and purified. Starch microparticles were used as the  
5  
6 adjuvant. The recombinant cholera toxin B subunit (rCTB) was included as mucosal antigen-  
7  
8 uptake enhancer. BALB/c mice were immunized orally or subcutaneously with SafB/D- and  
9  
10 rCTB-conjugated microparticles and intranasally or subcutaneously with SafB/D mixed with  
11  
12 rCTB. The systemic and mucosal immune responses were studied. An oral challenge with *S.*  
13  
14 *enteritidis* was performed. All the immunized groups, except the group receiving oral  
15  
16 immunization, responded with high IgM–IgG titers to SafB/D. Analysis of the subclass ratio  
17  
18 (IgG1/IgG2a1IgG2b) indicated a mixed Th1 and Th2 response, with Th1 predominating. Only  
19  
20 the group receiving intranasal immunization got the mucosal response, measured as specific  
21  
22 IgA/total IgA (from fecal samples), significantly higher than that in the untreated control group  
23  
24 ( $P < 0.05$ ). Spleens were removed 6 days after oral challenge and Salmonella CFU were counted.  
25  
26 The group immunized subcutaneously with SafB/D- and rCTB-conjugated microparticles had  
27  
28 significantly lower CFU counts than the untreated control group ( $P < 0.05$ ).  
29  
30  
31  
32  
33  
34

35 ***Application of sefA gene for design of a live recombinant Salmonella vaccine.*** Lopes *et al.*  
36  
37 (2006) cloned the *sefA* gene, which encodes the main subunit of the SEF14 fimbrial protein, into  
38  
39 a temperature-sensitive expression vector and transformed it into a nonpathogenic, avirulent  
40  
41 strain of *E. coli*. The recombinant strain was used as a vaccine to elicit specific immune response  
42  
43 against the SefA protein of *S. enteritidis* in 1-day-old chickens. The recombinant strain was  
44  
45 reisolated from the intestines of treated birds for up to 21 days after treatment, demonstrating its  
46  
47 ability to colonize the intestinal tracts of 1-day-old chickens. In addition, IgA against the SefA  
48  
49 protein was detected by ELISA in intestinal secretions from treated birds 7 days after treatment  
50  
51 and in bile samples 14–21 days after treatment. Non-treated birds did not show any evidence of  
52  
53 intestinal colonization by the recombinant strain or anti-SefA IgA response in their bile or  
54  
55 intestinal secretions. Thus, the preliminary evaluation of the recombinant strain showed a  
56  
57 potential use of this strain to elicit protection against *S. enteritidis* infection in chickens.  
58  
59  
60

1  
2 ***Vaccination with E. coli polyadhesin Dr against chronic urinary tract infection. E. coli***  
3  
4 expressing Dr fimbria and related adhesins are associated with urinary tract infection, including  
5  
6 cystitis and/or pyelonephritis and diarrhea. Children and pregnant women are prone to recurrent  
7  
8 or persistent infections caused by these organisms (Garcia *et al.*, 1996). Goluszko *et al.* (2005)  
9  
10 used purified *E. coli* Dr fimbrial antigen to vaccinate C3H/HeJ mice against an experimental  
11  
12 urinary tract infection due to a homologous strain bearing Dr polyadhesins. They demonstrated  
13  
14 reduced mortality in the vaccinated animals. Immune sera with high titers of anti-Dr antibody  
15  
16 inhibited bacterial binding to bladders and kidneys but did not affect the rate of renal  
17  
18  
19  
20  
21 colonization.

22  
23  
24 ***Oral vaccination with E. coli F4 (K88) poly-adhesive fimbriae against intestinal infection.***  
25  
26 Enterotoxigenic *E. coli* (EPEC) is the leading cause of diarrhea in piglets and newborn calves.  
27  
28 Massive efforts have therefore been made to develop a vaccine for the induction of protective  
29  
30 mucosal immunity against EPEC. Verdonck *et al.* (2009) showed that as a result of oral  
31  
32 immunization of piglets with F4 fimbriae purified from pathogenic enterotoxigenic *E. coli*, the  
33  
34 fimbriae bind to the F4 receptor (F4R) in the intestine and induce a protective F4-specific  
35  
36 immune response. F4 fimbriae are very stable polymeric structures composed of some minor  
37  
38 subunits and a major subunit FaeG that is also the fimbrial adhesin. Verdonck *et al.* (2009)  
39  
40 identified with the mutagenesis experiments FaeG amino acids 97 (N to K) and 201 (I to V) as  
41  
42 determinants for F4 polymeric stability. The interaction between the FaeG subunits in mutant F4  
43  
44 fimbriae is reduced but both mutant and wild type fimbriae behaved identically in F4R binding  
45  
46 and showed equal stability in the gastro-intestinal lumen. Oral immunization experiments  
47  
48 indicated that a higher degree of polymerisation of the fimbriae in the intestine was correlated  
49  
50 with a better F4-specific mucosal immunogenicity. Hu *et al.* (2009) developed recombinant  
51  
52 *Lactococcus lactis* which expresses K88 (F4) fimbrial polyadhesin FaeG for oral vaccination.  
53  
54 They demonstrated protective immune response in mice to FaeG. Recently Remer *et al.* (2009)  
55  
56 constructed the recombinant strain EcN pMut2-kanK88 (EcN-K88) stably expressing the  
57  
58  
59  
60

1  
2 determinant for the K88 fimbrial adhesin of ETEC on the bacterial surface. After oral application  
3  
4 of EcN-K88 to mice for one week, EcN-K88 as well as wild-type EcN and EcN mock-  
5  
6 transformed with the plasmid vector only could be detected in faecal samples for a minimum of  
7  
8 7 days after the last feeding, indicating that EcN can transiently colonise the murine intestine.  
9  
10 Oral application of EcN-K88 resulted in significant IgG serum titres against K88 as early as 7  
11  
12 days after the initial feeding with EcN-K88, but no significant IgA titres. In contrast, Remer *et*  
13  
14 *al.* (2009) failed to detect any specific T cell responses towards the K88 antigen both in spleen  
15  
16 and mesenteric lymph nodes. Although dendritic cells readily upregulated maturation and  
17  
18 activation markers in response to K88 stimulation, accompanied by secretion of interleukin (IL)-  
19  
20 12, IL-6, IL-10, and tumour necrosis factor, restimulation of T cells from mice having received  
21  
22 EcN-K88 with K88-loaded dendritic cells did not result in detectable T cell proliferation and IL-  
23  
24 2 secretion, but rather induced an IL-10 bias. While the serum antibody responses clearly  
25  
26 demonstrate that K88 is recognized by the humoral immune system, the findings of Remer *et al.*  
27  
28 (2009) indicate that oral application of probiotic EcN expressing the K88 fimbrial adhesin does  
29  
30 not induce a selective T cell response towards the antigen.  
31  
32  
33  
34  
35  
36  
37  
38

39 **Applications of polyadhesins for expression of heterologous proteins. *Application of***  
40 ***polyadhesins for design of antiviral vaccines.*** The potential of the major structural subunit DraE  
41  
42 of *E. coli* Dr fimbriae has been used to display a peptide of glycoprotein D derived from *Herpes*  
43  
44 *simplex* virus (HSV) type 1 (Zalewska *et al.*, 2003). The heterologous sequence mimicking an  
45  
46 epitope from glycoprotein D was inserted in one copy into the *draE* gene in place of a predicted  
47  
48 11-amino acid sequence in the N-terminal region of surface-exposed domain 2 within the  
49  
50 conserved disulfide loop (from Cys21 to Cys53). The inserted epitope was displayed on the  
51  
52 surface of the chimeric DraE protein as evidenced by immunofluorescence and was recognized  
53  
54 by monoclonal antibodies to the target HSV glycoprotein D antigen. Conversely, immunization  
55  
56 of rabbits with purified chimeric Dr-HSV fimbriae resulted in a serum that specifically  
57  
58  
59  
60



1  
2 recognized the 11-amino acid epitope of HSV glycoprotein D, indicating the utility of the  
3  
4 strategy employed (Zalewska *et al.*, 2003).  
5

6  
7 ***Application of polyadhesins for expression of cytokines.*** The ability of the Caf1M  
8  
9 chaperone/Caf1A usher pathway to express large amounts of F1 antigen (Caf1) in *E. coli* was  
10 investigated to facilitate secretion of full-length heterologous proteins fused to the Caf1 subunit  
11 (Zavialov *et al.*, 2001). Despite correct processing of chimeric protein composed of a modified  
12 Caf1 signal peptide, mature human IL-1 $\beta$  (hIL-1 $\beta$ ), and mature Caf1, the processed product  
13 (hIL-1 $\beta$ -Caf1) remained insoluble. Coexpression of this chimera with a functional Caf1M  
14 chaperone led to the accumulation of soluble hIL-1 $\beta$ -Caf1 in the periplasm. Soluble hIL-1 $\beta$ -  
15 Caf1 reacted with monoclonal antibodies directed against structural epitopes of hIL-1 $\beta$ . The  
16 results indicate that the Caf1M-induced release of hIL-1  $\beta$ -Caf1 from the inner membrane  
17 promotes folding of the hIL-1 $\beta$  domain. Similar results were obtained with the fusion of Caf1 to  
18 hIL-1ra or to human GM-CSF. Following co-expression of the hIL-1 $\beta$ : Caf1 precursor with the  
19 Caf1M chaperone and Caf1A outer membrane protein, hIL-1 $\beta$ -Caf1 could be detected on the  
20 cell surface of *E. coli* (Zavialov *et al.*, 2001). These results demonstrated for the first time the  
21 potential of the chaperone/usher secretion pathway in the transport of subunits with large  
22 heterogeneous N-terminal fusions. This represented a novel means for the delivery of correctly  
23 folded heterologous proteins to the periplasm and cell surface as either polymers or cleavable  
24 monomeric domains (Korpela *et al.*, 1999).  
25  
26  
27  
28  
29  
30  
31  
32  
33  
34  
35  
36  
37  
38  
39  
40  
41  
42  
43  
44  
45  
46  
47  
48  
49

## 50 Applications of Monoadhesins

51  
52  
53  
54 ***Applications of monoadhesins for vaccine design. Vaccination with FimH adhesin***  
55 ***against infection by uropathogenic E. coli.*** Virtually all uropathogenic strains of *E. coli*, the  
56 primary cause of cystitis, assemble adhesive surface organelles called type 1 pili that contain the  
57 FimH adhesin. Langermann *et al.* (1997) demonstrated that sera from animals vaccinated with  
58  
59  
60



1  
2 candidate FimH vaccines inhibited uropathogenic *E. coli* from binding to human bladder cells *in*  
3  
4 *vitro*. They found that immunization with FimH reduced *in vivo* colonization of the bladder  
5  
6 mucosa by more than 99% in a murine cystitis model, and immunoglobulin G to FimH was  
7  
8 detected in urinary samples from protected mice. Furthermore, passive systemic administration  
9  
10 of immune sera to FimH also resulted in reduced bladder colonization by uropathogenic *E. coli*.  
11  
12 Later Langermann *et al.* (2000) studied 4 monkeys inoculated with 100 µg of FimCH adhesin-  
13  
14 chaperone complex mixed with MF59 adjuvant, and 4 monkeys given adjuvant only  
15  
16 intramuscularly. After 2 doses (day 0 and week 4), a booster at 48 weeks elicited a strong IgG  
17  
18 antibody response to FimH in the vaccinated monkeys. All 8 monkeys were challenged with 1  
19  
20 ml of 10<sup>8</sup> *E. coli* cystitis isolate NU14. Three of the 4 vaccinated monkeys were protected from  
21  
22 bacteruria and pyuria; all control monkeys were infected. These findings suggest that a vaccine  
23  
24 based on the FimH adhesin of *E. coli* type 1 pili may have utility in preventing cystitis in  
25  
26 humans.  
27  
28  
29  
30  
31  
32

33 **Monoadhesins as targets for specific inhibition of adhesion.** Mannose-binding type 1 pili  
34  
35 are important virulence factors for the establishment of *E. coli* urinary tract infections (UTIs).  
36  
37 These infections are initiated by adhesion of uropathogenic *E. coli* to uroplakin receptors in the  
38  
39 uroepithelium via the FimH adhesin located at the tips of type 1 pili. Blocking of bacterial  
40  
41 adhesion is able to prevent infection. Bouckaert *et al.* (2005) provided the binding data of the  
42  
43 molecular events underlying type 1 fimbrial adherence, by crystallographic analyses of the FimH  
44  
45 receptor binding domains from an uropathogenic and a K-12 strain, and affinity measurements  
46  
47 with mannose, common mono- and disaccharides, and a series of alkyl and aryl mannosides.  
48  
49 Their results illustrate that the lectin domain of the FimH adhesin is a stable and functional entity  
50  
51 and that an exogenous butyl  $\alpha$ -D-mannoside, bound in the crystal structures, exhibits a  
52  
53 significantly better affinity for FimH ( $K_d=0.15$  µM) than mannose ( $K_d=2.3$  µM). Exploration of  
54  
55 the binding affinities of  $\alpha$ -D-mannosides with longer alkyl tails revealed affinities up to 5 nM.  
56  
57 Aryl mannosides and fructose can also bind with high affinities to the FimH lectin domain, with  
58  
59  
60

1 a 100-fold improvement and 15-fold reduction in affinity, respectively, compared with mannose.  
2  
3  
4 Taken together, these relative FimH affinities correlate exceptionally well with the relative  
5  
6 concentrations of the same glycans needed for the inhibition of adherence of type 1 piliated *E.*  
7  
8 *coli*. Wellens *et al.* (2008) demonstrated that  $\alpha$ -D-mannose based inhibitors of FimH not only  
9  
10 block bacterial adhesion on uroepithelial cells but also antagonize invasion and biofilm  
11  
12 formation. Heptyl  $\alpha$ -D-mannose prevents binding of type 1-piliated *E. coli* to the human bladder  
13  
14 cell line 5637 and reduces both adhesion and invasion of the UTI89 cystitis isolate instilled in  
15  
16 mouse bladder via catheterization. Heptyl  $\alpha$ -D-mannose also specifically inhibited biofilm  
17  
18 formation at micromolar concentrations. The structural basis of the great inhibitory potential of  
19  
20 alkyl and aryl  $\alpha$ -D-mannosides was elucidated in the crystal structure of the FimH receptor-  
21  
22 binding domain in complex with oligomannose-3. FimH interacts with  
23  
24 Man<sub>1,3</sub>Man $\beta$ <sub>1,4</sub>GlcNAc $\beta$ <sub>1,4</sub>GlcNAc in an extended binding site. The interactions along the  
25  
26  $\alpha$ <sub>1,3</sub> glycosidic bond and the first  $\beta$ <sub>1,4</sub> linkage to the chitobiose unit are conserved with those of  
27  
28 FimH with butyl  $\alpha$ -D-mannose. The strong stacking of the central mannose with the aromatic  
29  
30 ring of Tyr48 is congruent with the high affinity found for synthetic inhibitors in which this  
31  
32 mannose is substituted with an aromatic group.  
33  
34  
35  
36  
37  
38  
39

40 **Chaperone/usher assembly-translocation machinery as target for a new generation of**  
41 **antimicrobials interrupting assembly of adhesive organelles.** Pinkner *et al.* (2006) rationally  
42  
43 designed small compounds that specifically inhibit biogenesis of adhesive pili assembled by the  
44  
45 chaperone–usher pathway in Gram-negative pathogens. The activity of a family of bicyclic 2-  
46  
47 pyridones, termed pilicides, was evaluated in two different pilus biogenesis systems in  
48  
49 uropathogenic *E. coli*. Hemagglutination mediated by either type 1 or P pili, adherence to  
50  
51 bladder cells, and biofilm formation mediated by type 1 pili were all reduced by  $\approx$ 90% in  
52  
53 laboratory and clinical *E. coli* strains. Fig. 16 shows stereoisomer of the PapD–pilicide complex  
54  
55 (Pinkner *et al.*, 2006) in overlay with the FimD<sub>1–125</sub> N-terminal usher domain in complex with  
56  
57 the FimC-FimH<sub>158–279</sub> chaperone–adhesion complex (Fig. 16; Nishiyama *et al.*, 2005). The  
58  
59  
60

1  
2 conserved hydrophobic patch across the back of the F1-C1-D1  $\beta$ -sheet formed by residues  
3  
4 I90/I93, L32/L32, and L54/V56 (FimC/PapD) forms part of both the usher-interaction site and  
5  
6 the pilicide-binding site. In the chaperone–pilicide interaction, the plane of the 2-pyridone  
7  
8 system and the R1-cyclopropyl and R2-CH<sub>2</sub>-naphthyl substituents coincide with and mimic the  
9  
10 interactions made by the F4, L19, and F22 side chains from the usher N-terminal domain. The  
11  
12 overlay demonstrates the steric clash between the pilicide and the usher N-terminal domain.  
13  
14 Point mutations in the pilicide-binding site dramatically reduced pilus formation but did not  
15  
16 block the ability of PapD to bind subunits and mediate their folding (Pinkner *et al.*, 2006).  
17  
18 Surface plasmon resonance experiments confirmed that the pilicide interfered with the binding of  
19  
20 chaperone–subunit complexes to the usher (Pinkner *et al.*, 2006). These pilicides thus target key  
21  
22 virulence factors in pathogenic bacteria and represent a promising proof of concept for  
23  
24 developing drugs that function by targeting virulence factors.  
25  
26  
27  
28  
29  
30  
31  
32

### 33 CONCLUSIONS AND FUTURE PERSPECTIVES

34  
35  
36  
37 Extensively antibiotic-resistant strains of Gram-negative pathogens emerged during the last  
38  
39 dozen of years whereas safe and effective vaccines against many of them currently are absent.  
40  
41 There are now a growing number of reports of cases of infections caused by Gram-negative  
42  
43 organisms for which no adequate therapeutic options exist (de Jong & Ekdahl, 2006; Giske *et al.*,  
44  
45 2008). This return to the pre-antibiotic era has become a reality both in Europe as in other parts  
46  
47 of the world. Targeting bacterial virulence is an alternative approach to antimicrobial therapy  
48  
49 that offers promising opportunities to inhibit pathogenesis and its consequences without placing  
50  
51 immediate life-or-death pressure on the target bacterium. Two general strategies exist to inhibit  
52  
53 fimbrial adhesion mediated functions (Cegelski *et al.*, 2008; Cusumano & Hultgren, 2009):  
54  
55  
56  
57 (1) The specific inhibition of adhesion, which involves physically precluding pathogen binding  
58  
59 to host cells, for example, with carbohydrate derivatives of host ligands.  
60

1  
2 (2) The interruption of fimbrial adhesion assembly, which also blocks adhesion as well as  
3  
4 invasion and intracellular biofilm formation.  
5

6  
7 The first strategy is most effective for specific inhibition of monoadhesins. It was  
8  
9 demonstrated that  $\alpha$ -D-mannose based inhibitors of FimH adhesin not only block bacterial  
10  
11 adhesion on uroepithelial cells but also antagonize invasion and biofilm formation (Bouckaert *et*  
12  
13 *al.*, 2005; Wellens *et al.*, 2008).  
14

15  
16 The second general strategy to inhibit fimbrial adhesion mediated functions is targeted to the  
17  
18 classical chaperone/usher assembly-translocation machinery (Pinkner *et al.*, 2006; Aberg &  
19  
20 Almqvist, 2007). The recently solved structure of the usher translocator pore of the twinned-pore  
21  
22 translocation machinery created a ground for a rational design of a new generation of  
23  
24 antimicrobials interrupting assembly of adhesive organelles. However, chaperone/usher  
25  
26 machinery contains a few crucial details that are not studied well yet. They are likely to be the  
27  
28 major direction for future studies.  
29  
30  
31

32  
33 The revealed strong correlation between a number of residues in a F1-G1 loop of  
34  
35 chaperones and a number of subunits operating by them was as the basis for the novel function-  
36  
37 structural classification of the fimbrial adhesins. The FGS chaperone-assembled polyadhesive  
38  
39 fimbriae were discovered in addition to the previously found family of the FGL chaperone-  
40  
41 assembled polyadhesins. The FGL and FGS chaperone-assembled polyadhesins are encoded  
42  
43 exclusively by the gene clusters of the  $\gamma$ 3- and  $\kappa$ -monophyletic groups, respectively, while gene  
44  
45 clusters belonging to the  $\gamma$ 1-,  $\gamma$ 2-,  $\gamma$ 4-, and  $\pi$ -fimbrial clades exclusively encode monoadhesins  
46  
47 (Nuccio & Bäumler, 2007). Poly-adhesive binding possesses an advantage over mono-adhesive  
48  
49 binding because it would result in formation of more powerful and tight contact between the  
50  
51 pathogen and the host cell and it may lead to a massive aggregation of the receptors. This  
52  
53 subsequently would trigger subversive signals directed to mislead functions of host cells, in  
54  
55 particular, the cells of immune system. Anti-immune function is likely to be common for all  
56  
57 fimbrial polyadhesins including FGS chaperone-assembled poly-adhesive fimbriae/pili. Hence,  
58  
59  
60

1  
2 a search for binding to immune system associated receptors could be a starting point for  
3  
4 functional characterization of known and newly revealed members of both FGL and FGS  
5  
6 chaperone-assembled families of polyadhesins.  
7

8  
9 The fimbrial polyadhesins that are represented by the linear homopolymers of hundreds to  
10  
11 thousands of subunits have very high potential for cross-linking of B cell receptors and  
12  
13 stimulation of antibody production. They are specific and very powerful surface antigens  
14  
15 typical only for pathogenic strains. Therefore they are promising candidates for development of  
16  
17 recombinant vaccines against Gram-negative infections and for medical diagnostics of them.  
18  
19 The exploitation of these extraordinary properties of fimbrial polyadhesins is of great  
20  
21 importance because Gram-negative infections are a burden problem worldwide with  
22  
23 considerable negative economic impact and health risk to people.  
24  
25  
26  
27

28 In particular, the outbreak of pneumonic plague in Surat in 1994 and its spread to other  
29  
30 cities in India, lasted only a little over 2 weeks, but it created an unprecedented panic that had  
31  
32 global repercussions (Dutt *et al.*, 2006). At first, the Surat hospital doctors could not diagnose  
33  
34 the disease, but when they did, immediate intervention, in the form of prevention and treatment  
35  
36 (administration of antibodies) ceased the disease spreading beyond Surat, Delhi, Calcutta,  
37  
38 Bombay and their vicinities. Fewer than 1,200 people were diagnosed with plague. A DNA-  
39  
40 based study in 2000 decisively concluded that the Surat episode was a plague, but the Indian  
41  
42 isolates were genetically more heterogeneous compared to others in the world. The last  
43  
44 outbreak of primary pneumonic plague took place in the Shimla District of Himachal Pradesh  
45  
46 State in northern India during February 2002 (Gupta & Sharma, 2007). Sixteen cases of plague  
47  
48 were reported with a case-fatality rate of 25%.  
49  
50  
51  
52

53  
54 The infections caused by two other representatives of *Yersinia* genus, *Y. enterocolitica* and  
55  
56 *Y. pseudotuberculosis*, also have a significant health concern in India and worldwide. *Y.*  
57  
58 *enterocolitica* is the important food-borne enteropathogen that causes a variety of syndromes  
59  
60 (Viridi & Sachdeva, 2005). Most commonly, it causes gastroenteritis, terminal ileitis and

1  
2 mesenteric lymphadenitis. Postinfectious sequelae includes reactive arthritis and erythema  
3  
4 nodosum. *Y. pseudotuberculosis* also causes a variety of gastrointestinal and extraintestinal  
5  
6 infections in humans (Kumar *et al.*, 2009). Encoded by the *caf* gene cluster (Fig. 1) F1 capsular  
7  
8 antigen from *Y. pestis* is the most specific and potent antigen for medical diagnostics of bubonic  
9  
10 and pneumonic plague. The identical *psa* gene clusters present in *Y. pestis* and *Y.*  
11  
12 *pseudotuberculosis* (Fig. 1) that encodes for proteins for expression and assembly of the  
13  
14 fimbrial pH6 antigen. Positive detection of pH6 antigen without any traces of F1 antigen is  
15  
16 indicator of infection caused by *Y. pseudotuberculosis* or evidence of F1<sup>+</sup> strain of *Y. pestis*. *Y.*  
17  
18 *enterocolitica* contains a closely related to *psa* gene cluster *myf* (Fig. 1) encoding the Myf  
19  
20 fimbriae, which is built up of MyfA subunits. *Y. enterocolitica* is very heterogeneous (Viridi &  
21  
22 Sachdeva, 2005). Therefore specific medical diagnostics of pathogenic strains of *Y.*  
23  
24 *enterocolitica* is still unsolved problem. The Myf polyadhesin is promising conservative antigen  
25  
26 for indication of infection caused by *Y. enterocolitica*.  
27  
28  
29  
30  
31  
32

33 *Salmonella* spp. is the extremely heterogeneous species (Layton & Galyov, 2007). There are  
34  
35 over 2500 serotypes of *Salmonella* spp. Specific medical diagnostics of pathogenic strains from  
36  
37 *Salmonella* is still unsolved problem. The *Salmonella* spp. gene clusters *saf* and *sef* (Fig. 1)  
38  
39 encode for proteins for expression and assembly of the atypical fimbriae Saf and the  
40  
41 filamentous fimbriae-like structures SEF14/18. These gene clusters encode two distinct adhesin  
42  
43 subunits: the variable major polyadhesin subunits SefA or SafA and the conservative minor  
44  
45 SefD or SafD subunits (Fig. 1). The SefB chaperone of *S. enteritidis* assists in the assembly of  
46  
47 two distinct cell-surface structures, SEF14 and SEF18, which are homopolymers of SefA and  
48  
49 SefD subunits, respectively (Clouthier *et al.*, 1994). The SafD subunit is identical for *S.*  
50  
51 *enteritidis*, *S. Typhi*, *S. Paratyphi A*, *S. choleraesuis* and *S. typhimurium*, and the SefD subunit  
52  
53 is identical for *S. Paratyphi A* and *S. enteritidis*. Therefore SefD and SafD subunits and mAbs  
54  
55 to them can be used for medical diagnostics of main *Salmonella* infections.  
56  
57  
58  
59  
60

## Acknowledgements

This work was supported by grants from the European Commission/Research Executive Agency under a Marie Curie International Incoming Fellowship (235538) and a grant from the Academy of Finland (112900) to V. Z., and the FORMAS (221-2007-1057) and Swedish Research Council (K2008-58X-20689-01-3) to A. Z.

## References

- Aberg V & Almqvist F (2007) Pilicides-small molecules targeting bacterial virulence. *Org Biomol Chem* **5**: 1827–1834.
- Adams LM, Simmons CP, Rezmann L, Strugnell RA & Robins-Browne RM (1997) Identification and characterization of a K88- and CS31A-like operon of a rabbit enteropathogenic *Escherichia coli* strain which encodes fimbriae involved in the colonization of rabbit intestine. *Infect Immun* **65**: 5222–5230.
- Adinda W, Garofalo C, Nguyen H, Van Gerven N, Slättegård R, Hernalsteens J-P, Wyns L, Oscarson S, De Greve H, Hultgren S, Bouckaert J (2008) Intervening with Urinary Tract Infections Using Anti-Adhesives Based on the Crystal Structure of the FimH–Oligomannose-3 Complex. *PLoS ONE* **3**: e2040.
- Ahrens R, Ott M, Ritter A, Hoschuetzky H, Buehler T, Lottspeich F, Boulnois GJ, Jann K & Hacker J (1993) Genetic analysis of the gene cluster encoding nonfimbrial adhesin I from an *Escherichia coli* uropathogen. *Infect Immun* **61**: 2505–2512.
- Allen BL, Gerlach GF & Clegg S (1991) Nucleotide sequence and functions of *mrk* determinants necessary for expression of type 3 fimbriae in *Klebsiella pneumoniae*. *J Bacteriol* **173**: 916–920.



- 1  
2 Alvarez ML, Pinyerd HL, Crisantes JD, Rigano MM, Pinkhasov J, Walmsley AM, Mason HS &  
3  
4 Cardineau GA (2006) Plant-made subunit vaccine against pneumonic and bubonic plague is  
5  
6 orally immunogenic in mice. *Vaccine* **24**: 2477–2490.  
7  
8  
9 Anantha RP, McVeigh AL, Lee LH, Agnew MK, Cassels FJ, Scott DA, Whittam TS & Savarino  
10  
11 SJ (2004) Evolutionary and functional relationships of colonization factor antigen I and other  
12  
13 class 5 adhesive fimbriae of enterotoxigenic *Escherichia coli*. *Infect Immun* **72**: 7190–7201.  
14  
15  
16 Anderson KL, Billington J, Pettigrew D, Cota E, Simpson P, Roversi P, Chen H, Urvil P, du  
17  
18 Merle L & Barlow P (2004) An atomic resolution model for assembly, architecture, and  
19  
20 function of the Dr adhesins. *Mol Cell* **101**: 647–657.  
21  
22  
23 Anderson KL, Cota E, Simpson P, Chen HA, du Merle L, Le Bouguéne C & Matthews S  
24  
25 (2004b) Complete resonance assignments of a ‘donor-strand complemented’ AfaE: the  
26  
27 afimbrial adhesin from diffusely adherent *E coli*. *J Biomol NMR* **29**: 409–410.  
28  
29  
30 Anderson BN, Ding AM, Nilsson LM, Kusuma K, Tchesnokova V, Vogel V, Sokurenko EV &  
31  
32 Thomas WE (2007) Weak rolling adhesion enhances bacterial surface colonization. *J*  
33  
34 *Bacteriol* **189**: 1794–1802.  
35  
36  
37 Anderson GW, Worsham PL, Bolt CR, Andrews GP, Welkos SL, Friedlander AM & Burans JP  
38  
39 (1997) Protection of mice from fatal bubonic and pneumonic plague by passive  
40  
41 immunization with monoclonal antibodies against the F1 protein of *Yersinia pestis*. *Am J*  
42  
43 *Trop Med Hyg* **56**: 471–473.  
44  
45  
46  
47  
48 Anisimov AP, Bakhteeva IV, Panfertsev EA, Svetoch TE, Kravchenko TV, Platonov ME,  
49  
50 Titareva GM, Kombarova TI, Ivanov SA, Rakin AV, Amoako KK & Dentovskaya SV  
51  
52 (2009) The subcutaneous inoculation of pH 6 antigen mutants of *Yersinia pestis* does not  
53  
54 affect virulence and immune response in mice. *J Med Microbiol* **58**: 26–36.  
55  
56  
57  
58 Aprikian P, Tchesnokova V, Kidd B, Yakovenko O, Yarov-Yarovoy V, Trinchina E, Vogel V,  
59  
60 Thomas W & Sokurenko E (2007) Interdomain interaction in the FimH adhesin of  
*Escherichia coli* regulates the affinity to mannose. *J Biol Chem* **282**: 23437–23446.

- 1  
2 Bahrani FK & Mobley HLT (1994) *Proteus mirabilis* MR/P fimbrial operon: genetic  
3  
4 organization, nucleotide sequence, and conditions for expression. *J Bacteriol* **176**: 3412–  
5  
6 3419.  
7  
8
- 9 Bakker D, Vader CEM, Roosendaal B, Mooj FR, Oudega B & de Graaf FK (1991) Structure and  
10  
11 function of periplasmic chaperone-like proteins involved in the biosynthesis of K88 and K99  
12  
13 fimbriae in enterotoxigenic *Escherichia coli*. *Mol Microbiol* **5**: 875–886.  
14  
15
- 16 Bann JG, Pinkner JS, Frieden C & Hultgren SJ (2004) Catalysis of protein folding by chaperones  
17  
18 in pathogenic bacteria. *Proc Natl Acad Sci USA* **101**: 17389–17393.  
19  
20
- 21 Barbe V, Vallenet D, Fonknechten N, Kreimeyer A, Oztas S, Labarre L, Cruveiller S, Robert K,  
22  
23 Duprat S, Wincker P, Ornston LN, Weissenbach J, Marlière P, Cohen GN & Médigue C  
24  
25 (2004) Unique features revealed by the genome sequence of *Acinetobacter* sp. ADP1, a  
26  
27 versatile and naturally transformation competent bacterium. *Nucl Acids Res* **32**: 5766–5779.  
28  
29
- 30 Bäumlér AJ & Heffron F (1995) Identification and sequence analysis of *lpfABCDE*, a putative  
31  
32 fimbrial operon of *Salmonella typhimurium*. *J Bacteriol* **177**: 2087–2097.  
33  
34
- 35 Bäumlér AJ, Tsolis RM, Bowe FA, Kusters JG, Hoffmann S & Heffron F (1996) The *pef*  
36  
37 fimbrial operon of *Salmonella typhimurium* mediates adhesion to murine small intestine and  
38  
39 is necessary for fluid accumulation in the infant mouse. *Infect Immun* **64**: 61–68.  
40  
41
- 42 Beaulieu JF (1999) Integrins and human intestinal cell functions. *Front Biosci* **4**: D310–D321.  
43  
44
- 45 Benchimol S, Fuks A, Jothy S, Beauchemin N, Shirota K & Stanners CP (1989)  
46  
47 Carcinoembryonic antigen, a human tumor marker, functions as an intercellular adhesion  
48  
49 molecule. *Cell* **57**: 327–334.  
50  
51
- 52 Bendtsen JD, Nielsen H, von Heijne G & Brunak S (2004) Improved prediction of signal  
53  
54 peptides: SignalP 3.0. *J Mol Biol* **340**: 783–795.  
55  
56
- 57 Ben-Efraim S, Aronson M & Bichowsky-Slomnicki L (1961) New antigenic component of  
58  
59 *Pasteurella pestis* formed under specific conditions of pH and temperature. *J Bacteriol* **81**:  
60  
704–714.

- 1  
2 Berger CN, Billker O, Meyer TF, Servin AL & Kansau I (2004) Differential recognition of  
3  
4 members of the carcinoembryonic antigen family by Afa/Dr adhesins of diffusely adhering  
5  
6 *Escherichia coli* (Afa/Dr DAEC) *Mol Microbiol* **52**: 963–983.  
7  
8
- 9 Bergsten G, Wullt B, Svanborg C (2005) *Escherichia coli*, fimbriae, bacterial persistence and  
10  
11 host response induction in the human urinary tract. *Int J Med Microbiol* **295**: 487–502.  
12  
13
- 14 Bernier C, Gounon P & Le Bouguéne C (2002) Identification of an aggregative adhesion  
15  
16 fimbria (AAF) type III-encoding operon in enteroaggregative *Escherichia coli* as a sensitive  
17  
18 probe for detecting the AAF-encoding operon family. *Infect Immun* **70**: 4302–4311.  
19  
20
- 21 Bertin Y, Girardeau J-P, Der Vartanian M & Martin C (1993) The ClpE protein involved in  
22  
23 biogenesis of the CS31A capsule-like antigen is a member of a periplasmic chaperone family  
24  
25 in Gram-negative bacteria. *FEMS Microbiol Lett* **108**: 59–68.  
26  
27
- 28 Betis F, Brest P, Hofman V, Guignot J, Bernet-Camard MF, Rossi B, Servin A & Hofman P  
29  
30 (2003a) The Afa/Dr adhesins of diffusely adhering *Escherichia coli* stimulate interleukin-8  
31  
32 secretion, activate mitogen-activated protein kinases, and promote polymorphonuclear  
33  
34 transepithelial migration in T84 polarized epithelial cells. *Infect Immun* **71**: 1068–1074.  
35  
36
- 37 Betis F, Brest P, Hofman V, Guignot J, Kansau I, Rossi B, Servin A & Hofman P (2003b)  
38  
39 Afa/Dr diffusely adhering *Escherichia coli* infection in T84 cell monolayers induces  
40  
41 increased neutrophils transepithelial migration, which in turn promotes cytokine-dependent  
42  
43 upregulation of decay-accelerating factor (CD55), the receptor for Afa/Dr adhesins. *Infect*  
44  
45 *Immun* **71**: 1774–1783.  
46  
47  
48
- 49 Bilge SS, Clausen CR, Lau W & Moseley SL (1989) Molecular characterization of a fimbrial  
50  
51 adhesin, F1845, mediating diffuse adherence of diarrhea-associated *Escherichia coli* to HEp-  
52  
53 2 cells. *J Bacteriol* **171**: 4281–4289.  
54  
55
- 56 Bonci A, Chiesurin A, Muscas P & Rossolini GM (1997) Relatedness and phylogeny within the  
57  
58 family of periplasmic chaperones involved in the assembly of pili or capsule-like structures  
59  
60 of gram-negative bacteria. *J Mol Evol* **44**: 299–309.

- 1  
2 Bork P, Holm L & Sander C (1994) The immunoglobulin fold: structural classification, sequence  
3  
4 patterns and common core. *J Mol Biol* **242**: 309–320.  
5  
6  
7 Bouckaert J, Berglund J, Schembri M, De Genst E, Cools L, Wuhrer M, Hung C-S, Pinkner J,  
8  
9 Slättégård R, Zavialov A, Choudhury D, Langermann S, Hultgren SJ, Wyns L, Klemm P,  
10  
11 Oscarson S, Knight SD & De Greve H (2005) Receptor binding studies disclose a novel class  
12  
13 of high-affinity inhibitors of the *Escherichia coli* FimH adhesin. *Mol Microbiol* **55**: 441–455.  
14  
15  
16 Bouckaert J, Mackenzie J, de Paz JL, Chipwaza B, Choudhury D, Zavialov A, Mannerstedt K,  
17  
18 Anderson J, Piérard D, Wyns L, Seeberger PH, Oscarson S, De Greve H & Knight SD (2006)  
19  
20 The affinity of the FimH fimbrial adhesin is receptor-driven and quasi-independent of  
21  
22 *Escherichia coli* pathotypes. *Mol Microbiol* **61**: 1556–1568.  
23  
24  
25  
26 Boulton IC & Gray-Owen SD (2002) Neisserial binding to CEACAM1 arrests the activation and  
27  
28 proliferation of CD41 T lymphocytes. *Nat Immunol* **3**: 229–236.  
29  
30  
31 Bower JM, Eto DS & Mulvey MA (2005) Covert operations of uropathogenic *Escherichia coli*  
32  
33 within the urinary tract. *Traffic* **6**: 18–31.  
34  
35  
36 Bradbury J (2002) *Neisseria gonorrhoeae* evades host immunity by switching off T lymphocytes.  
37  
38 *Lancet* **359**: 681.  
39  
40  
41 Brest P, Betis F, Cuburu N, Selva E, Herrant M, Servin A, Auburger P & Hofman P (2004)  
42  
43 Increased rate of apoptosis and diminished phagocytic ability of human neutrophils infected  
44  
45 with Afa/Dr diffusely adhering *Escherichia coli* strains. *Infect Immun* **72**: 5741–5749.  
46  
47  
48 Brodbeck WG, Liu D, Sperry J, Mold C & Medof ME (1996) Localization of classical and  
49  
50 alternative pathway regulatory activity within the decay-accelerating factor. *J Immunol* **156**:  
51  
52 2528–2533.  
53  
54  
55 Brunder W, Khan AS, Hacker J & Karch H (2001) Novel type of fimbriae encoded by the large  
56  
57 plasmid of sorbitol-fermenting enterohemorrhagic *Escherichia coli* O157: H2. *Infect Immun*  
58  
59 **69**: 4447–4457.  
60

- 1  
2 Cane G, Moal VL, Pagès G, Servin AL, Hofman P & Vouret-Craviari V (2007) Up-regulation of  
3  
4 intestinal vascular endothelial growth factor by Afa/Dr diffusely adhering *Escherichia coli*.  
5  
6 *PLoS ONE* **2**: e1359.  
7  
8  
9 Cantey JR, Blake RK, Williford JR & Moseley SL. (1999) Characterization of the *Escherichia*  
10  
11 *coli* AF/R1 Pilus Operon: Novel Genes Necessary for Transcriptional Regulation and for  
12  
13 Pilus-Mediated Adherence. *Infect Immun* **67**: 2292–2298.  
14  
15  
16 Caras IW, Weddell GN, Davitz MA, Nussenzweig V & Martin DW (1987) Signal for attachment  
17  
18 of a phospholipid membrane anchor in decay accelerating factor. *Science* **238**: 1280–1283.  
19  
20  
21 Carnoy C & Moseley SL. (1997) Mutational analysis of receptor binding mediated by the Dr  
22  
23 family of *Escherichia coli* adhesins. *Mol Microbiol* **23**: 365–379.  
24  
25  
26 Carroll MC, Alicot EM, Katzman PJ, Klickstein LB, Smith JA & Fearon DT (1988)  
27  
28 Organization of the genes encoding complement receptors type 1 and 2, decay-accelerating  
29  
30 factor, and C4-binding protein in the RCA locus on human chromosome 1. *J Exp Med* **167**:  
31  
32 1271–1280.  
33  
34  
35 Cathelyn JS, Crosby SD, Lathem WW, Goldman WE & Miller VL (2006) RovA, a global  
36  
37 regulator of *Yersinia pestis*, specifically required for bubonic plague. *Proc Natl Acad Sci*  
38  
39 *USA* **103**: 13514–13519.  
40  
41  
42 Cegelski L, Marshall GR, Eldridge GR & Hultgren SJ (2008) The biology and future prospects  
43  
44 of antivirulence therapies. *Nat Rev Microbiol* **6**: 17–27.  
45  
46  
47 Chapman DAG, Zavialov AV, Chernovskaya TV, Karlyshev AV, Zav'yalova GA, Vasiliev AM,  
48  
49 Dudich IV, Abramov VM, Zav'yalov VP & Macintyre S (1999) Structure and functional  
50  
51 significance of the FGL sequence of the periplasmic chaperone, Caf1M, of *Yersinia pestis*. *J*  
52  
53 *Bacteriol* **181**: 2422–2429.  
54  
55  
56 Chattopadhyay S, Feldgarden M, Weissman SJ, Dykhuizen DE, van Belle G & Sokurenko EV  
57  
58 (2007) Haplotype diversity in "source-sink" dynamics of *Escherichia coli* urovirulence. *J*  
59  
60 *Mol Evol* **64**: 204–214.

- 1  
2  
3  
4  
5  
6  
7  
8  
9  
10  
11  
12  
13  
14  
15  
16  
17  
18  
19  
20  
21  
22  
23  
24  
25  
26  
27  
28  
29  
30  
31  
32  
33  
34  
35  
36  
37  
38  
39  
40  
41  
42  
43  
44  
45  
46  
47  
48  
49  
50  
51  
52  
53  
54  
55  
56  
57  
58  
59  
60
- Chen T, Zimmermann W, Parker J, Chen I, Maeda A & Bolland S (2001) Biliary glycoprotein (BGP<sub>a</sub>, CD66<sub>a</sub>, CEACAM1) mediates inhibitory signals. *J Leukoc Biol* **70**: 335–340.
- Chen TH & Elberg SS (1977) Scanning electron microscopic study of virulent *Yersinia pestis* and *Yersinia pseudotuberculosis* type 1. *Infect Immun* **15**: 972–977.
- Chessa D, Dorsey CW, Winter M & Bäumlér AJ (2008) Binding specificity of *Salmonella* plasmid-encoded fimbriae assessed by glycomics. *J Biol Chem* **283**: 8118–8124.
- Chichester JA, Musiychuk K, Farrance C, Mett V, Lyons J, Mett V & Yusibov (2009) A single component two-valent LcrV-F1 vaccine protects non-human primates against pneumonic plague. *Vaccine* **27**: 3471–3474.
- Chiu CH, Tang P, Chu C, Hu S, Bao Q, Yu J, Chou Y-Y, Wang H-S & Lee Y-S (2005) The genome sequence of *Salmonella enterica* serovar Choleraesuis, a highly invasive and resistant zoonotic pathogen. *Nucl Acids Res* **33**: 1690–1698.
- Choudhury D, Thompson A, Stojanoff V, Langermann S, Pinkner J, Hultgren SJ & Knight SD (1999) X-ray structure of the FimC-FimH chaperone-adhesin complex from uropathogenic *Escherichia coli*. *Science* **285**: 1061–1066.
- Cleri DJ, Vernaleo JR, Lombardi LJ, Rabbar MS, Mathew A, Marton R & Reyelt MC (1997) Plague pneumonia disease caused by *Yersinia pestis*. *Semin Respir Infect* **12**: 12–23.
- Clouthier SC, Collinson SK & Kay WW (1994) Unique fimbriae-like structures encoded by *sefD* of the SEF14 fimbrial gene cluster of *Salmonella enteritidis*. *Mol Microbiol* **12**: 893–901.
- Clouthier SC, Müller KH, Doran JL, Collinson SK & Kay WW (1993) Characterization of three fimbrial genes, *sefABC*, of *Salmonella enteritidis*. *J Bacteriol* **175**: 2523–2533.
- Cornelis GR & Wolf-Watz H (1997) The *Yersinia* Yop virulon: a bacterial system for subverting eukaryotic cells. *Mol Microbiol* **23**: 861–867.
- Cota E, Chen HA, Anderson KL, Simpson P, du Merle L, Bernier-Fébreau C, Piątek R, Zalewska B, Nowicki B, Kur J, Le Bouguéne C & Matthews S (2004) Letter to the editor:



1  
2 complete resonance assignments of the ‘donor-strand complemented’ AfaD: the afimbrial  
3  
4 invasin from diffusely adherent *E coli*. *J Biomol NMR* **29**: 411–412.  
5  
6

7  
8 Cota E, Jones C, Simpson P, Altroff H, Anderson KL, du Merle L, Guignot J, Servin A, Le  
9  
10 Bouguéne C, Mardon H & Matthews S (2006) The solution structure of the invasive tip  
11  
12 complex from Afa/Dr fibrils. *Mol Microbiol* **62**: 356–366.  
13  
14

15  
16 Coyne KE, Hall SE, Thompson S, Arce MA, Kinoshita T, Fujita T, Anstee DJ, Rosse W &  
17  
18 Lublin DM (1992) Mapping of epitopes, glycosylation sites, and complement regulatory  
19  
20 domains in human decay accelerating factor. *J Immunol* **149**: 2906–2913.  
21  
22

23  
24 Craig L, Pique ME, Tainer JA (2004) Type IV pilus structure and bacterial pathogenicity. *Nat*  
25  
26 *Rev Microbiol* **2**: 363–378.  
27

28  
29 Crump JA, Luby SP & Mintz ED (2004) The global burden of typhoid fever. *Bull World Health*  
30  
31 *Organ* **82**: 346–353.  
32

33  
34 Cusumano CK & Hultgren SJ (2009) Bacterial adhesion - a source of alternate antibiotic targets.  
35  
36 *IDrugs* **12**: 699–705.  
37

38  
39 Davitz MA, Low MG & Nussenzweig V (1986) Release of decay accelerating factor (DAF) from  
40  
41 the cell membrane by phosphatidylinositol specific phospholipase C (PIPLC) Selective  
42  
43 modification of a complement regulatory protein. *J Exp Med* **163**: 1150–1161.  
44

45  
46 De Bord KL, Anderson DM, Marketon MM, Overheim KA, DePaolo RW, Ciletti NA, Jabri B &  
47  
48 Schneewind O (2006) Immunogenicity and protective immunity against bubonic plague and  
49  
50 pneumonic plague by immunization of mice with the recombinant V10 antigen, a variant of  
51  
52 LcrV. *Infect Immun* **74**: 4910–4914.  
53

54  
55 De Greve H, Wyns L & Bouckaert J (2007) Combining sites of bacterial fimbriae. *Curr Opin*  
56  
57 *Struct Biol* **17**: 506–512.  
58  
59  
60



- 1  
2 Deisenhofer J (1981) Crystallographic refinement and atomic models of a human Fc fragment  
3  
4 and its complex with fragment B of protein A from *Staphylococcus aureus* at 2.9- and 2.8-Å  
5  
6 resolution. *Biochemistry* **20**: 2361–2370.  
7  
8
- 9 De Jong B & Ekdahl B (2006) The comparative burden of salmonellosis in the European Union  
10  
11 member states, associated and candidate countries. *BMC Public Health* **6**: 4.  
12  
13
- 14 DeLano WL (2002) The PyMOL user's manual. Palo Alto, CA, USA.  
15
- 16 Delepelaire P (2004) Type I secretion in Gram-negative bacteria. *Biochim Biophys Acta* **1694**:  
17  
18 149–161.  
19
- 20 Del Prete G, Santi L, Andrianaivoarimanana V, Amedei A, Domarle O, D' Elios MM, Arntzen  
21  
22 CJ, Rahalison L & Mason HS (2009) Plant-derived recombinant F1, V, and F1-V fusion  
23  
24 antigens of *Yersinia pestis* activate human cells of the innate and adaptive immune system.  
25  
26  
27 *Int J Immunopathol Pharmacol* **22**: 133–143.  
28  
29
- 30 Deng W, Liou SR, Plunkett G, Mayhew GF, Rose DJ, Burl V, Kodoyianni V, Schwartz DC &  
31  
32 Blattner FR. (2003) Comparative genomics of *Salmonella enterica* serovar Typhi strains Ty2  
33  
34 and CT18. *J Bacteriol* **185**: 2330–2337.  
35  
36
- 37 Derewenda U, Mateja A, Devedjiev Y, Routzahn KM, Evdokimov AG, Derewenda ZS &  
38  
39 Waugh DS (2004) The structure of *Yersinia pestis* V-antigen, an essential virulence factor  
40  
41 and mediator of immunity against plague. *Structure (Cambridge)* **12**: 357–358.  
42  
43
- 44 Diard S, Toribio AL, Boum Y, Vigier F, Kansau I, Bouvet O & Servin A (2006) Environmental  
45  
46 signals implicated in Dr fimbriae release by pathogenic *Escherichia coli*. *Microbes Infect* **8**:  
47  
48 1851–1858.  
49
- 50  
51 Dobrindt U, Blum-Oehler G, Hartsch T, Gottschalk G, Ron RZ, Fünfstück R & Hacker J. (2001)  
52  
53 S-Fimbria-encoding determinant *sfaI* is located on pathogenicity island III536 of  
54  
55 uropathogenic *Escherichia coli* strain 536. *Infect Immun* **69**: 4248–4256.  
56  
57  
58  
59  
60

- 1  
2 Dodson KW, Jacob-Dubuisson F, Striker RT & Hultgren SJ (1993) Outer-membrane PapC  
3  
4 molecular usher discriminately recognizes periplasmic chaperone-pilus subunit complexes.  
5  
6 *Proc Natl Acad Sci USA* **90**: 3670–3674.  
7  
8
- 9 Dodson KW, Pinkner JS, Rose RG, Magnusson T, Hultgren S & Waksman G (2001) Structural  
10  
11 basis of the interaction of the pyelonephritic *E coli* adhesin to its human kidney receptor. *Cell*  
12  
13 **105**: 733–743.  
14  
15
- 16 Donda A, Mori L, Shamshiev A, Carena A, Mottet C, Heim MH, Beglinger C, Grunert F,  
17  
18 Rochlitz C, Terracciano L, Jantscheff P, De Libero G (2000) Locally inducible CD66a  
19  
20 (CEACAM1) as an amplifier of the human intestinal T cell response. *Eur J Immunol* **30**:  
21  
22 2593–2603.  
23  
24
- 25 Du Y, Rosqvist R & Forsberg Å (2002) Role of fraction 1 antigen of *Yersinia pestis* in inhibition  
26  
27 of phagocytosis. *Infect Immun* **70**: 1453–1460.  
28  
29
- 30 Dutt AK, Akhtar R & McVeigh M (2006) Surat plague of 1994 re-examined. *Southeast Asian J*  
31  
32 *Trop Med Public Health* **37**: 755–760.  
33  
34
- 35 Edwards RA, Cao J & Schifferli DM (1996) Identification of major and minor chaperone proteins  
36  
37 involved in the export of 987P fimbriae. *J Bacteriol* **178**: 3426–3433.  
38  
39
- 40 Edwards RA, Schifferli DM & Maloy SR (2000) A role for *Salmonella* fimbriae in  
41  
42 intraperitoneal infections. *Proc Natl Acad Sci USA* **97**: 1258–1262.  
43  
44
- 45 Elias WP, Czczulin JR, Henderson IR, Trabulsi LR & Nataro JP (1999) Organization of  
46  
47 biogenesis genes for aggregative adherence fimbria II defines a virulence gene cluster in  
48  
49 enteroaggregative *Escherichia coli*. *J Bacteriol* **181**: 1779–1785.  
50  
51
- 52 Emmerth M, Goebel W, Miller SI & Hueck CJ (1999) Genomic subtraction identifies  
53  
54 *Salmonella typhimurium* prophages, F-related plasmid sequences, and a novel fimbrial  
55  
56 operon, *stf*, which are absent in *Salmonella typhi*. *J Bacteriol* **181**: 5652–5661.  
57  
58
- 59 Erilov D, Puorger C & Glockshuber R (2007) Quantitative analysis of nonequilibrium,  
60  
denaturant-dependent protein folding transitions. *J Am Chem Soc* **129**: 8938–8939.

- 1  
2 Eto DS, Jones TA, Sundsbak JL & Mulvey MA (2007) Integrin-mediated host cell invasion by  
3  
4 Type 1–piliated uropathogenic *Escherichia coli*. *PLoS Pathog* **3**: e100.  
5  
6  
7 Eyles JE, Williamson ID & Alpar HO (2000) Protection studies following bronchopulmonary  
8  
9 and intramuscular immunisation with *Yersinia pestis* F1 and V subunit vaccines co-  
10  
11 encapsulated in biodegradable microspheres: a comparison of efficacy. *Vaccine* **18**: 3266–  
12  
13 3271.  
14  
15  
16 Fahlgren A, Baranov V, Frangsmyr L, Zoubir F, Hammarstrom ML & Hammarstrom S (2003)  
17  
18 Interferon-gamma tempers the expression of carcinoembryonic antigen family molecules in  
19  
20 human colon cells: a possible role in innate mucosal defence. *Scand J Immunol* **58**: 628–641.  
21  
22  
23 Fang L, Nowicki BJ, Dong YL & Yallampalli C (1999) Localized increase in nitric oxide  
24  
25 production and the expression of nitric oxide synthase isoforms in rat uterus with  
26  
27 experimental intrauterine infection. *Amer J Obstet Gynecol* **181**: 601–609.  
28  
29  
30 Fang L, Nowicki B & Yallampalli C (2001) Differential expression of uterine NO in pregnant  
31  
32 and nonpregnant rats with intrauterine bacterial infection. *Amer J Physiol Regul Integr Comp*  
33  
34 *Physiol* **280**: R1356–R1363.  
35  
36  
37 Fischer H, Ellström P, Ekström K, Gustafsson L, Gustafsson M & Svanborg C (2007) Ceramide  
38  
39 as a TLR4 agonist; a putative signalling intermediate between sphingolipid receptors for  
40  
41 microbial ligands and TLR4. *Cell Microbiol* **9**: 1239–1251.  
42  
43  
44 Folkesson A, Advani A, Sukupolvi S, Pfeifer JD, Normark S & Löfdahl S (1999) Multiple  
45  
46 insertions of fimbrial operons correlate with the evolution of *Salmonella* serovars responsible  
47  
48 for human disease. *Mol Microbiol* **33**: 612–622.  
49  
50  
51 Forero M, Yakovenko O, Sokurenko EV, Thomas WE & Vogel V (2006) Uncoiling mechanics  
52  
53 of *Escherichia coli* Type I fimbriae are optimized for catch bonds. *PLoS Biology* **4**: e298.  
54  
55  
56 Foxman B & Brown P (2003) Epidemiology of urinary tract infections: Transmission and risk  
57  
58 factors, incidence and costs. *Infect Dis Clin North Am* **17**: 227–241.  
59  
60

- 1  
2 Foxman B, Barlow R, D'Arcy H, Gillespie B & Sobel JD (2000) Urinary tract infection: Self-  
3 reported incidence and associated costs. *Ann Epidemiol* **10**: 509–515.  
4  
5  
6  
7  
8 Fronzes R, Christie PJ & Waksman G (2009a) The structural biology of type IV secretion  
9 systems. *Nat Rev Microbiol* **7**: 703–714.  
10  
11  
12  
13 Fronzes R, Remaut H & Waksman G (2008) Architectures and biogenesis of non-flagellar  
14 protein appendages in Gram-negative bacteria. *EMBO J* **27**: 2271–2280.  
15  
16  
17  
18  
19 Fronzes R, Schäfer E, Wang L, Saibil, HR, Orlova EV & Waksman G (2009b) Structure of a  
20 type IV secretion system core complex. *Science* **323**: 266–268.  
21  
22  
23  
24 Fujita T, Inoue T, Ogawa K, Iida K & Tamura N (1987) The mechanism of action of decay-  
25 accelerating factor (DAF) DAF inhibits the assembly of C3 convertases by dissociating C2a  
26 and Bb. *J Exp Med* **166**: 1221–1228.  
27  
28  
29  
30  
31 Galván EM, Chen H & Schifferli DM (2006) The Psa fimbriae of *Yersinia pestis* interact with  
32 phosphatidylcholine on alveolar epithelial cells and pulmonary surfactant. *Infect Immun* **75**:  
33 1272–1279.  
34  
35  
36  
37  
38 Galyov EE, Karlyshev AV, Chernovskaya TV, Dolgikh DA, Smirnov OY, Volkovoy KI,  
39 Abramov VM & Zav'yalov VP (1991) Expression of the envelope antigen F1 of *Yersinia*  
40 *pestis* is mediated by the product of *cafIM* gene having homology with the chaperone PapD  
41 of *Escherichia coli*. *FEBS Lett* **286**: 79–82.  
42  
43  
44  
45  
46  
47  
48 Galyov EE, Smirnov OY, Karlyshev AV, Volkovoy KI, Denesyuk AI, Nazimov IV, Rubtsov  
49 KS, Abramov VM, Dalvadyanz SM & Zav'yalov VP (1990) Nucleotide sequence of the  
50 *Yersinia pestis* gene encoding F1 antigen and the primary structure of the protein. *FEBS Lett*  
51 **277**: 230–232.  
52  
53  
54  
55  
56  
57 Garcia MI, Labigne A & Le Bouguéne C (1994) Nucleotide sequence of the afimbrial-adhesin-  
58 encoding *afa-3* gene cluster and its translocation via flanking IS1 insertion sequences. *J*  
59 *Bacteriol* **176**: 7601–7613.  
60

- 1  
2 Garcia MI, Gounon P, Courcoux P, Labigne A & Le Bouguenec C (1996) The afimbrial  
3  
4 adhesive sheath encoded by the *afa-3* gene cluster of pathogenic *Escherichia coli* is  
5  
6 composed of two  
7  
8 adhesins. *Mol Microbiol* **19**: 683–693.  
9  
10  
11 Gerlach RG & Hensel M (2007) Protein secretion systems and adhesins: The molecular armory  
12  
13 of Gram-negative pathogens. *Int J Med Microbiol* **297**: 401–415.  
14  
15  
16 Giske CG, Monnet DL, Cars O & Carmeli Y (2008) Clinical and economic impact of common  
17  
18 multidrug-resistant Gram-negative bacilli. *Antimicrob Agents Chemother* **52**: 813–821.  
19  
20  
21 Glynn A, Roy CJ, Powell BS, Adamovicz JJ, Freytag LC & Clements JD (2005) Protection  
22  
23 against aerosolized *Yersinia pestis* challenge following homologous and heterologous prime-  
24  
25 boost with recombinant plague antigens. *Infect Immun* **73**: 5256–5261.  
26  
27  
28 Gohl O, Friedrich A, Hoppert M & Averhoff B (2006) The thin pili of *Acinetobacter* sp. strain  
29  
30 BD413 mediate adhesion to biotic and abiotic surfaces. *Appl Env Microb* **72**: 1394–1401.  
31  
32  
33 Goluszko P, Goluszko E, Nowicki B, Nowicki S, Popov V & Wang H-Q (2005) Vaccination  
34  
35 with purified Dr fimbriae reduces mortality associated with chronic urinary tract infection  
36  
37 due to *Escherichia coli* bearing Dr adhesin. *Infect Immun* **73**: 627–631.  
38  
39  
40 Goluszko P, Niesel D, Nowicki B, Selvarangan R, Nowicki S, Hart A, Pawelczyk E, Das M,  
41  
42 Urvil P & Hasan R (2001) Dr operon-associated invasiveness of *Escherichia coli* from  
43  
44 pregnant patients with pyelonephritis. *Infect Immun* **69**: 4678–4680.  
45  
46  
47 Gossert AD, Bettendorff P, Puorger C, Vetsch M, Herrmann T, Glockshuber R & Wüthrich K  
48  
49 (2008) NMR structure of the *Escherichia coli* Type 1 pilus subunit FimF and its interactions  
50  
51 with other pilus subunits. *J Mol Biol* **375**: 752–763.  
52  
53  
54 Gounon P, Jouve M & Le Bouguenec C (2000) Immunocytochemistry of the AfaE adhesin and  
55  
56 AfaD invasin produced by pathogenic *Escherichia coli* strains during interaction of the  
57  
58 bacteria with HeLa cells by high resolution scanning electron microscopy. *Microbes Infect* **2**:  
59  
60 359–365.

- 1  
2 Grunert F & Kuroki M (1998) CEA family members expressed on hematopoietic cells and their  
3 possible role in cell adhesion and signaling. *Cell Adhesion and Communication Mediated by*  
4 *the CEA Family-Basic and Clinical Perspective*. Harwood Academic Publisher, Amsterdam,  
5 *Netherlands* (CP Stanners ed.), p. 99–120.  
6  
7  
8  
9  
10  
11 Guignot J, Hudault S, Kansau I, Chau I & Servin AL (2009) DAF and CEACAMs receptor-  
12 mediated internalization and intracellular lifestyle of Afa/Dr diffusely adhering *Escherichia*  
13 *coli* into epithelial cells. *Infect Immun* **77**: 517–531.  
14  
15  
16  
17  
18 Guignot J, Peiffer I, Bernet-Camard M-F, Lublin DM, Carnoy C, Moseley SL & Servin A (2000)  
19 Recruitment of CD55 and CD66e brush border-associated glycosylphosphatidylinositol-  
20 anchored proteins by members of the Afa/Dr diffusely adhering family of *Escherichia coli*  
21 that infect the human polarized intestinal Caco-2/TC7 cells. *Infect Immun* **68**: 3554–3563.  
22  
23  
24  
25  
26  
27  
28 Gupta ML & Sharma A (2007) Pneumonic plague, Northern India, 2002. *Emerg Infect Dis* **13**:  
29 664–666.  
30  
31  
32  
33 Hamid N & Jain SK (2007) Immunological, cellular and molecular events in typhoid fever.  
34 *Indian J Biochem Biophys* **44**: 320–330.  
35  
36  
37  
38 Hammar M, Bian Z & Normark S (1996) Nucleator-dependent intercellular assembly of  
39 adhesive curli organelles in *E coli*. *Proc Natl Acad Sci USA* **93**: 6562–6566.  
40  
41  
42  
43 Hammarstrom S (1999) The carcinoembryonic antigen (CEA) family: structures, suggested  
44 functions and expression in normal and malignant tissues. *Seminars Cancer Biol* **9**: 67–81.  
45  
46  
47  
48 Hart A, Nowicki BJ, Reisner B, Pawelczyk E, Goluszko P, Urvil P, Anderson G & Nowicki S  
49 (2001) Ampicillin-resistant *Escherichia coli* in gestational pyelonephritis: increased  
50 occurrence and association with the colonization factor Dr adhesin. *J Infect Dis* **183**: 1526–  
51 1529.  
52  
53  
54  
55  
56  
57  
58  
59  
60 Hart A, Pham T, Nowicki S, Whorton EB, Martens MG, Anderson GD & Nowicki BJ (1996)  
Gestational pyelonephritis-associated *Escherichia coli* isolates represent a nonrandom,  
closely related population. *Amer J Obstet Gynecol* **174**: 983-989.

- 1  
2 Hart E, Tauschek M, Bennett-Wood V, Hartland EL & Robins-Browne RM (2009) Rabbit-  
3  
4 specific fimbriae, Ral, alter the patterns of *in vitro* adherence and intestinal colonisation of  
5  
6 rabbits by human-specific enteropathogenic *E. coli*. *Microbes Infect* **11**: 803–810.  
7  
8
- 9 Hasan RJ, Pawelczyk E, Urvil PT, Venkatarajan MS, Goluszko P, Kur J, Selvarangan R,  
10  
11 Nowicki S, Braun WA & Nowicki BJ (2002) Structure-function analysis of decay-  
12  
13 accelerating factor: identification of residues important for binding of the *Escherichia coli* Dr  
14  
15 adhesin and complement regulation. *Infect Immun* **70**: 4485–4493.  
16  
17
- 18 Heath DG, Anderson GW, Mauro JM, Welkos SL, Andrews GP, Adamovicz J & Friedlander  
19  
20 AM (1998) Protection against experimental bubonic and pneumonic plague by a recombinant  
21  
22 capsular F1-V antigen fusion protein vaccine. *Vaccine* **16**: 1131–1137.  
23  
24
- 25 Hill J, Copse C, Leary S, Stagg AJ, Williamson ED & Titball RW (2003) Synergistic protection  
26  
27 of mice against plague with monoclonal antibodies specific for the F1 and V antigens of  
28  
29 *Yersinia pestis*. *Infect Immun* **71**: 2234–2238.  
30  
31
- 32 Hill J, Eyles JE, Elvin SJ, Healey GD, Lukaszewski RA & Titball RW (2006) Administration of  
33  
34 antibody to the lung protects mice against pneumonic plague. *Infect Immun* **74**: 3068–3070.  
35  
36
- 37 Holmgren A & Branden CI (1989) Crystal structure of chaperone protein PapD reveals an  
38  
39 immunoglobulin fold. *Nature* **342**: 248–251.  
40  
41
- 42 Honarvar S, Choi B-K & Schifferli DM (2003) Phase variation of the 987P-like CS18 fimbriae  
43  
44 of human enterotoxigenic *Escherichia coli* is regulated by site-specific recombinases. *Mol*  
45  
46 *Microbiol* **48**: 157–171.  
47  
48
- 49 Honko AN, Sriranganathan N, Lees CJ & Mizel SB (2006) Flagellin is an effective adjuvant for  
50  
51 immunization against lethal respiratory challenge with *Yersinia pestis*. *Infect Immun* **74**:  
52  
53 1113–1120.  
54  
55
- 56 Hu CX, Xu ZR, Li WF, Niu D, Lu P & Fu LL (2009) Secretory expression of K88 (F4) fimbrial  
57  
58 adhesin FaeG by recombinant *Lactococcus lactis* for oral vaccination and its protective  
59  
60 immune response in mice. *Biotechnol Lett* **31**: 991–997.



- 1  
2 Huang XZ & Lindler LE (2004) The pH6 antigen is an antiphagocytic factor produced by  
3  
4 *Yersinia pestis* independent of *Yersinia* outer proteins and capsule antigen. *Infect Immun* **72**:  
5  
6 7212–7219.  
7  
8
- 9 Hung DL, Knight SD, Woods RM, Pinkner JS & Hultgren SJ (1996) Molecular basis of two  
10  
11 subfamilies of immunoglobulin-like chaperones. *EMBO J* **15**: 3792–3805.  
12  
13
- 14 Hung DL, Pinkner JS, Knight SD & Hultgren SJ (1999) Structural basis of chaperone self-  
15  
16 capping in P pilus biogenesis. *Proc Natl Acad Sci USA* **96**: 8178–8183.  
17  
18
- 19 Iriarte M & Cornelis GR (1995) MyfF, an element of the network regulating the synthesis of  
20  
21 fibrillae in *Yersinia enterocolitica*. *J Bacteriol* **177**: 738–744.  
22  
23
- 24 Iriarte M, Vanooteghem JC, Delor I, Diaz R, Knutton S & Cornelis GR (1993) The Myf fibrillae  
25  
26 of *Yersinia enterocolitica*. *Mol Microbiol* **9**: 507–520.  
27  
28
- 29 Jacob-Dubuisson F, Striker R & Hultgren SJ (1994) Chaperone assisted self-assembly of pili  
30  
31 independent of cellular energy. *J Biol Chem* **269**: 12447–12455.  
32  
33
- 34 Jalajakumar MB, Thomas CJ, Halter R & Manning PA (1989) Genes for biosynthesis and  
35  
36 assembly of CS3 pili of CFA/II enterotoxigenic *Escherichia coli*: novel regulation of pilus  
37  
38 production by bypassing an amber codon. *Mol Microbiol* **12**: 1685–1695.  
39  
40
- 41 Jedrzejczak R, Dauter Z, Dauter M, Piątek R, Zalewska B, Mroz M, Bury K, Nowicki B & Kur J  
42  
43 (2006) Structure of DraD invasin from uropathogenic *Escherichia coli*: a dimer with  
44  
45 swapped beta-tails. *Acta Crystallogr D Biol Crystallogr* **62**: 157–164.  
46  
47
- 48 Joardar V, Lindeberg M, Jackson RW, Selengut J, Dodson R, Brinkac LM, Daugherty SC,  
49  
50 DeBoy R, Durkin AS, Giglio MG, Madupu R, Nelson WC, Rosovitz MJ, Sullivan S,  
51  
52 Crabtree J, Creasy T, Davidsen T, Haft DH, Zafar N, Zhou L, Halpin R, Holley T, Khouri H,  
53  
54 Feldblyum T, White O, Fraser CM, Chatterjee AK, Cartinhour S, Schneider DJ, Mansfield J,  
55  
56 Collmer A & Buell CR (2005) Whole-genome sequence analysis of *Pseudomonas syringae*  
57  
58 pv. phaseolicola 1448A reveals divergence among pathovars in genes involved in virulence  
59  
60 and transposition. *J Bacteriol* **187**: 6488–6498.

- 1  
2 Johnson JR (1991) Virulence factors in *Escherichia coli* urinary tract infection. *Clin Microbiol*  
3  
4 *Rev* **4**: 80–128.  
5  
6 Johnson JR, Skubitz KM, Nowicki BJ, Jacques-Palaz K & Rakita RM (1995) Nonlethal  
7  
8 adherence to human neutrophils mediated by Dr antigen-specific adhesins of *Escherichia*  
9  
10 *coli*. *Infect Immun* **63**: 309–316.  
11  
12  
13 Jones T, Adamovicz JJ, Cyr SL, Bolt CR, Bellerose N, Pitt LM, Lowell GH & Burt DS (2006)  
14  
15 Intranasal Protollintrade mark/F1-V vaccine elicits respiratory and serum antibody responses  
16  
17 and protects mice against lethal aerosolized plague infection. *Vaccine* **24**: 1625–1632.  
18  
19  
20 Jones CH, Dodson K & Hultgren SJ (1996) Structure, function and assembly of adhesive P pili.  
21  
22 *Urinary Tract Infections: Molecular Pathogenesis and Clinical Management*. ASM Press:  
23  
24 Washington, DC (Mobley HLT & Warren JW eds), pp. 175–219.  
25  
26  
27 Jones CH, Pinkner JS, Nicholes AV, Slonim LN, Abraham SN & Hultgren SJ (1993) FimC is a  
28  
29 periplasmic PapD-like chaperone that directs assembly of type 1 pili in bacteria. *Proc Natl*  
30  
31 *Acad Sci USA* **90**: 8397–8401.  
32  
33  
34 Jouve M, Garcia MI, Courcoux P, Labigne A, Gounon P & Le Bouguéne C (1997) Adhesion to  
35  
36 and invasion of HeLa cells by pathogenic *Escherichia coli* carrying the *afa-3* gene cluster are  
37  
38 mediated by the AfaE and AfaD proteins, respectively. *Infect Immun* **56**: 4082–4089.  
39  
40  
41 Kammerer R, Hahn S, Singer BB, Luo JS & von Kleist S (1998) Biliary glycoprotein (CD66a), a  
42  
43 cell adhesion molecule of the immunoglobulin superfamily, on human lymphocytes:  
44  
45 structure, expression and involvement in T cell activation. *Eur J Immunol* **28**: 3664–3674.  
46  
47  
48 Kammerer R, Stober D, Singer BB, Obrink B & Reimann J (2001) Carcinoembryonic antigen-  
49  
50 related cell adhesion molecule 1 on murine dendritic cells is a potent regulator of T cell  
51  
52 stimulation. *J Immunol* **166**: 6537–6544.  
53  
54  
55 Karlyshev AV, Galyov EE, Abramov VM & Zav'yalov VP (1992) *cafIR* gene and its role in the  
56  
57 regulation of capsule formation of *Y pestis*. *FEBS Lett* **305**: 37–40.  
58  
59  
60

1  
2 Karlyshev AV, Galyov EE, Smirnov OY, Abramov VM & Zav'yalov VP (1994) Structure and  
3  
4 regulation of a gene cluster involved in capsule formation of *Y pestis*, p. 321–330. *Biological*  
5  
6 *Membranes: Structure, Biogenesis and Dynamic, NATO-ASI Series*, (Op den Kamp JAF ed.)  
7  
8 vol. H-82, Springer-Verlag.

9  
10  
11 Karlyshev AV, Galyov EE, Smirnov OY, Guzaev AP, Abramov VM & Zav'yalov VP (1992) A  
12  
13 new gene of the *fl* operon of *Y pestis* involved in the capsule biogenesis. *FEBS Lett* **297**: 77–  
14  
15 80.

16  
17  
18 Kaul AK, Khan S, Martens MG, Crosson JT, Lupo VR & Kaul R (1999) Experimental  
19  
20 gestational pyelonephritis induces preterm births and low birth weights in C3H/HeJ mice.  
21  
22 *Infect Immun* **67**: 5958–5966.

23  
24  
25 Keller R, Ordoñez JG, de Oliveira RR, Trabulsi LR, Baldwin TJ & Knutton S (2002) Afa, a  
26  
27 diffuse adherence fibrillar adhesin associated with enteropathogenic *Escherichia coli*. *Infect*  
28  
29 *Immun* **70**: 2681–2689.

30  
31  
32 Kida Y, Kobayashi M, Takao S, Akira T, Yoshimasa O, Sigemasa H, Toshikazu Y & Kohji H  
33  
34 (2005) Interleukin-1 stimulates cytokines, prostaglandin E2 and matrix metalloproteinase-1  
35  
36 production via activation of MAPK/AP-1 and NF- $\kappa$ B in human gingival fibroblasts. *Cytokine*  
37  
38 **29**: 159–168.

39  
40  
41 Kline KA, Fälker S, Dahlberg S, Normark S & Henriques-Normark B (2009) Bacterial adhesins  
42  
43 in host-microbe interactions. *Cell Host Microbe* **5**: 580–592.

44  
45  
46 Knight SD, Berglund J & Choudhury D (2000) Bacterial adhesins: structural studies reveal  
47  
48 chaperone function and pilus biogenesis. *Curr Opin Chem Biol* **4**: 653–660.

49  
50  
51 Knutton S, McConnel MM, Rowe B & McNeish AS (1989) Adhesion and ultrastructural  
52  
53 properties of human enterotoxigenic *Escherichia coli* producing colonization factor antigens  
54  
55 III and IV. *Infect Immun* **57**: 3364–3371.

56  
57  
58 Korotkova N, Chattopadhyay S, Tabata TA, Beskhlebnaya V, Vigdorovich V, Kaiser BK, Strong  
59  
60 RK, Dykhuizen DE, Sokurenko EV & Moseley SL (2007) Selection for functional diversity

1  
2 drives accumulation of point mutations in Dr adhesins of *Escherichia coli*. *Mol Microbiol*  
3  
4 **64**: 180–194.

5  
6 Korotkova N, Cota E, Lebedin Y, Monpouet S, Guignot J, Servin AL, Matthews S & Moseley  
7  
8 SL (2006a) A subfamily of Dr adhesions of *Escherichia coli* bind independently to decay-  
9  
10 accelerating factor and the N-domain of carcinoembryonic antigen. *J Biol Chem* **281**: 29120–  
11  
12 29130.

13  
14  
15 Korotkova N, Le Trong I, Samudrala R, Korotkov K, Van Loy CP, Bui AL, Moseley SL &  
16  
17 Stenkamp RE (2006b) Crystal structure and mutational analysis of the DaaE adhesin of  
18  
19 *Escherichia coli*. *J Biol Chem* **281**: 22367–22377.

20  
21  
22 Korotkova N, Yang Y, Le Trong I, Cota E, Demeler B, Marchant J, Thomas WE, Stenkamp RE,  
23  
24 Moseley SL & Matthews S (2008a) Binding of Dr adhesins of *Escherichia coli* to  
25  
26 carcinoembryonic antigen triggers receptor dissociation. *Mol Microbiol* **67**: 420–434.

27  
28  
29 Korotkova N, Yarova-Yarovaya Y, Tchesnokova V, Yazvenko N, Carl MA, Stapleton AE &  
30  
31 Moseley SL (2008b) *Escherichia coli* DraE adhesin-associated bacterial internalization by  
32  
33 epithelial cells is promoted independently by decay-accelerating factor and carcinoembryonic  
34  
35 antigen-related cell adhesion molecule binding and does not require the DraD invasin *Infect*  
36  
37 *Immun* **76**: 3869–3880.

38  
39  
40 Korpela T, Macintyre-Ayane S, Zavialov A, Battchikova N, Petrovskaya L, Zav'yalov V &  
41  
42 Korobko V (1999) Microbial protein expression system. *US patent 6919198*.

43  
44  
45 Kuehn MJ, Heuser J, Normark S & Hultgren SJ (1992) P pili in uropathogenic *E. coli* are  
46  
47 composite fibres with distinct fibrillar adhesive tips. *Nature* **356**: 252–255.

48  
49  
50 Kumar S, Balakrishna K, Agarwal GS, Merwyn S, Rai GP, Batra HV, Sardesai AA &  
51  
52 Gowrishankar J (2009) Th1-type immune response to infection by pYV-cured phoP-phoQ  
53  
54 null mutant of *Yersinia pseudotuberculosis* is defective in mouse model. *Antonie van*  
55  
56 *Leeuwenhoek* **95**: 91–100.

- 1  
2 Lalioui L & Le Bouguéne C (2001) *afa-8* Gene cluster is carried by a pathogenicity island  
3  
4 inserted into the tRNA<sup>Phe</sup> of human and bovine pathogenic *Escherichia coli* isolates. *Infect*  
5  
6 *Immun* **69**: 937–948.  
7  
8
- 9 Lalioui L, Jouve M, Gounon P & Le Bouguéne C (1999) Molecular cloning and  
10  
11 characterization of the *afa-7* and *afa-8* gene clusters encoding Afimbrial adhesins in  
12  
13 *Escherichia coli* strains associated with diarrhea or septicemia in calves. *Infect Immun* **10**:  
14  
15 5048–5059.  
16  
17
- 18 Lane MC & Mobley HLT (2007) Role of P-fimbrial-mediated adherence in pyelonephritis and  
19  
20 persistence of uropathogenic *Escherichia coli* (UPEC) in the mammalian kidney. *Kidney*  
21  
22 *Intern* **72**: 19–25.  
23  
24
- 25 Langermann S, Möllby R, Burlein J, Palaszynski S, Auguste G, DeFusco A, Strouse R,  
26  
27 Schenerman MA, Hultgren SJ, Pinkner JS, Winberg J, Guldevall L, Söderhäll M, Ishikawa  
28  
29 K, Normark S & Koenig S (2000) Vaccination with FimH adhesin protects cynomolgus  
30  
31 monkeys from colonization and infection by uropathogenic *Escherichia coli*. *J Infect Dis*  
32  
33 **181**: 774–778.  
34  
35
- 36 Langermann S, Palaszynski S, Barnhart M, Auguste G, Pinkner JS, Burlein J, Barren P, Koenig  
37  
38 S, Leath S, Jones CH & Hultgren SJ (1997) Prevention of mucosal *Escherichia coli* infection  
39  
40 by FimH-adhesin-based systemic vaccination. *Science* **276**: 607–611.  
41  
42
- 43 Layton AN & Galyov EE (2007) Salmonella-induced enteritis: molecular pathogenesis and  
44  
45 therapeutic implications. *Expert Rev Mol Med* **9**: 1–17.  
46  
47
- 48 Le Bouguéne C & Bertin Y (1999) AFA and F17 adhesins produced by pathogenic *Escherichia*  
49  
50 *coli* strains in domestic animals. *Vet Res* **30**: 317–342.  
51  
52
- 53 Le Bouguéne C & Servin AL (2006) Diffusely adherent *Escherichia coli* strains expressing  
54  
55 Afa/Dr adhesins (Afa/Dr DAEC): hitherto unrecognized pathogens. *FEMS Microbiol Lett*  
56  
57 **256**: 185–194.  
58  
59  
60

- 1  
2 Le Bouguéne C (2005) Adhesins and invasins of pathogenic *Escherichia coli*. *Int J Med*  
3  
4 *Microbiol* **295**: 471–478.  
5  
6  
7 Leffler H & Svanborg-Edén C (1980) Chemical identification of a glycosphingolipid receptor for  
8  
9 *E coli* attaching to human urinary tract epithelial cells and agglutinating human erythrocytes.  
10  
11 *FEMS Microbiol Lett* **8**: 127–134.  
12  
13  
14 Leffler H & Svanborg-Edén C (1981) Glycolipid receptors for uropathogenic *Escherichia coli* on  
15  
16 human erythrocytes and uroepithelial cells. *Infect Immun* **34**: 920–929.  
17  
18  
19 Lemaitre N, Sebbane F, Long D & Hinnebusch BJ (2006) *Yersinia pestis* YopJ suppresses  
20  
21 tumour necrosis factor  $\alpha$  induction and contributes to apoptosis of immune cells in the lymph  
22  
23 node but is not required for virulence in a rat model of bubonic plague. *Infect Immun* **74**:  
24  
25 5126–5131.  
26  
27  
28 Levine MM, Ristaino P, Marley G, Smyth C, Knutton S, Boedeker E, Black R, Young C,  
29  
30 Clements ML, Cheney C & Patnaik R (1984) Coli surface antigens 1 and 3 of colonization  
31  
32 factor antigen II-positive enterotoxigenic *Escherichia coli*: morphology, purification, and  
33  
34 immune responses in humans. *Infect Immun* **44**: 409–420.  
35  
36  
37 Li Y, Cui Y, Hauck Y, Platonov ME, Dai E, Song Y, Guo Z, Pourcel C, Dentovskaya SV,  
38  
39 Anisimov AP, Yang R & Vergnaud G (2009) Genotyping and phylogenetic analysis of  
40  
41 *Yersinia pestis* by MLVA: Insights into the worldwide expansion of Central Asia plague foci.  
42  
43 *PLoS ONE* **4**: e6000.  
44  
45  
46  
47 Li Y, Han W, Lei L, Li Z & Shi L (2009) MrkD adhesin of *Klebsiella pneumoniae* expression,  
48  
49 purification and analysis of adhesive activity. *Wei Sheng Wu Xue Bao* **49**: 638–642.  
50  
51  
52 Li B, Jiang L, Song Q, Yang J, Chen Z, Guo Z, Zhou D, Du Z, Song Y, Wang J, Wang H, Yu S,  
53  
54 Wang J & Yang R (2005) Protein microarray for profiling antibody responses to *Yersinia*  
55  
56 *pestis* live vaccine. *Infect Immun* **73**: 3734–3739.  
57  
58  
59 Li H, Qian L, Chen Z, Thibault D, Liu G, Liu T & Thanassi DG (2004) The outer membrane  
60  
usher forms a twin-pore secretion complex. *J Mol Biol* **344**: 1397–1407.

- 1  
2 Li Y-F, Poole S, Rasulova F, McVeigh AL, Savarino SJ & Xia D (2007) A receptor-binding site  
3  
4 as revealed by the crystal structure of CfaE, the colonization factor antigen I fimbrial adhesin  
5  
6 of enterotoxigenic *Escherichia coli*. *J Biol Chem* **282**: 23970–23980.  
7  
8
- 9 Li B & Yang R (2008) Interaction between *Yersinia pestis* and the host immune system. *Infect*  
10  
11 *Immun* **76**: 1804–1811.  
12  
13
- 14 Lindberg F, Lund B, Johansson L & Normark S (1987) Localization of the receptor binding  
15  
16 protein adhesin at the tip of the bacterial pilus. *Nature* **328**: 84–87.  
17  
18
- 19 Lindler LE & Tall BD (1993) *Yersinia pestis* pH6 antigen forms fimbriae and is induced by  
20  
21 intracellular association with macrophages. *Mol Microbiol* **8**: 311–324.  
22  
23
- 24 Lindler LE, Klempner MS & Straley SC (1990) *Yersinia pestis* pH6 antigen: genetic,  
25  
26 biochemical, and virulence characterization of a protein involved in the pathogenesis of  
27  
28 bubonic plague. *Infect Immun* **58**: 2569–2577.  
29  
30
- 31 Linke D, Riess T, Autenrieth IB, Lupas A & Kempf VA (2006) Trimeric autotransporter  
32  
33 adhesins: variable structure, common function. *Trends Microbiol* **14**: 264–270.  
34  
35
- 36 Lintermans PF, Pohl P, Deboeck F, Bertels A, Schlicker C, Vandekerckhove J, van Damme J,  
37  
38 van Montagu M & de Greve H (1988) Isolation and nucleotide sequence of the F17-A gene  
39  
40 encoding the structural protein of the F17 fimbriae in bovine enterotoxigenic *Escherichia*  
41  
42 *coli*. *Infect Immun* **56**: 1475–1484.  
43  
44
- 45 Liu F, Chen H, Galván EM, Lasaro MA & Schifferli DM (2006) Effects of Psa and F1 on the  
46  
47 adhesive and invasive interactions of *Yersinia pestis* with human respiratory tract epithelial  
48  
49 cells. *Infect Immun* **74**: 5636–5644.  
50  
51
- 52 Lopes VC, Velayudhan BT, Halvorson DA & Nagaraja KV (2006) Preliminary evaluation of the  
53  
54 use of the *sefA* fimbrial gene to elicit immune response against *Salmonella enterica* serotype  
55  
56 *Enteritidis* in chickens. *Avian Dis* **50**: 185–190.  
57  
58  
59  
60



- 1  
2 Louvard D, Kedinger M & Hauri HP (1992) The differentiating intestinal epithelial cell:  
3  
4 establishment and maintenance of functions through interactions between cellular structures.  
5  
6 *Annu Rev Cell Biol* **8**: 157–195.  
7  
8  
9 Lublin DM & Atkinson JP (1989) Decay-accelerating factor: biochemistry, molecular biology,  
10  
11 and function. *Annu Rev Immun* **7**: 35-58.  
12  
13  
14 MacIntyre S, Zyrianova IM, Chernovskaya TV, Leonard M, Rudenko EG, Zav'yalov VP &  
15  
16 Chapman DAG (2001) An extended hydrophobic interactive surface of *Yersinia pestis*  
17  
18 Caf1M chaperone is essential for subunit binding and F1 capsule assembly. *Mol Microbiol*  
19  
20 **39**: 12–25.  
21  
22  
23 Makoveichuk E, Cherepanov P, Lundberg S, Forsberg Å & Olivecrona G (2003) pH6 antigen of  
24  
25 *Yersinia pestis* interacts with plasma lipoproteins and cell membranes. *Lipid Res* **44**: 320–  
26  
27 330.  
28  
29  
30 Marketon MM, Depaolo RW, Debord KL, Jabri B & Schneewind O (2005) Plague bacteria  
31  
32 target immune cells during infection. *Science* **309**: 1739–1741.  
33  
34  
35 Marklund B-I, Tennent JM, Garcia E, Hamers A, Bdga M, Lindberg F, Gaastra W & Normark S  
36  
37 (1992) Horizontal gene transfer of the *Escherichia coli* *pap* and *prs* pili operons as a  
38  
39 mechanism for the development of tissue-specific adhesive properties. *Mol Microbiol* **6**:  
40  
41 2225–2242.  
42  
43  
44 Massad G & Mobley HLT (1994) Genetic organization and complete sequence of the *Proteus*  
45  
46 *mirabilis* *pmf* fimbrial operon. *Gene* **150**: 101–104.  
47  
48  
49 Massad G, Fulkerson GF, Watson DC & Mobley HL (1996) *Proteus mirabilis* ambient-  
50  
51 temperature fimbriae: cloning and nucleotide sequence of the *atf* gene cluster. *Infect Immun*  
52  
53 **64**: 4390–4395.  
54  
55  
56 McClelland M, Sanderson KE, Spieth J, Clifton SW, Latreille P, Courtney L, Porwollik S, Ali J,  
57  
58 Dante M, Du F, Hou S, Layman D, Leonard S, Nguyen C, Scott K, Holmes A, Grewal N,  
59  
60 Mulvaney E, Ryan E, Sun H, Florea L, Miller W, Stoneking T, Nhan M, Waterston R &

- 1  
2 Wilson RK. (2001) Complete genome sequence of *Salmonella enterica* serovar  
3  
4 Typhimurium LT2. *Nature* **413**: 852–856.  
5  
6  
7 McClelland M., Sanderson KE, Clifton SW, Latreille P, Porwollik S, Sabo A, Meyer R, Bieri T,  
8  
9 Ozersky P, McLellan M, Harkins CR, Wang C, Nguyen C, Berghoff A, Elliott G, Kohlberg  
10  
11 S, Strong C, Du F, Carter J, Kremizki C, Layman D, Leonard S, Sun H, Fulton L, Nash W,  
12  
13 Miner T, Minx P, Delehaunty K, Fronick C, Magrini V, Nhan M, Warren W, Florea L,  
14  
15 Spieth J & Wilson RK (2004) Comparison of genome degradation in Paratyphi A and Typhi,  
16  
17 human-restricted serovars of *Salmonella enterica* that cause typhoid. *Nat Genet* **36**: 1268–  
18  
19 1274.  
20  
21  
22  
23 Merckel MC, Tanskanen J, Edelman S, Westerlund-Wikström B, Korhonen TK & Goldman A  
24  
25 (2003) The structural basis of receptor-binding by *Escherichia coli* associated with diarrhea  
26  
27 and septicemia. *J Mol Biol* **331**: 897–905.  
28  
29  
30 Meslet-Cladiere LM, Pimenta A, Duchaud E, Holland IB & Blight MA (2004) *In vivo* expression  
31  
32 of the mannose-resistant fimbriae of *Photobacterium temperata* K122 during insect infection. *J*  
33  
34 *Bacteriol* **186**: 611–622.  
35  
36  
37 Mueller CA, Broz P, Muller SA, Ringler P, Erne-Brand F, Sorg I, Kuhn M, Engel A & Cornelis  
38  
39 GR (2005) The V-antigen of *Yersinia* forms a distinct structure at the tip of injectosome  
40  
41 needles. *Science* **310**: 674–676.  
42  
43  
44 Munera D, Hultgren S & Fernandez LA (2007) Recognition of the N-terminal lectin domain of  
45  
46 FimH adhesin by the usher FimD is required for type 1 pilus biogenesis. *Mol Microbiol* **64**:  
47  
48 333–346.  
49  
50  
51 Musson JA, Morton M, Walker N, Harper HM, McNeill HV, Williamson ED & Robinson JH  
52  
53 (2006) Sequential proteolytic processing of the capsular Caf1 antigen of *Yersinia pestis* for  
54  
55 MHC class II restricted presentation to T lymphocytes. *J Biol Chem* **281**: 26129–26135.  
56  
57  
58 Nakajima A, Iijima H, Neurath MF, Nagaishi T, Nieuwenhuis EES, Raychowdhury R, Glickman  
59  
60 J, Blau DM, Russell S, Holmes KV & Blumberg RS (2002) Activation-induced expression of

1  
2       carcinoembryonic antigen-cell adhesion molecule 1 regulates mouse T lymphocyte function.

3  
4       *J Immunol* **168**: 1028–1035.

5  
6       Nataro JP & Kaper JB (1998) Diarrheagenic *Escherichia coli*. *Clin Microbiol Rev* **11**: 142–201.

7  
8       Ng TW, Akman L, Osisami M & Thanassi DG (2004) The usher N terminus is the initial  
9       targeting site for chaperone-subunit complexes and participates in subsequent pilus  
10       biogenesis events. *J Bacteriol* **186**: 5321–5331.

11  
12       Niemann HH, Schubert WD & Heinz DW (2004) Adhesins and invasins of pathogenic bacteria:  
13       a structural view. *Microbes Infect* **6**: 101–112.

14  
15       Nilsson LM, Thomas WE, Sokurenko EV & Vogel V (2006) Elevated shear stress protects  
16       *Escherichia coli* cells adhering to surfaces via catch bonds from detachment by soluble  
17       inhibitors. *Appl Environ Microbiol* **72**: 3005–3010.

18  
19       Nilsson LM, Thomas WE, Sokurenko EV & Vogel V (2008) Beyond induced-fit receptor-ligand  
20       interactions: structural changes that can significantly extend bond lifetimes. *Structure* **16**:  
21       1047–1058.

22  
23       Nilsson LM, Thomas WE, Trintchina E, Vogel V & Sokurenko EV (2006) Catch bond-mediated  
24       adhesion without a shear threshold: trimannose versus monomannose interactions with the  
25       FimH adhesin of *Escherichia coli*. *J Biol Chem* **281**: 16656–16663.

26  
27       Nilsson LM, Yakovenko O, Tchesnokova V, Thomas WE, Schembri MA, Vogel V, Klemm P &  
28       Sokurenko EV (2007) The cysteine bond in the *Escherichia coli* FimH adhesin is critical for  
29       adhesion under flow conditions. *Mol Microbiol* **65**: 1158–1169.

30  
31       Nishiyama M, Horst R, Eidam OT, Herrmann T, Ignatov O, Vetsch M, Bettendorff P, Jelesarov  
32       I, Grütter MG, Wüthrich K, Glockshuber R & Capitani G (2005) Structural basis of  
33       chaperone-subunit complex recognition by the type 1 pilus assembly platform FimD. *The*  
34       *EMBO J* **24**: 1–12.

- 1  
2 Nishiyama M, Vetsch M, Puorger C, Jelesarov I & Glockshuber R (2003) Identification and  
3  
4 characterization of the chaperone subunit complex-binding domain from the Type 1 pilus  
5  
6 assembly platform FimD. *J Mol Biol* **330**: 513–525.  
7  
8  
9 Nouvion AL & Beauchemin N (2009) CEACAM1 as a central modulator of metabolism, tumor  
10  
11 progression, angiogenesis and immunity. *Med Sci (Paris)* **25**: 247–252.  
12  
13  
14 Nowicki B, Hart A, Coyne KE, Lublin DM & Nowicki S (1993) Short consensus repeat-3  
15  
16 domain of recombinant decayaccelerating factor is recognized by *Escherichia coli*  
17  
18 recombinant Dr adhesin in a model of a cell-cell interaction. *J Exp Med* **178**: 2115–2121.  
19  
20  
21 Nowicki B, Fang L, Singhal J, Nowicki S & Yallampalli C (1997) Lethal outcome of uterine  
22  
23 infection in pregnant but not in nonpregnant rats and increased death rate with inhibition of  
24  
25 nitric oxide. *Amer J Reprod Immunol* **38**: 309–312.  
26  
27  
28 Nowicki B, Martens M, Hart A & Nowicki S (1994) Gestational age-dependent distribution of  
29  
30 *Escherichia coli* fimbriae in pregnant patients with pyelonephritis. *Ann NY Acad Sci* **730**:  
31  
32 290-291.  
33  
34  
35 Nowicki B, Moulds J, Hull R & Hull S (1988) A hemagglutinin of uropathogenic *Escherichia*  
36  
37 *coli* recognizes the Dr blood group antigen. *Infect Immun* **56**: 1057–1060.  
38  
39  
40 Nuccio S-P & Bäumler AJ (2007) Evolution of the chaperone/usher assembly pathway: fimbrial  
41  
42 classification goes greek. *Microbiol Mol Biol Rev* **71**: 551–575.  
43  
44  
45 Öbrink B (1997) CEA adhesion molecules: multifunctional proteins with signal-regulatory  
46  
47 properties. *Curr Opin Cell Biol* **9**: 616–626.  
48  
49  
50 Osman S, Remaut H, Waksman G & Orlova EV (2008) Structural Analysis of the Saf Pilus by  
51  
52 Electron Microscopy and Image Processing. *J Mol Biol* **379**: 174–187.  
53  
54  
55 Payne D, Tatham D, Williamson ED & Titball RW (1998) pH6 antigen of *Yersinia pestis* binds  
56  
57 to  $\beta$ 1-linked galactosyl residues in glycosphingolipids. *Infect Immun* **66**: 4545–4548.  
58  
59  
60 Peiffer I, Servin A & Bernet-Camard M-F (1998) Piracy of decay-accelerating factor (CD55)  
signal transduction by the diffusely adhering strain *Escherichia coli* C1845 promotes

1  
2 cytoskeletal F-Actin rearrangements in cultured human intestinal INT407 cells. *Infect Immun*  
3  
4 **66**: 4036–4042.

5  
6 Peiffer I, Blanc-Potard A-B, Bernet-Camard M-F, Guignot J, Barbat A & Servin A (2000a)  
7  
8 Afa/Dr diffusely adhering *Escherichia coli* C1845 infection promotes selective injuries in the  
9  
10 junctional domain of polarized human intestinal Caco-2/TC7 cells. *Infect Immun* **68**: 3431–  
11  
12 3442.

13  
14 Peiffer I, Guignot J, Barbat A, Carnoy C, Moseley SL, Nowicki BJ, Servin A & Bernet-Camard  
15  
16 M-F (2000) Structural and functional lesions in brush border of human polarized intestinal  
17  
18 Caco-2/TC7 cells infected by members of the Afa/Dr diffusely adhering family of  
19  
20 *Escherichia coli*. *Infect Immun* **68**: 5979–5990.

21  
22 Pereverzev YV, Prezhdo OV, Forero M, Sokurenko EV & Thomas WE (2005) The two-pathway  
23  
24 model for the catch-slip transition in biological adhesion. *Biophys J* **89**: 1446–1454.

25  
26 Pereverzev YV, Prezhdo OV & Sokurenko EV (2009) Allosteric role of the large-scale domain  
27  
28 opening in biological catch-binding. *Phys Rev E Stat Nonlin Soft Matter Phys* **79**: 051913.

29  
30 Perry RD & Fetherston JD (1997) *Yersinia pestis* – etiologic agent of plague. *Clin Microbiol Rev*  
31  
32 **10**: 35–66.

33  
34 Pettigrew D, Anderson KL, Billington J, Cota E, Simpson P, Urvil P, Rabuzin Roversi FP,  
35  
36 Nowicki B, du Merle L, Le Bouguéne C, Matthews S & Lea SM (2004) High resolution  
37  
38 studies of the Afa/Dr adhesin DraE and its interaction with chloramphenicol. *J Biol Chem*  
39  
40 **279**: 46851–46857.

41  
42 Pettigrew DM, Roversi P, Davies SG, Russell AJ & Lea SM (2009) A structural study of the  
43  
44 interaction between the Dr haemagglutinin DraE and derivatives of chloramphenicol. *Acta*  
45  
46 *Crystallogr D Biol Crystallogr* **65**: 513–522.

47  
48 Pham TQ, Goluszko P, Popov V, Nowicki S & Nowicki BJ (1997) Molecular cloning and  
49  
50 characterization of Dr-II A nonfimbrial adhesin-I-like adhesin isolated from gestational  
51  
52  
53  
54  
55  
56  
57  
58  
59  
60

1  
2 pyelonephritis-associated *Escherichia coli* that binds to decayaccelerating factor. *Infect*  
3  
4  
5 *Immun* **10**: 4309–4318.

6  
7 Piątek R, Zalewska B, Kolaj O, Ferens M, Nowicki B & Kur J (2005) Molecular aspects of  
8  
9 biogenesis of *Escherichia coli* Dr fimbriae: characterization of DraB-DraE complexes. *Infect*  
10  
11 *Immun* **73**: 135–145.

12  
13  
14 Pinkner JS, Remaut H, Buelens F, Miller E, Åberg V, Pemberton N, Hedenström M, Larsson F,  
15  
16 Seed P, Waksman G, Hultgren SJ & Almqvist F (2006) Rationally designed small  
17  
18 compounds inhibit pilus biogenesis in uropathogenic bacteria. *Proc Natl Acad Sci USA* **103**:  
19  
20 17897–17902.

21  
22  
23  
24 Poole ST, McVeigh AL, Anantha RP, Lee LH, Akay YM, Pontzer EA, Scott DA, Bullitt E &  
25  
26 Savarino SJ (2007) Donor strand complementation governs intersubunit interaction of  
27  
28 fimbriae of the alternate chaperone pathway. *Mol Microbiol* **63**: 1372–1384.

29  
30  
31 Proft T & Baker EN (2009) Pili in Gram-negative and Gram-positive bacteria - structure,  
32  
33 assembly and their role in disease. *Cell Mol Life Sci* **66**: 613–635.

34  
35  
36 Pujol C, Klein KA, Romanov GA, Palmer LE, Ciota C, Zhao Z & Bliska JB (2009) *Yersinia*  
37  
38 *pestis* can reside in autophagosomes and avoid xenophagy in murine macrophages by  
39  
40 preventing vacuole acidification. *Infect Immun* **77**: 2251–2261.

41  
42  
43 Read TD, Dowdell M, Satola SW & Farley MM (1996) Duplication of pilus gene complexes of  
44  
45 *Haemophilus influenzae* biogroup aegyptius. *J Bacteriol* **178**: 6564–6570.

46  
47  
48 Remaut H, Rose RJ, Hannan TJ, Hultgren SJ, Radford SE, Ashcroft AE & Waksman G (2006)  
49  
50 Donor-strand exchange in chaperone-assisted pilus assembly proceeds through a concerted  $\beta$   
51  
52 strand displacement mechanism. *Mol Cell* **22**: 831–842.

53  
54  
55 Remaut H, Tang C, Henderson N, Pinkner J, Wang T, Hultgren S, Thanassi D, Waksman G & Li  
56  
57 H (2008) Fiber formation across the bacterial outer membrane by the chaperone/usher  
58  
59 pathway. *Cell* **133**: 640–652.  
60

- 1  
2 Remer KA, Bartrow M, Roeger B, Moll H, Sonnenborn U & Oelschlaeger TA (2009) Split  
3  
4 immune response after oral vaccination of mice with recombinant *Escherichia coli* Nissle  
5  
6 1917 expressing fimbrial adhesin K88. *Int J Med Microbiol* (Epub ahead of print).  
7  
8
- 9 Remi F, Remaut H & Waksman G (2008) Architectures and biogenesis of non-flagellar protein  
10  
11 appendages in Gram-negative bacteria. *The EMBO Journal* **27**: 2271–2280.  
12  
13
- 14 Rey-Campos J, Rubinstein P & de Cordoba SR (1988) A physical map of the human regulator of  
15  
16 complement activation gene cluster linking the complement genes CR1, CR2, DAF, and  
17  
18 C4BP. *J Exp Med* **167**: 664–669.  
19  
20
- 21 Richardson JS & Richardson DC (2002) Natural beta-sheet proteins use negative design to avoid  
22  
23 edge-to-edge aggregation. *Proc Natl Acad Sci USA* **99**: 2754–2759.  
24  
25
- 26 Riegman N, Kusters R, van Veggel H, Bergmans H, van Bergen P, Henegouwen E, Hacker J &  
27  
28 van Die I (1990) F1C fimbriae of a uropathogenic *Escherichia coli* strain: genetic and  
29  
30 functional organization of the *foc* gene cluster and identification of minor subunits. *J*  
31  
32 *Bacteriol* **172**: 1114–1120.  
33  
34
- 35 Rose RJ, Welsh TS, Waksman G, Ashcroft AE, Radford SE & Paci E (2008) Donor-strand  
36  
37 exchange in chaperone-assisted pilus assembly revealed in atomic detail by molecular  
38  
39 dynamics. *J Mol Biol* **375**: 908–919.  
40  
41
- 42 Rougeaux C, Berger CN & Servin AL (2008) CEACAM1-4L down-regulates hDAF-associated  
43  
44 signaling after being recognized by the Dr adhesin of diffusely adhering *Escherichia coli*.  
45  
46 *Cell Microbiol* **10**: 632–654.  
47  
48
- 49 Saarela S (1999) Functional and molecular characterization of the GafD fimbrial lectin of  
50  
51 *Escherichia coli*. *Academic dissertation University of Helsinki, Finland*.  
52  
53
- 54 Saarela S, Taira S, Nurmiaho-Lassila E-L, Makkonen A & Rhen M (1995) The *Escherichia coli*  
55  
56 G-fimbrial lectin protein participates both in fimbrial biogenesis and in recognition of the  
57  
58 receptor N-acetyl-D-glucosamine. *J Bacteriol* **177**: 1477–1484.  
59  
60



- 1  
2 Saarela S, Westerlund-Wikström B, Rhen M & Korhonen TK (1996) The GafD protein of the G  
3  
4 (F17) fimbrial complex confers adhesiveness of *Escherichia coli* to laminin. *Infect Immun*  
5  
6 **64**: 2857–2860.  
7  
8
- 9 Sabhnani L, Manocha M, Sridevi K, Shashikiran D, Rayanade R & Rao DN (2003) Developing  
10  
11 subunit immunogens using B and T cell epitopes and their constructs derived from the F1  
12  
13 antigen of *Yersinia pestis* using novel delivery vehicles. *FEMS Immun Med Microbiol* **38**:  
14  
15 215–229.  
16  
17
- 18 Sabhnani L & Rao DN (2000) Identification of immunodominant epitope of F1 antigen of  
19  
20 *Yersinia pestis*. *FEMS Immun Med Microbiol* **27**: 155–162.  
21  
22
- 23 Salih O, Remaut H, Waksman G & Orlova EV (2008) Structural analysis of the Saf pilus by  
24  
25 electron microscopy and image processing. *J Mol Biol* **379**: 174–187.  
26  
27
- 28 Santi L, Giritch A, Roy CJ, Marillonnet S, Klimyuk V, Gleba Y, Webb R, Arntzen CJ & Mason  
29  
30 HS (2006) Protection conferred by recombinant *Yersinia pestis* antigens produced by a rapid  
31  
32 and highly scalable plant expression system. *Proc Natl Acad Sci USA* **103**: 861–866.  
33  
34
- 35 Sanchez R, Kanarek L, Koninkx J, Hendriks H, Lintermans P, Bertels A, Charlier G & Van  
36  
37 Driessche E (1993) Inhibition of adhesion of enterotoxigenic *Escherichia coli* cells  
38  
39 expressing F17 fimbriae to small intestinal mucus and brush-border membranes of young  
40  
41 calves. *Microb Pathog* **15**: 407–419.  
42  
43
- 44 Sauer FG, Barnhart M, Choudhury D, Knight SD, Waksman G & Hultgren SJ (2000)  
45  
46 Chaperone-assisted pilus assembly and bacterial attachment. *Curr Opin Struct Biol* **10**: 548–  
47  
48 556.  
49  
50
- 51 Sauer FG, Futterer K, Pinkner JS, Dodson KW, Hultgren SJ & Waksman G (1999) Structural  
52  
53 basis of chaperone function and pilus biogenesis. *Science* **285**: 1058–1061.  
54  
55
- 56 Sauer FG, Pinkner JS, Waksman G & Hultgren SJ (2002) Chaperone priming of pilus subunits  
57  
58 facilitates a topological transition that drives fiber formation. *Cell* **111**: 543–551.  
59  
60

- 1  
2 Sauer FG, Remaut H, Hultgren SJ & Waksman G (2004) Fiber assembly by the chaperone–usher  
3 pathway. *Biochim Biophys Acta* **1694**: 259–267.  
4  
5  
6  
7 Saulino ET, Thanassi DG, Pinkner JS, Hultgren SJ, Lombardo MJ, Roth R & Heuser J (1998)  
8  
9 Ramifications of kinetic partitioning on usher-mediated pilus biogenesis. *EMBO J* **17**: 2177–  
10 2185.  
11  
12  
13  
14 Savarino SJ, Fox P, Deng Y & Nataro JP (1994) Identification and characterization of a gene  
15  
16 cluster mediating enteroaggregative *Escherichia coli* aggregative adherence fimbria I  
17  
18 biogenesis. *J Bacteriol* **176**: 4949–4957.  
19  
20  
21 Scaletsky ICA, Michalski J, Torres AG, Dulguer MV & Kaper JB (2005) Identification and  
22  
23 characterization of the locus for diffuse adherence, which encodes a novel afimbrial adhesin  
24  
25 found in atypical enteropathogenic *Escherichia coli*. *Infect Immun* **73**: 4753–4765.  
26  
27  
28 Schembri MA, Sokurenko EV & Klemm P (2000) Functional flexibility of the FimH adhesin:  
29  
30 insights from a random mutant library. *Infect Immun* **68**: 2638–2646.  
31  
32  
33 Sebbane F, Jarrett C, Gardner D, Long D & Hinnebusch BJ (2009) The *Yersinia pestis*  
34  
35 *cafIM1A1* fimbrial capsule operon promotes transmission by flea bite in a mouse model of  
36  
37 bubonic plague. *Infect Immun* **77**: 1222–1229.  
38  
39  
40 Sebbane F, Lemaitre N, Sturdevant DE, Rebeil R, Virtaneva K, Porcella SF & Hinnebusch BJ  
41  
42 (2006) Adaptive response of *Yersinia pestis* to extracellular effectors of innate immunity  
43  
44 during bubonic plague. *Proc Natl Acad Sci USA* **103**: 11766–11771.  
45  
46  
47 Selvarangan R, Goluszko P, Singhal J, Carnoy C, Moseley S, Hudson B, Nowicki S & Nowicki  
48  
49 B (2004) Interaction of Dr adhesin with collagen Type IV is a critical step in *Escherichia coli*  
50  
51 renal persistence. *Infect Immun* **72**: 4827–4835.  
52  
53  
54 Servin AL (2005) Pathogenesis of Afa/Dr diffusely adhering *Escherichia coli*. *Clin Microbiol*  
55  
56 *Rev* **18**: 264–292.  
57  
58  
59 Sharma RK, Sodhi A & Batra HV (2005a) Involvement of c-Jun N-terminal kinase in rF1  
60  
mediated activation of murine peritoneal macrophages in vitro. *J Clin Immunol* **3**: 215–223.

- 1  
2 Sharma RK, Sodhi A, Batra HV & Tuteja U (2005b) Phosphorilation of p42/44 MAP kinase is  
3  
4 required for rF1-induced activation of murine peritoneal macrophages. *Mol Immunol* **42**:  
5  
6 1385–1392.  
7  
8
- 9 Smiley ST (2008a) Current challenges in the development of vaccines for pneumonic plague.  
10  
11 *Expert Rev Vaccines* **7**: 209–221.  
12  
13
- 14 Smiley ST (2008b) Immune defense against pneumonic plague. *Immunol Rev* **225**: 256–271.  
15  
16
- 17 So SS & Thanassi DG (2006) Analysis of the requirements for pilus biogenesis at the outer  
18  
19 membrane usher and the function of the usher C-terminus. *Mol Microbiol* **60**: 364–375.  
20  
21
- 22 Sodhi A, Sharma RK, Batra HV & Tuteja U (2004) Recombinant fraction 1 protein of *Yersinia*  
23  
24 *pestis* activates murine peritoneal macrophages *in vitro*. *Cell Immunol* **229**: 52–61.  
25  
26
- 27 Sokurenko EV, Chesnokova V, Doyle RJ & Hasty DL (1997) Diversity of the *Escherichia coli*  
28  
29 Type 1 fimbrial lectin: differential binding to mannosides and uroepithelial cells. *J Biol*  
30  
31 *Chem* **272**: 17880–17886.  
32  
33
- 34 Sokurenko EV, Chesnokova V, Dykhuizen DE, Ofek I, Wu X-R, Krogfelt KA, Struve C,  
35  
36 Schembri MA & Hasty DL (1998) Pathogenic adaptation of *Escherichia coli* by natural  
37  
38 variation of the FimH adhesin. *Proc Natl Acad Sci USA* **95**: 8922–8926.  
39  
40
- 41 Sokurenko EV, Courtney HS, Abraham SN, Klemm P & Hasty DL (1992) Functional  
42  
43 heterogeneity of Type 1 fimbriae of *Escherichia coli*. *Infect Immun* **60**: 4709–4719.  
44  
45
- 46 Sokurenko EV, Courtney HS, Maslow J, Siitonen A & Hasty DL (1995) Quantitative differences  
47  
48 in adhesiveness of Type 1 fimbriated *Escherichia coli* due to structural differences in *fimH*  
49  
50 genes. *J Bacteriol* **177**: 3680–3686.  
51  
52
- 53 Sokurenko EV, Courtney HS, Ohman DE, Klemm P & Hasty DL (1994) Heterogeneity due to  
54  
55 minor sequence variations among *fimH* genes. *J Bacteriol* **176**: 748–755.  
56  
57
- 58 Soto GE & Hultgren SJ (1999) Bacterial adhesins: common themes and variations in architecture  
59  
60 and assembly. *J Bacteriol* **181**: 1059–1071.

- 1  
2  
3  
4  
5  
6  
7  
8  
9  
10  
11  
12  
13  
14  
15  
16  
17  
18  
19  
20  
21  
22  
23  
24  
25  
26  
27  
28  
29  
30  
31  
32  
33  
34  
35  
36  
37  
38  
39  
40  
41  
42  
43  
44  
45  
46  
47  
48  
49  
50  
51  
52  
53  
54  
55  
56  
57  
58  
59  
60
- Stahlhut SG, Chattopadhyay S, Struve C, Weissman SJ, Aprikian P, Libby SJ, Fang FC, Krogfelt KA & Sokurenko EV (2009) Population variability of the FimH type 1 fimbrial adhesin in *Klebsiella pneumoniae*. *J Bacteriol* **191**: 1941–1950.
- Strindelius L, Folkesson A, Normark S & Sjöholm I (2004) Immunogenic properties of the *Salmonella* atypical fimbriae in BALB/c mice. *Vaccine* **22**: 1448–1456.
- Sung MA, Fleming K, Chen HA & Matthews S (2001) The solution structure of PapGII from uropathogenic *Escherichia coli* and its recognition of glycolipid receptors. *EMBO Rep* **2**: 621–627.
- Tchesnokova V, Aprikian P, Yakovenko O, LaRock C, Kidd B, Vogel V, Thomas W & Sokurenko E (2008) Integrin-like allosteric properties of the catch-bond forming FimH adhesin of *E coli*. *J Biol Chem* **283**: 7823–7833.
- Thanassi DG, Saulino ET & Hultgren SJ (1998) The chaperone/usher pathway: a major terminal branch of the general secretory pathway. *Curr Opin Microbiol* **1**: 223–231.
- Thanassi DG, Stathopoulos C, Dodson K, Geiger D & Hultgren SJ (2002) Bacterial outer membrane ushers contain distinct targeting and assembly domains for pilus biogenesis. *J Bacteriol* **184**: 6260–6269.
- Thomas WE, Nilsson LM, Forero M, Sokurenko EV & Vogel V (2004) Shear-dependent 'stick-and-roll' adhesion of type 1 fimbriated *Escherichia coli*. *Mol Microbiol* **53**: 1545–1557.
- Thomas WE, Trintchina E, Forero M, Vogel V & Sokurenko EV (2002) Bacterial adhesion to target cells enhanced by shear force. *Cell* **109**: 913–923.
- Thomas WE, Vogel V & Sokurenko E (2008) Biophysics of catch bonds. *Annu Rev Biophys* **37**: 399–416.
- Thomas RJ, Webber D, Collinge A, Stagg AJ, Bailey SC, Nunez A, Gates A, Jayasekera PN, Taylor RR, Eley S & Titball RW (2009) Different pathologies but equal levels of responsiveness to the recombinant F1 and V antigen vaccine and ciprofloxacin in a murine model of plague caused by small- and large-particle aerosols. *Infect Immun* **77**: 1315–1323.

- 1  
2 Thompson JA, Grunert F & Zimmerman W (1991) Carcinoembryonic antigen family: molecular  
3  
4 biology and clinical perspective. *J Clin Lab Anal* **5**: 344–366.  
5  
6  
7 Tieng V, Le Bouguenec C, du Merle L, Bertheau P, Desreumaux P, Janin A, Charron D &  
8  
9 Toubert A (2002) Binding of *Escherichia coli* adhesin AfaE to CD55 triggers cell-surface  
10  
11 expression of the MHC class I-related molecule MICA *Proc Natl Acad Sci USA* **99**: 2977–  
12  
13 2982.  
14  
15  
16 Torres AG, Blanco M, Valenzuela P, Slater TM, Patel SD, Dahbi G, López C, Barriga XF,  
17  
18 Blanco JE, Gomes TA, Vidal R & Blanco J (2009) The Long Polar Fimbriae genes of  
19  
20 pathogenic *Escherichia coli* strains as reliable markers to identify virulent isolates. *J Clin*  
21  
22 *Microbiol* **47**: 2442–2451.  
23  
24  
25  
26 Tripathi V, Chitralkha KT, Bakshi AR, Tomar D, Deshmukh RA, Baig MA & Rao DN (2006)  
27  
28 Inducing systemic and mucosal immune responses to B-T construct of F1 antigen of *Yersinia*  
29  
30 *pestis* in microsphere delivery. *Vaccine* **24**: 3279–3289.  
31  
32  
33 van den Broeck W, Cox E, Oudega C & Goddeeris BM (2000) The F4 fimbrial antigen of  
34  
35 *Escherichia coli* and its receptors. *Vet Microbiol* **71**: 223–244.  
36  
37  
38 van Ham SM, van Alphen L, Mooj FR & JPM van Putten (1994) The fimbrial gene cluster of  
39  
40 *Haemophilus influenzae* type b. *Mol Microbiol* **13**: 673–684.  
41  
42  
43 Van Loy CP, Sokurenko EV & Moseley SL (2002) The major structural subunits of Dr and  
44  
45 F1845 fimbriae are adhesions. *Infect Immun* **70**: 1694–1702.  
46  
47  
48 Van Molle I, Moonens K, Buts L, Garcia-Pino A, Panjikar S, Wyns L, De Greve H & Bouckaert  
49  
50 J (2009) The F4 fimbrial chaperone FaeE is stable as a monomer that does not require self-  
51  
52 capping of its pilin-interactive surfaces. *Acta Crystallogr D Biol Crystallogr* **65**: 411–420.  
53  
54  
55 Velan B, Bar-Haim E, Zauberman A, Mamroud E, Shafferman A & Cohen S (2006)  
56  
57 Discordance in the effects of *Yersinia pestis* on dendritic cell functions: induction of  
58  
59 maturation and paralysis of migration. *Infect Immun* **74**: 6365–6376.  
60

- 1  
2 Verdonck F, Joensuu JJ, Stuyven E, De Meyer J, Muilu M, Pirhonen M, Goddeeris BM, Mast J,  
3  
4 Niklander-Teeri V & Cox E (2009) The polymeric stability of the *Escherichia coli* F4 (K88)  
5  
6 fimbriae enhances its mucosal immunogenicity following oral immunization. *Vaccine* **26**:  
7  
8 5728–5735.  
9
- 10  
11 Verger D, Bullitt E, Hultgren SJ & Waksman G (2007) Crystal structure of the P pilus rod  
12  
13 subunit PapA *PLoS Pathogens* **3**: e73.  
14
- 15  
16 Verger D, Rose RJ, Paci E, Costakes G, Daviter T, Hultgren S, Remaut H, Ashcroft AE, Radford  
17  
18 SE & Waksman G (2008) Structural determinants of polymerization reactivity of the P pilus  
19  
20 adaptor subunit PapF. *Structure* **16**: 1724-1731.  
21
- 22  
23 Vetsch M, Pourger C, Spirig T, Grauschopf U, Weber-Ban EU & Glockshuber R (2004) Pilus  
24  
25 chaperones represent a new type of protein folding catalyst. *Nature* **431**: 329–333.  
26
- 27  
28 Viboud GI & Bliska JB (2005) *Yersinia* outer proteins: role in modulation of host cell signaling  
29  
30 responses and pathogenesis. *Annu Rev Microbiol* **59**: 69–89.  
31
- 32  
33 Virdi JS & Sachdeva P (2005) Molecular heterogeneity in *Yersinia enterocolitica* and *Y.*  
34  
35 *enterocolitica*-like species – implications for epidemiology, typing and taxonomy. *FEMS*  
36  
37 *Immun Med Microbiol* **45**: 1–10.  
38
- 39  
40 Waksman G & Hultgren SJ (2009) Structural biology of the chaperone–usher pathway of pilus  
41  
42 biogenesis. *Nature Rev Microbiol* **7**: 765–774.  
43
- 44  
45 Wang H, Min G, Glockshuber R, Sun TT & Kong XP (2009) Uropathogenic *E. coli* adhesin-  
46  
47 induced host cell receptor conformational changes: implications in transmembrane signaling  
48  
49 transduction. *J Mol Biol* (Epub ahead of print).  
50
- 51  
52 Watts C (2004) The exogenous pathway for antigen presentation on major histocompatibility  
53  
54 complex class II and CD1 molecules. *Nature Immun* **5**: 685–692.  
55
- 56  
57 Weissman SJ, Chattopadhyay S, Aprikian P, Obata-Yasuoka M, Yarova-Yarovaya Y, Stapleton  
58  
59 A, Ba-Thein W, Dykhuizen D, Johnson JR & Sokurenko EV (2006) Clonal analysis reveals  
60

1  
2 high rate of structural mutations in fimbrial adhesins of extraintestinal pathogenic  
3  
4 *Escherichia coli*. *Mol Microbiol* **59**: 975–988.

5  
6 Wellens A, Garofalo C, Nguyen H, Van Gerven N, Slättegård R, Hernalsteens J-P, Wyns L,  
7  
8 Oscarson S, De Greve H, Hultgren S & Bouckaert J (2008) Intervening with Urinary Tract  
9  
10 Infections Using Anti-Adhesives Based on the Crystal Structure of the FimH–Oligomannose-  
11  
12 3 Complex. *PLoS ONE* **3**: e2040.

13  
14 Welkos SL, Andrews GP, Lindler LE, Snellings NJ & Strachan SD (2004) Mu dII(Ap lac)  
15  
16 mutagenesis of *Yersinia pestis* plasmid pFra and identification of temperature-regulated loci  
17  
18 associated with virulence. *Plasmid* **51**: 1–11.

19  
20 Westerlund B & Korhonen TK (1993) Bacterial proteins binding to the mammalian extracellular  
21  
22 matrix. *Mol Microbiol* **9**: 687–694.

23  
24 Westerlund B, Kuusela P, Risteli J, Risteli L, Vartio T, Rauvala H, Virkola R & Korhonen TK  
25  
26 (1989) The O75X adhesin of uropathogenic *Escherichia coli* is a type IV collagen-binding  
27  
28 protein. *Mol Microbiol* **3**: 329–337.

29  
30 Westerlund-Wikström B & Korhonen TK (2005) Molecular structure of adhesin domains in  
31  
32 *Escherichia coli* fimbriae. *Int J Med Microb* **295**: 479–486.

33  
34 Willems RJL, van der Heide HGJ & Mooi FR (1992) Characterization of a *Bordetella pertussis*  
35  
36 fimbrial gene cluster which is located directly downstream of the filamentous haemagglutinin  
37  
38 gene. *Mol Microbiol* **6**: 2661–2671.

39  
40 Williamson ED, Eley SM, Stagg AJ, Green M, Russell P & Titball RW (1997) A sub-unit  
41  
42 vaccine elicits IgG in serum, spleen cell cultures and bronchial washings and protects  
43  
44 immunized animals against pneumonic plague. *Vaccine* **15**: 1079–1084.

45  
46 Williamson ED, Flick-Smith HC, LeButt C, Rowland CA, Jones SM, Waters EL, Gwyther RJ,  
47  
48 Miller J, Packer PJ & Irving M (2005) Human immune response to a plague vaccine  
49  
50 comprising recombinant F1 and V antigens. *Infect Immun* **73**: 3598–3608.



- 1  
2  
3  
4  
5  
6  
7  
8  
9  
10  
11  
12  
13  
14  
15  
16  
17  
18  
19  
20  
21  
22  
23  
24  
25  
26  
27  
28  
29  
30  
31  
32  
33  
34  
35  
36  
37  
38  
39  
40  
41  
42  
43  
44  
45  
46  
47  
48  
49  
50  
51  
52  
53  
54  
55  
56  
57  
58  
59  
60
- Wolf MK, De Haan LAM, Cassels FJ, Willshaw GA, Warren R, Boedeker EC & Gastra W (1997) The CS6 colonization factor of human enterotoxigenic *Escherichia coli* contains two heterologous major subunits. *FEMS Microbiol Lett* **148**: 35–42.
- Wroblewska-Seniuk K, Selvarangan R, Hart A, Pladzyk R, Goluszko P, Jafari A, du Merle L, Nowicki S, Yallampalli C, Le Bouguéne C & Nowicki B (2005) Dra/AfaE adhesin of uropathogenic Dr/Afa1 *Escherichia coli* mediates mortality in pregnant rats. *Infect Immun* **73**: 7597–7601.
- Yakovenko O, Sharma S, Forero M, Tchesnokova V, Aprikian P, Kidd B, Mach A, Vogel V, Sokurenko E & Thomas WE (2008) FimH forms catch bonds that are enhanced by mechanical force due to allosteric regulation. *J Biol Chem* **283**: 11596–11605.
- Yamamoto D, Hernandez RT, Blanco M, Greune L, Schmidt MA, Carneiro SM, Dahbi G, Blanco JE, Mora A, Blanco J & Gomes TAT (2009) Invasiveness as a putative additional virulence mechanism of some atypical Enteropathogenic *Escherichia coli* strains with different uncommon intimin types. *BMC Microbiology* **9**: 146.
- Yang Y & Isberg RR (1997) Transcriptional regulation of the *Yersinia pseudotuberculosis* pH6 antigen adhesin by two envelope-associated components. *Mol Microbiol* **24**: 499–510.
- Yen MR, Peabody CR, Partovi SM, Zhai Y, Tseng YH & Saier MH (2002) Protein-translocating outer membrane porins of gram-negative bacteria. *Biochim Biophys Acta* **1562**: 6–31.
- Yu S & Lowe AW (2009) The pancreatic zymogen granule membrane protein, GP2, binds *Escherichia coli* type 1 Fimbriae. *BMC Gastroenterology* **9**: 58.
- Yu X, Visweswaran GR, Duck Z, Marupakula S, MacIntyre S, Knight SD & Zavialov AV (2009) Caf1A usher possesses a Caf1 subunit-like domain that is crucial for Caf1 fibre secretion. *Biochem J* **418**: 541–551.
- Zalewska B, Piątek R, Bury K, Samet A, Nowicki B, Nowicki S & Kur J (2005) A surface-exposed DraD protein of uropathogenic *Escherichia coli* bearing Dr fimbriae may be

1  
2 expressed and secreted independently from DraC usher and DraE adhesion. *Microbiology*  
3  
4 **151**: 2477–2486.

5  
6 Zalewska B, Piątek R, Konopa G, Nowicki B, Nowicki S & Kur J (2003) Chimeric Dr fimbriae  
7  
8 with a herpes simplex virus type 1 epitope as a model for a recombinant vaccine. *Infect*  
9  
10  
11 *Immun* **71**: 5505–5513.

12  
13 Zalewska- Piątek B, Bury K, Piątek R, Bruździak P & Kur J (2008) Type II secretory pathway  
14  
15 for surface secretion of DraD invasin from the uropathogenic *Escherichia coli* Dr<sup>+</sup> strain. *J*  
16  
17 *Bacteriol* **190**: 5044–5056.

18  
19 Zavalov A, Zav'yalova G, Korpela T & Zav'yalov V (2007) FGL chaperone-assembled fimbrial  
20  
21 polyadhesins: anti-immune armament of Gram-negative bacterial pathogens. *FEMS*  
22  
23 *Microbiol Rev* **31**: 478–514.

24  
25 Zavalov AV & Knight SD (2007) A novel self-capping mechanism controls aggregation of  
26  
27 periplasmic chaperone Caf1M *Mol Microbiol* **64**: 153–164.

28  
29 Zavalov AV, Batchikova NV, Korpela T, Petrovskaya LE, Korobko VG, Kersley J, MacIntyre S  
30  
31 & Zav'yalov VP (2001) Secretion of recombinant proteins via the chaperone/usher pathway  
32  
33 in *Escherichia coli*. *Appl Environ Microbiol* **67**: 1805–1814.

34  
35 Zavalov AV, Berglund J, Pudney AF, Fooks LJ, Ibrahim TM, MacIntyre S & Knight SD (2003)  
36  
37 Structure and biogenesis of the capsular F1 antigen from *Yersinia pestis*: preserved folding  
38  
39 energy drives fiber formation. *Cell* **113**: 587–596.

40  
41 Zavalov AV, Kersley J, Korpela T, Zav'yalov VP, MacIntyre S & Knight SD (2002) Donor  
42  
43 strand complementation mechanism in the biogenesis of non-pilus systems. *Mol Microbiol*  
44  
45 **45**: 983–995.

46  
47 Zavalov AV, Tischenko VM, Fooks LJ, Brandsdal BO, Aquist J, Zav'yalov VP, MacIntyre S &  
48  
49 Knight SD (2005) Resolving the energy paradox of chaperone-mediated fibre assembly.  
50  
51  
52 *Biochem J* **389**: 685–694.  
53  
54  
55  
56  
57  
58  
59  
60

1  
2  
3  
4  
5  
6  
7  
8  
9  
10  
11  
12  
13  
14  
15  
16  
17  
18  
19  
20  
21  
22  
23  
24  
25  
26  
27  
28  
29  
30  
31  
32  
33  
34  
35  
36  
37  
38  
39  
40  
41  
42  
43  
44  
45  
46  
47  
48  
49  
50  
51  
52  
53  
54  
55  
56  
57  
58  
59  
60

Zav'yalov VP, Abramov VM, Cherepanov PG, Spirina GV, Chernovskaya TV, Vasiliev AM & Zav'yalova GA (1996) pH6 antigen (PsaA protein) of *Yersinia pestis*, a novel bacterial Fc-receptor. *FEMS Immun Med Microbiol* **14**: 53–57.

Zav'yalov VP, Chernovskaya TV, Chapman DAG, Karlishev AV, MacIntyre S, Zavialov AV, Vasiliev AM, Denesyuk AI, Dudich IV, Korpela T & Abramov VM (1997) Influence of the conserved disulphide bond, exposed to the putative binding pocket, on the structure and function of the immunoglobulin-like periplasmic molecular chaperone, Caf1M, of *Yersinia pestis*. *Biochem J* **324**: 571–578.

Zav'yalov VP, Chernovskaya TV, Navolotskaya EV, Karlishev AV, MacIntyre S, Vasiliev AM & Abramov VM (1995a) Specific high affinity binding of human interleukin 1 $\beta$  by Caf1A usher protein of *Yersinia pestis*. *FEBS Lett* **371**: 65–68.

Zav'yalov VP, Zav'yalova GA, Denesyuk AI & Korpela T (1995b) Modelling of steric structure of a periplasmic molecular chaperone Caf1M of *Yersinia pestis*, a prototype member of a subfamily with characteristic structural and functional features. *FEMS Immun Med Microbiol* **11**: 19–24.

Zhou H, Monack DM, Kayagaki N, Wertz I, Yin J, Wolf B & Dixit VM (2005) *Yersinia* virulence factor YopJ acts as a deubiquitinase to inhibit NF-kB activation. *J Exp Med* **202**: 1327–1332.

**Table 1.** Adhesive fimbrial organelles assembled on the Gram negative pathogen cell surface via classical chaperone-usher pathway<sup>a</sup>.

Organelle	Chaperone/usher	Bacterium	Disease	Reference(s)
Aggregative adherence fimbria II, AAF/II	AafD/C	<i>Escherichia coli</i>	Diarrhea	Elias <i>et al.</i> , 1999
n/d <sup>b</sup>	ACIAD0120/0121	<i>Acinetobacter</i> sp. strain ADP1	n/d	Barbe <i>et al.</i> , 2004; Gohl <i>et al.</i> , 2006
Thin pili, an external diameter of 2 to 3 nm	AcuD/C	<i>Acinetobacter</i> sp. strain BD413	n/d	Barbe <i>et al.</i> , 2004; Gohl <i>et al.</i> , 2006
Afimbrial adhesin, AFA-III	Afa-3B/C	<i>E. coli</i>	Diarrhea or cystitis	Garcia <i>et al.</i> , 1994
Afimbrial adhesin, AfaE-VIII	Afa-8B/C	<i>E. coli</i>	Diarrhea/septicaemia	Lalioui & Le Bouguéneq, 2001
AF/R1 pili	AfrC/B	<i>E. coli</i>	Diarrhea in rabbits	Cantey <i>et al.</i> , 1999
Aggregative adherence fimbria type I, AAF-I	AggD/C	<i>E. coli</i>	Diarrhea	Savarino <i>et al.</i> , 1994
Aggregative adhesion fimbria type III, AAF-III	Agg-3D/C	<i>E. coli</i>	Diarrhea	Bernier <i>et al.</i> , 2002
Ambient-temperature fimbriae	AtfB/C	<i>Proteus mirabilis</i>	Urinary tract infections	Massad <i>et al.</i> , 1996
Capsular F1 antigen	Caf1M/A	<i>Yersinia pestis</i>	Plague	Galyov <i>et al.</i> , 1990, 1991; Karlyshev <i>et al.</i> , 1992a,b, 1994
Colonization factor-3, CS-3 fimbriae	CS3-E/D	<i>E. coli</i>	Diarrhea	Jalajakumar <i>et al.</i> , 1989
Colonization factor, CS6	CssC/D	<i>E. coli</i>	Diarrhea	Wolf <i>et al.</i> , 1997
CS12 fimbria	CswB/C	<i>E. coli</i>	Diarrhea	EMBL accession number Q9ALL0
CS31A capsule-like antigen	ClpE/D	<i>E. coli</i>	Diarrhea	Bertin <i>et al.</i> , 1993
F1845 (DaaE) fimbrial adhesin	DaaB/C	<i>E. coli</i>	Diarrhea	Bilge <i>et al.</i> , 1989
Diffuse adherence fibrillar adhesin	DafaB/C	<i>E. coli</i>	Diarrhea	Keller <i>et al.</i> , 2002
Dr hemagglutinin flexible fimbriae	DraB/C	<i>E. coli</i>	Pyelonephritis	Piątek <i>et al.</i> , 2005; Servin, 2005; Van Loy <i>et al.</i> , 2002
F17 pili	F17D/C	<i>E. coli</i>	Diarrhea	Lintermans <i>et al.</i> , 1988
987P fimbriae	FasB/D	<i>E. coli</i>	Diarrhea in piglets	Emmerth <i>et al.</i> , 1999
K99 pili	FaeE/D	<i>E. coli</i>	Neonatal diarrhea in calves, lambs, and piglets	Bakker <i>et al.</i> , 1991
K88 pili	FanE/D	<i>E. coli</i>	Neonatal diarrhea in piglets	Bakker <i>et al.</i> , 1991
Type 2 and 3 pili	FimB/C	<i>Bordetella pertussis</i>	Whooping cough	Willems <i>et al.</i> , 1992
Type 1 pili	FimC/D	<i>E. coli</i>	Cystitis	Jones <i>et al.</i> , 1993
F1C pili	FocC/D	<i>E. coli</i>	Cystitis	Riegman <i>et al.</i> , 1990
CS18 fimbriae	FotB/D	<i>E. coli</i>	Diarrhea	Honarvar <i>et al.</i> , 2003
<i>Haemophilus influenzae</i> biogroup aegyptius fimbriae	HafB/E	<i>H. influenzae</i>	Meningitis, Brazilian purpuric fever	Read <i>et al.</i> , 1996

<i>H. influenzae</i> fimbriae	HifB/C	<i>H. influenzae</i> type b	Otitis media	van Ham <i>et al.</i> , 1994
Afimbrial adhesin	LdaE	<i>E. coli</i>	Diarrhea	Scaletsky <i>et al.</i> , 2005
Long polar fimbriae	LpfB/C	<i>Salmonella typhimurium</i>	Gastroenteritis	Bäumler & Heffron, 1995
Mannose-resistant fimbriae	MrfD/C	<i>Photorhabdus temperata</i>	Insect pathogen	Meslet-Cladiere <i>et al.</i> , 2004
Type 3 fimbriae	MrkB	<i>Klebsiella pneumoniae</i>	Pneumonia	Allen <i>et al.</i> , 1991
Mannose-resistant/Proteus-like MR/P pili	MrpD/C	<i>P. mirabilis</i>	Nosocomial urinary tract infections	Bahrani & Mobley, 1994
Mucoid <i>Yersinia</i> factor, Myf fimbriae	MyfB/C	<i>Y. enterocolitica</i>	Enterocolitis	Iriarte & Cornelis, 1995
Nonfimbrial adhesin, NFA-I	NfaE/C	<i>E. coli</i>	Urinary tract infections	Ahrens <i>et al.</i> , 1993; Servin, 2005
P pili	PapD/C	<i>E. coli</i>	Pyelonephritis or cystitis	Marklund <i>et al.</i> , 1992
Pef pili	PefD/C	<i>S. typhimurium</i>	Gastroenteritis	Bäumler <i>et al.</i> , 1996
PMF pili	PmfC/D	<i>P. mirabilis</i>	Nosocomial urinary tract infections	Massad & Mobley, 1994
Fimbrial pH6 antigen	PsaB/C	<i>Y. pestis</i> , <i>Y. pseudotuberculosis</i>	Plague Gastroenteritis	Massad & Mobley, 1994
Putative adhesin	PSPPH_A0063/ A0064	<i>Pseudomonas syringae</i>	Halo blight of bean	Joardar <i>et al.</i> , 2005
REPEC fimbriae	RalE/D	<i>E. coli</i>	Diarrhea in rabbits	Adams <i>et al.</i> , 1997
Atypical fimbriae Saf	SafB/C	<i>S. typhimurium</i>	Gastroenteritis	Folkesson <i>et al.</i> , 1999; McClelland <i>et al.</i> , 2001
Putative atypical fimbriae	SafB/C	<i>S. typhi</i>	Enteric typhoid fever	Deng <i>et al.</i> , 2003
Putative atypical fimbriae	SafB/C	<i>S. choleraesuis</i>	Sepsis, extraintestinal focal infections	Chiu <i>et al.</i> , 2005
Putative atypical fimbriae	SafB/C	<i>S. paratyphi A</i>	Enteric typhoid fever	McClelland <i>et al.</i> , 2004
Filamentous fimbriae-like structures SEF14/18	SefB/C	<i>S. enteritidis</i>	Gastroenteritis	Clouthier <i>et al.</i> , 1993, 1994
Putative fimbriae	SefB/C	<i>S. typhi</i>	Enteric typhoid fever	EMBL accession number A212T7
Putative fimbriae	SefB/C	<i>S. paratyphi A</i>	Enteric typhoid fever	McClelland <i>et al.</i> , 2004
S pili	SfaE/F	<i>E. coli</i>	Urinary tract infections	Dobrindt <i>et al.</i> , 2001
Sfp fimbriae	SfpD/C	<i>E. coli</i>	Diarrhea	Brunder <i>et al.</i> , 2001
Stf fimbriae	StfD/C	<i>S. typhimurium</i>	Systemic and fatal infection in inbred mice	Emmerth <i>et al.</i> , 1999

<sup>a</sup>The information is placed in alphabetical order of the names of chaperone/usher proteins.

<sup>b</sup>non-detected.

**Table 2.** Function-structure classification of superfamily of adhesive fimbrial organelles assembled on the Gram negative pathogen cell surface via classical chaperone/usher pathway.

SUBFAMILIES	FUNCTION	MORPHOLOGY	CHAPERONES	NUMBER OF SUBUNITS	ADHESIN SUBUNITS
<b>Family 1: Polyadhesins</b>					
Subfamily 1.1: FGL chaperone- assembled polyadhesins-1 <sup>a</sup> -1 <sup>b</sup>	Poly-adhesive binding	From thin flexible fibers (2 nm diameter) observed for Psa fimbriae to amorphous or capsule-like morphology for F1 antigen (by electron microscopy)	Caf1M, CS3-E, MyfB, NfaE, PsaB	1	The main structural subunit: Caf1, CS3, MyfA, NfaA, PsaA.
Subfamily 1.2: FGL chaperone- assembled polyadhesins- (1+1 <sup>c</sup> )-1	Poly-adhesive binding	Thin flexible fibres (2 nm diameter) were observed for Dr adhesin by electron microscopy	AafD, Afa-3B, Afa- 8B, AggD, Agg-3D, DaaB, DafaB, DraB	2	The main structural subunit: AafA, Afa-3E, Afa-8E, AggA, Agg-3A, DaaE, DafaE, DraE. Additional subunit (AafD, Afa-3D, Afa-8D, AggD, Agg-3D, DaaD, DafaD, DraD) is displayed on the tip of fibre with type II secretion system.
Subfamily 1.3: FGL chaperone- assembled polyadhesins-2-1	Poly-adhesive binding	Atypical fimbrial structures	SafB, SefB, CscC	2	The main structural subunits: CscA, CscB; SafA, SefA. SafD and SefD subunits might be displayed on the tip of fibre.
Subfamily 1.4: FGS chaperone- assembled polyadhesins-1-1	Poly-adhesive binding	Thin flexible pili with a poorly defined diameter (2-4 nm, Pef pili) or atypical fimbria (Atf)	AtfB, PefD	1	The main structural subunit: AtfA, PefA.
Subfamily 1.5: FGS chaperone- assembled polyadhesins-1-2	Poly-adhesive binding	n/d <sup>d</sup>	ACIAD0120, ACIAD0123	1	The main structural subunit ACIAD0122.

Subfamily 1.6: FGS chaperone- assembled polyadhesins-3-1	Poly-adhesive binding <sup>d</sup>	AF/R1 pili	AfrC	3	The main structural subunit AfrE <sup>d</sup> .
Subfamily 1.7: FGS chaperone- assembled polyadhesins-4-1	Poly-adhesive binding	Thin flexible pili with a poorly defined diameter (2-4 nm, K88 pili)	FanE	4	The main structural subunit FanH.
Subfamily 1.8: FGS chaperone- assembled polyadhesins-5-1	Poly-adhesive binding	Thin flexible pili with a poorly defined diameter (2-4 nm, K99 pili)	FaeE, LdaE, RalE	5	The main structural subunit FaeH, LdaH, RalG <sup>d</sup> .
<b>Family 2: Monoadhesins</b>					
Subfamily 2.1: FGS chaperone- assembled monoadhesins-2-1	Mono-adhesive binding	Thin pili	AcuD, F17D, FimB	2	One domain (adhesin) on the tip: AcuG, F17G, FimD.
Subfamily 2.2: FGS chaperone- assembled monoadhesins-3-1	Mono-adhesive binding	Fimbriae/pili	HifB, HafB, MrkB, LpfB, PmfD	3	One domain (adhesin) on the tip: AfrE, HifE, HafE, MrkD, LpfE, PmfE.
Subfamily 2.3: FGS chaperone- assembled monoadhesins-3-3	Mono-adhesive binding	Fimbriae/pili	FasB, FasC, FasE; CswB, CswC, CswE; FotB, FotC, FotE	3	One domain (adhesin) on the tip: FasG, CswG, FotG.
Subfamily 2.4: FGS chaperone- assembled monoadhesins-4-1	Mono-adhesive binding	Fimbriae/pili	FocC, StfD	4	One domain (adhesin) on the tip: FocH, StfG.
Subfamily 2.5: FGS chaperone- assembled monoadhesins-5-1	Mono-adhesive binding	Fimbriae/pili	FimC, SfpD, SfaE, MrpD	5	One domain (adhesin) on the tip: FimH, SfpG, SfaH, MrpH.
Subfamily 2.6: FGS chaperone- assembled monoadhesins-7-1	Mono-adhesive binding	Fimbriae/pili	MrfD, PapD	7	One domain (adhesin) on the tip: MrfH, PapG.

<sup>a</sup> number of subunits secreted via classical chaperone/usher pathway.

<sup>b</sup> number of periplasmic chaperones assisted assembly of fibre.

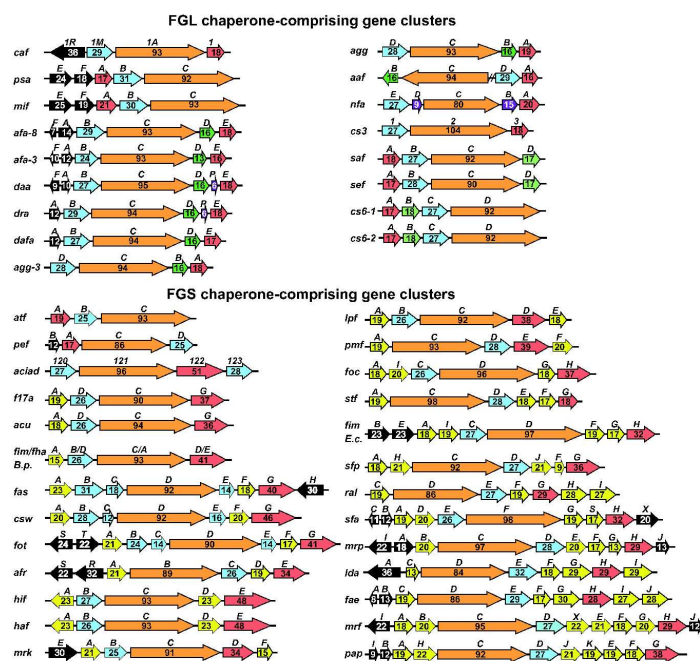


1  
2  
3  
4  
5  
6  
7  
8  
9  
10  
11  
12  
13  
14  
15  
16  
17  
18  
19  
20  
21  
22  
23  
24  
25  
26  
27  
28  
29  
30  
31  
32  
33  
34  
35  
36  
37  
38  
39  
40  
41  
42  
43  
44  
45  
46  
47  
48  
49  
50  
51  
52  
53  
54  
55  
56  
57  
58  
59  
60

<sup>c</sup> additional subunit displayed on the tip of fibre with type II secretion system.

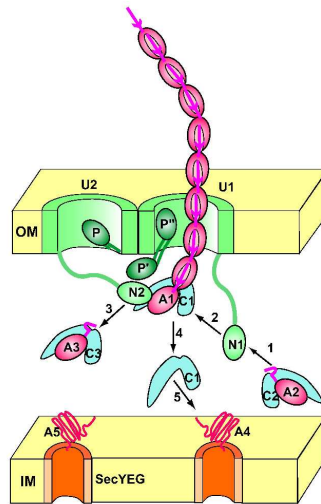
<sup>d</sup> based on high homology of the *ral* and *afr* gene clusters with the *fae* cluster.

For Peer Review



General organization of gene clusters encoding adhesive organelles assembled with classical chaperone/usher machinery (elaborated by the authors). The genes encoding periplasmic chaperones and outer membrane ushers are blue and light orange, accordingly. The genes encoding adhesin subunits, structural subunits and subunits with unknown function are red and yellow, correspondingly. The genes encoding regulatory proteins are black. The proteins with putative function are green. The proteins with unknown function are pink. The numbers designate a molecular weight of encoded protein in kDa.

209x297mm (600 x 600 DPI)

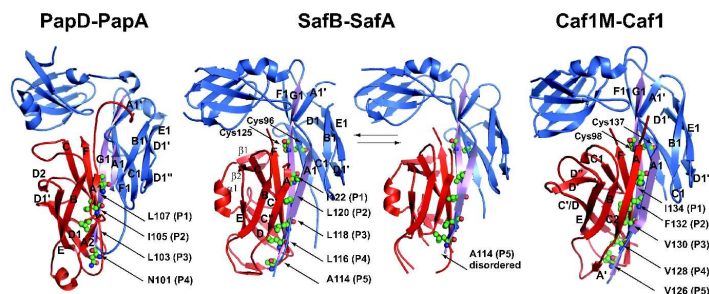


General scheme of functioning of the chaperone/usher machinery that drives formation of adhesive protein fibres on the bacterial surface. The subunits are connected in fiber by the "donor strand complementation" (shown by red arrows). The fiber is secreted through the pore (illustrated by split cylinder) in the outer membrane (OM) formed by the "usher protein" (marked by letter U). N1 and N2 indicate N-terminal domains of two different ushers (U1 and U2, accordingly). Letter P indicates position of the plug domain in U2 and P' and P'' indicate two different positions of the plug domain in U1 for the two alternative models of gating. The free N1 recruits the C2:A2 complex (step 1), and bring the complex within proximity of the N2-bound C1:A1 complex (step 2). Donor-strand exchange then releases N2 for recruitment of the C3:A3 complex (step 3) and releases C1 (step 4) for recruitment of next A4 subunit (step 5). The redrawing is based on the data published by Remaut et al. (2008).

209x297mm (600 x 600 DPI)

1  
2  
3  
4  
5  
6  
7  
8  
9  
10  
11  
12  
13  
14  
15  
16  
17  
18  
19  
20  
21  
22  
23  
24  
25  
26  
27  
28  
29  
30  
31  
32  
33  
34  
35  
36  
37  
38  
39  
40  
41  
42  
43  
44  
45  
46  
47  
48  
49  
50  
51  
52  
53  
54  
55  
56  
57  
58  
59  
60

For Peer Review



Ribbon presentation of the crystal structures of PapD-PapA, SafB-SafA and Caf1M-Caf1 complexes.

The chaperones are blue with G1 and A1 edge strands in violet, the subunits are red. The two conserved Cys residues in the whole FGL family which form disulfide bond are shown as ball-and-stick. The hydrophobic residues in G1 strand of the chaperones that interact with the P5-P1 pockets of the subunits are also shown as ball-and-stick. The SafB residue A114, which interacts with the P5 pocket, is in equilibrium between a bound (left, type I structure) and unbound (right, type II structure) state in the P5 pocket. The structures were redrawn based on the co-ordinates of atoms published by Remaut et al. (2006) (PDB accession numbers, 2CO6 and 2CO7), Verger et al. (2007) (PDB accession number, 2UY6) and Zavialov et al. (2003, 2005) (PDB accession number, 1P5V). All figures were prepared with PyMOL (DeLano, 2002).

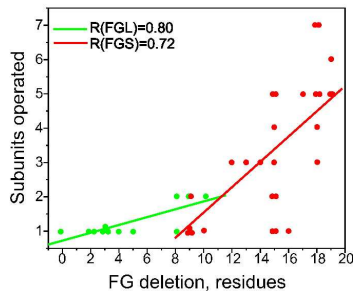
209x297mm (600 x 600 DPI)

1  
2  
3  
4  
5  
6  
7  
8  
9  
10  
11  
12  
13  
14  
15  
16  
17  
18  
19  
20  
21  
22  
23  
24  
25  
26  
27  
28  
29  
30  
31  
32  
33  
34  
35  
36  
37  
38  
39  
40  
41  
42  
43  
44  
45  
46  
47  
48  
49  
50  
51  
52  
53  
54  
55  
56  
57  
58  
59  
60

CHAPERONE	90	100	110	120	130	140	UniProtKB/ Swiss-Prot entry
CafM	DKESLQWLCVKGIPPKDED	INVDDATNKQKFNEDK	IGVFQIA	NNC	IKLLV	RR	P26926
Afa-8B	DRESLQWLCVKGIPPKHDD	RWAEEKGADK	--KKADK	ITQ	NNLS	SSCVKLV	Q9ADX2
MyfB	DRESLQWLCITGIPPKGDD	VWDNSQHDK	--NNMQD	UNN	ILS	GTCKLLV	F33407
PsaB	DRETQWLCITGIPPKNGD	AWGNTQNNP	---KNSS	ITD	QMS	STCKLV	F69965
AafD	DRETQWLCVKGIPPKANDR	WAENDSKN	---VLDN	KALN	HIS	WTCKLV	Q9X2M3
Agg-3D	DRETQWLCVKGIPPKSDEK	WAESNKN	---SLNN	ITN	QMS	STCKLV	Q8KWG7
AggD	DRESLQWLCVKAIPPKYED	KWAKEEVSG	---KKS	DKT	NN	QMS	F46004
DafaB	DRESLQWLCVKGIPPKEDR	WAEGKDG	---KKAD	K	SN	QMS	Q9AGX9
Afa-3B	DRESLQWLCVKGIPPKEDR	WAEGKDG	---KKAD	K	SN	QMS	P53516
DraB	DRESLQWLCVKGIPPKEDR	WAEGKDG	---KKAD	K	SN	QMS	Q68361
DaaB	DRESLQWLCVKGIPPKEDR	WAEGKDG	---KKAD	K	SN	QMS	MacIntyre et al., 2001
NfaE	DRESLQWLCVKGIPPKEDR	WAEGKDG	---KKAD	K	SN	QMS	P46738
CS3-1	DRESLQWLCVKGIPPKQGD	LWANNE	---KEF	GHK	IN	NTCKLV	P15483
Pseudomonas	DRESLQWLCVKGIPPKQGD	LWANNE	---KEF	GHK	IN	NTCKLV	Q48BA8
SafB S. tm.	DRESLQWLCVKGIPPKQGD	LWANNE	---KEF	GHK	IN	NTCKLV	Q82R33
SefB S. ent.	NEESLQWLCVKGIPPKQGD	LWANNE	---KEF	GHK	IN	NTCKLV	P33387
CssC1	SQESMRWLCIESMPPEK	STKINRK	---EGRT	D	SN	IS	P53518
CssC2	SQESMRWLCIESMPPEK	STKINRK	---EGRT	D	SN	IS	P53519
FasB	DQETIYVWVSNAI	EGGEEVKTQER	-----GKISAK	IS	IA	RYKVFMI	Q46992
CswB	DRETLPWAVSNLSL	GVVFTKLDNKE	-----GKITAK	IS	IA	RFKVPVLI	Q9ALL0
FotB	HKETLFWVNSL	GGDKTELKSID	-----DKITAK	IS	IA	RFKVPVLI	Q846B1
F17aD	DRESLFWLNVDL	IPAKPSFAGKSEK	-----AQGYNY	Q	IA	RSRIKLV	Q30925
HafB	DRESLFWLNVDL	IPKPAEFLA	-----KHGSF	Q	IA	RSRIKLV	P94812
HiFb	DRESLFWLNVDL	IPKPAEFLA	-----KHGSF	Q	IA	RSRIKLV	P35757
MrkB	DKETLWLNLEL	IPVEASQKNE	-----GQNI	Q	IA	RSRFKVI	P21646
AcuD	DRESLFWLNVDL	IPPEASANKD	-----KNL	IT	NN	RSRIKLV	Q6Q279
LpfB	DRESVFWLNVKAL	IPAKSEDAEA	-----KNV	Q	IA	RTKLV	P43661
FimB/FhaD	DRESVFWLNVKAL	IPAKSEDAEA	-----KNV	Q	IA	RTKLV	P33409
ACIAD0123	DRESQFWLNLYEI	IPKKLQSNQKP	-----ETNHQ	D	IS	QTQLKVF	Q6FFQ7
AtfB	DRESLFWMNVKAL	IPSLDEKLAN	-----ENT	Q	IA	RSRIKLV	P72210
FimC	DRESLFWMNVKAL	IPSMKSKLT	-----ENT	Q	IA	ISRIKLV	P31697
FocC	DRESLFWMNVKAL	IPAMDKARTG	-----ENY	Q	IA	VSRIKLV	Q6KDA4
SfaE	DRESLFWMNVKAL	IPAMDKARTG	-----ENY	Q	IA	VSRIKLV	Q9EXJ6
ACIAD0120	DRESVFWLNVDL	IPALRNKLD	-----QAM	V	IL	KSRIKLV	Q6FFR0
AfrC	DRESLFWLNVDL	IPPKVKVDGE	-----GSV	IA	AN	TRVKLV	Q85184
PeFD S. tm.	DRESLFWLNVDL	IPPKKASE	-----GNV	IA	AN	TKVLI	Q04821
FanE	DRESIFWLNVDL	IPPAKGD	-----GGS	IA	AN	NRVKLV	P25402
FaeE	DRESVFWLNVDL	IPPALE	-----GSG	IA	AN	RTKLV	P25401
LdaE	DRESVFWLNVDL	IPPALE	-----GSG	IA	AN	RTKLV	Q49JG0
Rale	DRESVFWLNVDL	IPPALE	-----GSG	IA	AN	RTKLV	P96324
MrpD	DRESVFWLNVDL	IPPRSK	-----PNV	Q	IA	QTRIKLV	Q51905
MrfD	DRESLFWLNVDL	IPPRSK	-----PNT	Q	IA	QTRIKLV	Q93MT3
PapD	DRESLFWLNVDL	IPPRSK	-----PNT	Q	IA	QTRIKLV	P15319
SfpD	DRESLFWLNVDL	IPPRSK	-----PNT	Q	IA	QTRIKLV	Q933Y4
StfD	DRETLPFWNVREI	IPQSDK	-----PNT	Q	IA	QTRIKLV	Q87659
PmfD	DRESLFWLNVDL	IPPAKQ	-----ANV	Q	IA	QSRIKLV	P53520

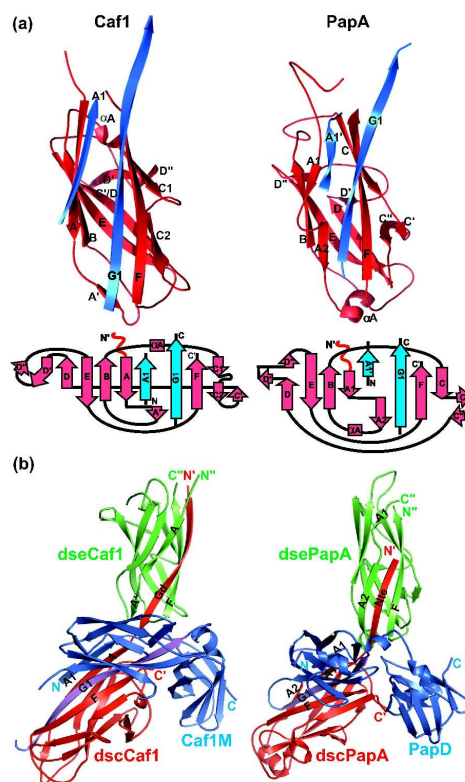
Functionally important sequences of the chaperones assembling fimbrial adhesins via chaperone/usher pathway (elaborated by the authors). Numbering in CafM sequence is indicated. Conserved Cys residues involved in disulphide bond formation in the FGL chaperones are yellow. Other residues conserved in the whole superfamily are green, including subunit anchoring Lys that is replaced by Pro in FasB, CswB and FotB operating only with adhesin subunits. Alternating bulky hydrophobic residues (from five to three in the FGL family; three in the FGS family) extending from the beginning of the G1  $\beta$ -strand are red. The conservative positions, that are typical for the CafM-like subfamily of FGL chaperones, are cyan. F1 and G1  $\beta$ -strands are shown by arrows (see Fig. 3 for details).

209x297mm (600 x 600 DPI)



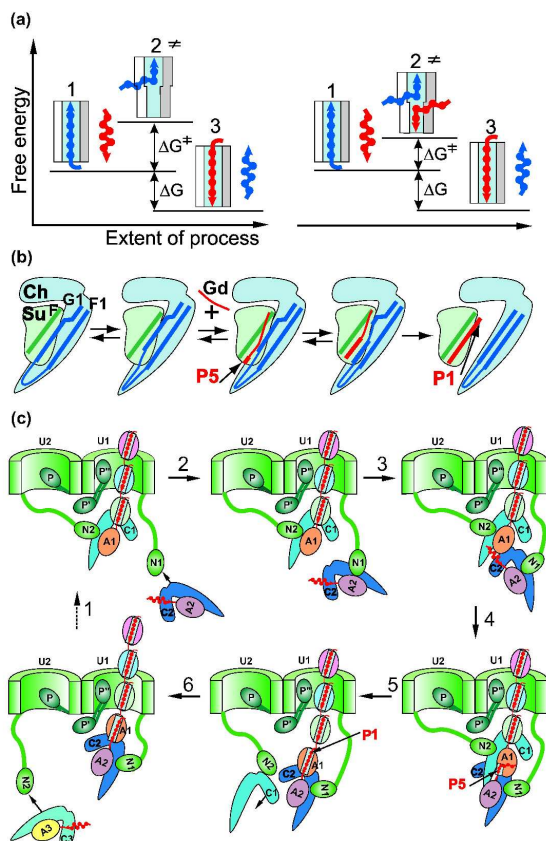
Plot of correlation (elaborated by the authors) between a number of deleted residues in a F1-G1 loop in a chaperone (FG deletion in residues shown on abscissa) in comparison with the F1-G1 loop of the Caf1M chaperone and a number of subunits operating by a chaperone (subunits operated shown on ordinate). The slopes of plots of correlation for FGL and FGS chaperones are different and are shown by green and red, correspondingly. The coefficient of correlation for FGL chaperones is equal to 0.80 and for FGS chaperones it is equal to 0.72.  
209x297mm (600 x 600 DPI)





(a) Comparison of PapA pilin domain and Caf1 polyadhesin subunit complemented with chaperones. PapA pilin domain and Caf1 polyadhesin subunit are shown red with donor strands from PapD and Caf1M chaperone (blue). Only interacting chaperone-subunit strands are shown. (b) A ribbon diagrams of the native PapD–PapA'–PapA'' and Caf1M–Caf1'–Caf1'' complexes. Caf1M and PapD are blue, except for G1 and A1  $\beta$ -strands (violet). The chaperone-bound Caf1' and PapA' subunits and N-terminal donor strands (Gd or Nte) are red; the Caf1'' and PapA'' subunits corresponding to the tip of growing fibers are green. The N- and C-termini are labelled in the same colours as the ribbons. The redrawing is based on the co-ordinates of atoms of structures published by Verger et al. (2007) (PDB accession number, 2UY6) and Zavialov et al. (2003, 2005) (PDB accession numbers, 1P5V and 1Z9S).

209x297mm (600 x 600 DPI)



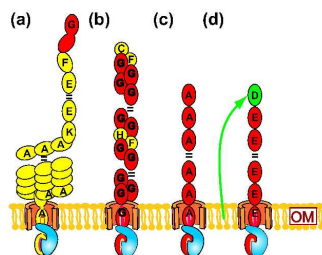
Model for the mechanism of donor strand exchange (DSE) in vitro and in vivo. (a) Models for usher-catalyzed assembly proposed by Zavialov et al. (2003). Left image: stepwise DSE in which the entire G1 donor strand is removed before the Gd strand is bound. Right image: sequential concerted DSE in which G1 is gradually replaced by Gd in a zip-in-zip-out mechanism. (1 and 3) correspond to the crystallographically observed chaperone-subunit and subunit-subunit structures, respectively. (2) presents the imaginary structures.  $\Delta G$  corresponds to the free energy for fiber formation from chaperone-subunit assembly complex and must necessarily be 0. Values for the different free energy terms are not known, and the figure is not meant to indicate even relative sizes of these terms. (b) Schematic presentation of DSE in vitro based on the experimental data (Remaut et al., 2006). Chaperone and subunit are labeled (Ch, light blue) and (Su, light green), respectively. In the chaperone, strands G1 and F1 are presented as solid dark blue lines. In the subunit, strand F, which directly interacts with the G1 donor strand, is depicted in dark green. An incoming N-terminal Gd

1  
2  
3 donor strand (depicted in red) forms a ternary complex with the chaperone-subunit complex at the  
4 P5 pocket (indicated by a thicker line). DSE then proceeds and terminates by dissociation of the  
5 chaperone-subunit complex and insertion of the P1 residue in the P1 pocket. (c) Schematic  
6 representation of a single incorporation cycle at the usher. Chaperone and usher are shown light  
7 blue and light orange, respectively. For clarity, subunits are differentiated by color with the  
8 incoming subunit in light cyan. The N-terminal and C-terminal domains of the usher are indicated.  
9 Redrawing based on Zavialov et al. (2003) and Remaut et al. (2006, 2008) and Fronzes et al.  
10 (2008).

11 209x297mm (600 x 600 DPI)

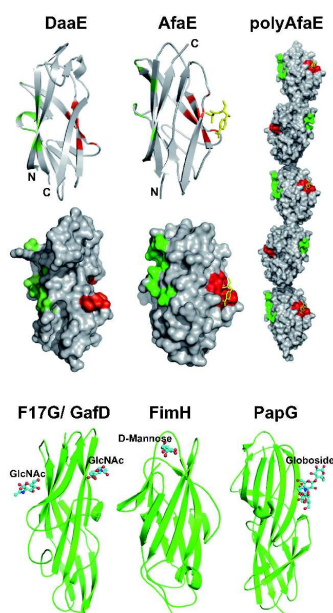
12  
13  
14  
15  
16  
17  
18  
19  
20  
21  
22  
23  
24  
25  
26  
27  
28  
29  
30  
31  
32  
33  
34  
35  
36  
37  
38  
39  
40  
41  
42  
43  
44  
45  
46  
47  
48  
49  
50  
51  
52  
53  
54  
55  
56  
57  
58  
59  
60

For Peer Review



Schematic presentation (elaborated by the authors) of the structure of FGS chaperone-assembled thick rigid mono-adhesive fimbriae/pili (a; P pili as example) (Sauer et al., 2000, 2004), FGS chaperone-assembled hetero-polyadhesins (b; F4, K88 pili as example) (van den Broeck et al., 2000), FGS chaperone-assembled homo-polyadhesins (c; PE fimbriae as example) (Chessa et al., 2008) and FGL chaperone-assembled polyadhesins (d; AfaE polyadhesin as example) (Anderson et al., 2004a). Periplasmic chaperones and outer membrane ushers are in blue and light orange, accordingly. Adhesin subunits are in red. Structural subunits are in yellow. Green arrow shows chaperone/usher independent secretion of AfaD subunit (shown in green) via type II secretion system (Zalewska-Piątek et al., 2008) and its potential display on the tip of the AfaE fimbrial polyadhesin (Anderson et al., 2004a).

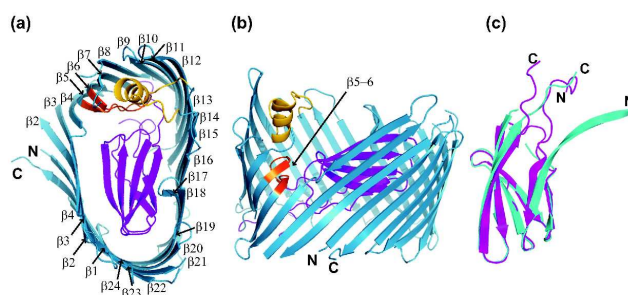
209x297mm (600 x 600 DPI)



Binding sites of FGL chaperone assembled polyadhesins (DaaE and AfaE) and FGS chaperone assembled mono-adhesive fimbriae/pili (GafD/F17G, FimH and PapG). A ribbon diagrams and solvent accessible surface presentations of DaaE subunit of a strand-swapped trimer of wild type DaaE of F1845 adhesin and self-complemented AfaE subunit of AFA-III adhesin with chloramphenicol as a yellow stick presentation. CD55/DAF and CEACAMS binding sites derived from DraE and DaaE mutagenesis are shown in green and red, respectively. Molecular surface rendering of a model for AfaE fiber was generated by assuming the same orientation between successive subunits as observed for Caf1' and Caf1'' in F1 fiber (Zavialov et al., 2003). The residues involved in binding with CD55/DAF and CEACAMS are in green and red, respectively. Ribbon presentations also are given for adhesin domains of GafD/F17G (PDB accession number, 1OIO), FimH (PDB accession number, 1KLF) and PapG (PDB accession number, 1J8R). Bound ligands, determined crystallographically, for GafD/F17G, FimH and PapG are also shown and labeled. The redrawing is

1  
2  
3 based on the data and co-ordinates of atoms of the structures published by Anderson et al. (2004a,  
4 b), Korotkova et al. (2006a, b), Pettigrew et al. (2004) and Li et al. (2007).  
5 209x297mm (600 x 600 DPI)  
6  
7  
8  
9  
10  
11  
12  
13  
14  
15  
16  
17  
18  
19  
20  
21  
22  
23  
24  
25  
26  
27  
28  
29  
30  
31  
32  
33  
34  
35  
36  
37  
38  
39  
40  
41  
42  
43  
44  
45  
46  
47  
48  
49  
50  
51  
52  
53  
54  
55  
56  
57  
58  
59  
60

For Peer Review



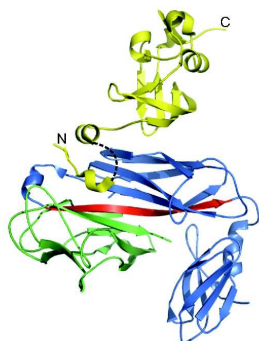
(a) Ribbon presentation of the PapC130–640 translocation channel (PDB accession number, 2VQI) viewed from the extracellular side. The  $\beta$ -barrel, plug domain,  $\beta$ 5–6 hairpin, and helix  $\alpha$ 1 are colored blue, magenta, orange, and yellow, respectively. Beta strands are labeled  $\beta$ 1 through  $\beta$ 24, the labels N and C indicate the N and C termini of the translocation channel. (b) Ribbon presentation of PapC130–640 viewed from the side. Structural elements are colored as in (a). The N and C termini, helix  $\alpha$ 1, strand  $\beta$ 4, and the  $\beta$ 5–6 hairpin are labeled. (c) Structural superposition of the Caf1A plug domain (232–320 amino acid fragment of Caf1A; PDB accession number, 3FCG) and the PapC plug domain (252–330 amino acid fragment of PapC; PDB accession number, 2VQI). Caf1A232–320 and PapC252–330 are in magenta and cyan, respectively. Beta strands are labeled according to the immunoglobulin fold classification. N- and C-terminal ends of structured fragments are indicated. The structures are redrawn based on the co-ordinates of atoms published by Remaut et al. (2008) and Yu et al. (2009).



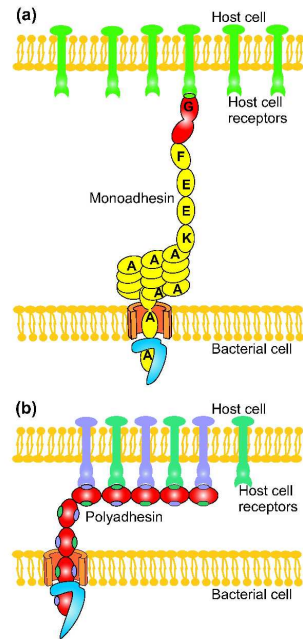
1  
2  
3  
4  
5  
6  
7  
8  
9  
10  
11  
12  
13  
14  
15  
16  
17  
18  
19  
20  
21  
22  
23  
24  
25  
26  
27  
28  
29  
30  
31  
32  
33  
34  
35  
36  
37  
38  
39  
40  
41  
42  
43  
44  
45  
46  
47  
48  
49  
50  
51  
52  
53  
54  
55  
56  
57  
58  
59  
60

209x297mm (600 x 600 DPI)

For Peer Review

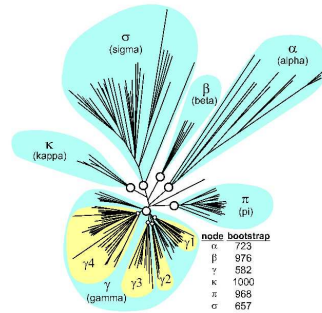


X-ray structure of the ternary N-terminal usher domain FimDN(1-125)-FimC chaperone-FimHP pilin complex. The ribbon diagram of the ternary complex is shown, with FimDN(1-125) N-terminal usher domain depicted in green, FimC chaperone in cyan and the pilin domain FimHP in yellow. The G1 donor strand of FimC chaperone is colored in blue. A black dashed line indicates residues 10-18 of FimDN N-terminal usher domain, for which no electron density was observed. The N- and C-termini of FimDN N-terminal usher domain are labeled in green. The structure is redrawn based on the coordinates of atoms published by Nishiyama et al. (2005) (PDB accession number, 1ZE3).  
209x297mm (600 x 600 DPI)

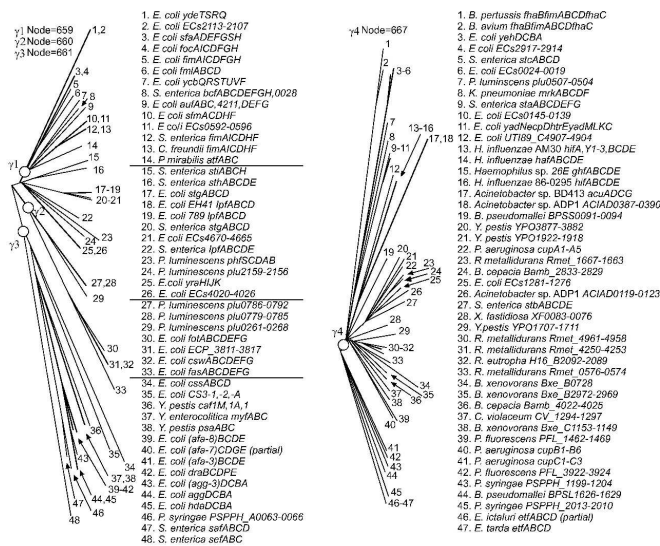


Schematic illustration (elaborated by the authors) a binding of mono-adhesive (a) and poly-adhesive (b) organelles to host cell receptors. Periplasmic chaperones and outer membrane ushers are in blue and orange, accordingly. Adhesin and pilin subunits are in red and yellow, respectively. Host receptors for moadhesins are shown by green. Two different types of host receptors for polyadhesins are shown by violet and greencyan.

209x297mm (600 x 600 DPI)

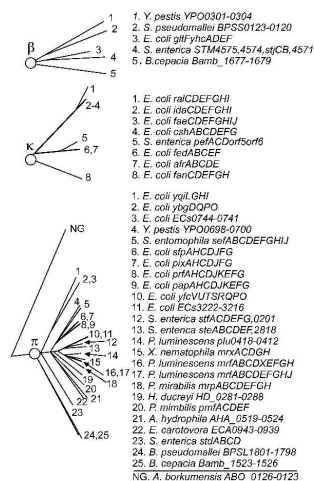


Phylogenetic tree of the fimbrial usher protein family (the redrawn is based on Nuccio & Bäumlner, 2007). The graph shows an unrooted phenogram generated using analysis of amino acid sequences of 189 ushers (Nuccio & Bäumlner, 2007). Ushers are grouped into six fimbrial clades (highlighted in light blue) termed  $\alpha$ ,  $\beta$ ,  $\gamma$ ,  $\kappa$ ,  $\pi$ , and  $\sigma$ -fimbriae. Ushers of  $\gamma$ -clade are subdivided into four clades (highlighted in yellow) termed  $\gamma_1$ ,  $\gamma_2$ ,  $\gamma_3$ , and  $\gamma_4$ -fimbriae. Bootstrap values of nodes defining these clades (indicated by open circles at the base of each fimbrial clade) are shown. For the details of generation of the phylogenetic tree and bootstrap values see Nuccio & Bäumlner (2007).  
209x297mm (600 x 600 DPI)

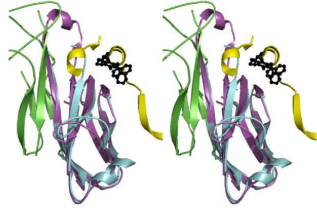


Phylogenetic relationship of operons belonging to the  $\gamma_1$ ,  $\gamma_2$ ,  $\gamma_3$ , and  $\gamma_4$ -fimbriae (the redrawn is based on Nuccio & Bäumer, 2007). The branch of the fimbrial usher protein tree representing  $\gamma_1$ ,  $\gamma_2$ ,  $\gamma_3$ , and  $\gamma_4$ -fimbriae is shown on the left. The bootstrap value for the node defining each subclade is displayed at the top and was generated in the analysis performed for Fig. 14. Numbers at the end of each branch of the phylogenetic tree correspond to the numbers given for each operon on the right.

209x297mm (600 x 600 DPI)



Phylogenetic relationship of operons belonging to the  $\beta$ ,  $\kappa$ , and n-fimbriae (the redrawing is based on Nuccio & Bäumlner, 2007). The branch of the fimbrial usher protein tree representing  $\beta$ ,  $\kappa$ , and n-fimbriae is shown on the left. The bootstrap value for the node defining each subclade is displayed at the top and was generated in the analysis performed for Fig. 14. Numbers at the end of each branch of the phylogenetic tree correspond to the numbers given for each operon on the right.  
209x297mm (600 x 600 DPI)



1  
2  
3  
4  
5  
6  
7  
8  
9  
10  
11  
12  
13  
14  
15  
16  
17  
18  
19  
20  
21  
22  
23  
24  
25  
26  
27  
28  
29  
30  
31  
32  
33  
34  
35  
36  
37  
38  
39  
40  
41  
42  
43  
44  
45  
46  
47  
48 Stereomage of the FimD1-125 N-terminal usher domain in complex with the FimC-FimH158-279  
49 chaperone-adhesion complex with the PapD- pilicide complex in overlay. PapD and pilicide are  
50 shown in light blue ribbon and ball-and-stick presentation, respectively. FimC and FimH158-279 are  
51 shown in magenta and green, with the FimD1-125 N-terminal domain shown in yellow. The  
52 redrawing is based on the co-ordinates of atoms of the structures published by Nishiyama et al.  
53 (2005) (PDB accession number, 1ZE3).  
54 209x297mm (600 x 600 DPI)  
55  
56  
57  
58  
59  
60